

2011

# Stathmin Depletion from Cells Lacking p53 Leads to Delayed Cell Cycle Progression and Apoptosis Due to Increased Microtubule Stability

Bruce Knighton Carney  
*Lehigh University*

Follow this and additional works at: <http://preserve.lehigh.edu/etd>

---

## Recommended Citation

Carney, Bruce Knighton, "Stathmin Depletion from Cells Lacking p53 Leads to Delayed Cell Cycle Progression and Apoptosis Due to Increased Microtubule Stability" (2011). *Theses and Dissertations*. Paper 1324.

This Dissertation is brought to you for free and open access by Lehigh Preserve. It has been accepted for inclusion in Theses and Dissertations by an authorized administrator of Lehigh Preserve. For more information, please contact [preserve@lehigh.edu](mailto:preserve@lehigh.edu).

**Stathmin Depletion from Cells Lacking p53 Leads to Delayed Cell Cycle  
Progression and Apoptosis Due to Increased Microtubule Stability.**

by

Bruce K. Carney

A Dissertation

Presented to the Graduate and Research Committee

of Lehigh University

in Candidacy for the Degree of

Doctor of Philosophy

in

Molecular Biology

Lehigh University

July 15, 2011

Copyright  
Bruce K. Carney

Approved and recommended for acceptance as a dissertation in partial fulfillment of the requirements for the degree of Doctor of Philosophy

**Stathmin Depletion from Cells Lacking p53 Leads to Delayed Cell Cycle Progression and Apoptosis Due to Increased Microtubule Stability.**

By Bruce K. Carney

July 15, 2011

---

Defense Date

---

Lynne Cassimeris, Ph.D.  
Committee Chair

---

Approved Date

Committee Members:

---

Robert Skibbens, Ph.D.  
Committee Member

---

M. Kathy Iovine, Ph.D.  
Committee Member

---

Maureen Murphy, Ph.D.  
External Member

## **Acknowledgements**

I would like to thank Lynne for her help and guidance throughout my time in her lab. Her passion and enthusiasm have made her a fantastic mentor. She has continuously pushed me to be the best I could be and was always there with helpful suggestions, thoughtful discussions, and constant support. Thanks to my committee for their many valuable ideas and discussions, as well as all their help and assistance along the way. You have all helped me immensely and I am very grateful for all you have done for me.

I would also like to thank past and present members of the Cassimeris lab group. Dr. James Warren, Dr. Bret Becker, and Justin Morabito thank you for all you taught me in the early parts of my time here. Without you, I would not have learned all the techniques that have helped me along the way. I would especially like to thank, Dr. Danielle Ringhoff and Victoria Caruso. You two have been amazing; I could not have asked for better labmates. Without both of you, I would not have made it to this point. Thank you for all the helpful discussions, advice, and a break from reality when I most needed it.

To the Department of Biological Sciences, thank you for allowing me the opportunity to further pursue my education. A special thanks to Maria Brace, Vicki Waldron, Carol Esposito, and Joann Deppert. You have been invaluable as resources and have made my time here much easier.

Thank you to the Cassbens Group for all your suggestions, BOGS for a chance to socialize outside of the department, and my fellow graduate students for making my time here more enjoyable. I would especially like to thank Marie for always making me smile, Tim for all his fantastic cooking, Mike for always being a sympathetic ear, Candice for putting up with me in the office, Kevin for always being there, and finally Dylan and Sue for always being up for a lunchtime get away and always making me laugh. You all have been fantastic friends and I will miss working with you.

Most importantly, thank you to my family. Without your love and support none of this would have been possible. Thank you for all you have done for me over the years.

## **Table of Contents**

Acknowledgements	iv
List of Figures	ix
List of Abbreviations	xi
Abstract	1

### **Chapter 1:**

<b><u>Introduction</u></b>	<b><u>3</u></b>
Introduction	3
Cytoskeleton	4
Microtubule Structure	4
Microtubule Dynamics	5
Assembly of Microtubules	6
Microtubule Associated Proteins (MAPs)	8
Stathmin/Oncoprotein 18	9
Cell Cycle	13
Apoptosis	14
p53: a DNA damage checkpoint protein	16
Dissertation Summary	17
Figures	19

**Chapter 2:**

**Stathmin/Oncoprotein 18, a microtubule regulatory protein, is required for survival**

**of both normal and cancer cell lines lacking the tumor suppressor, p53** **23**

Introduction	24
Methods	26
Results	30
Discussion	38
Conclusions	41
Figures	43

**Chapter 3:**

**Increasing Stable Microtubules Leads to G2 Delay in Human Cell Lines Lacking**

**p53** **56**

Introduction	57
Methods	59
Results	64
Discussion	71
Conclusions	77
Figures	78

**Chapter 4:**

**Conclusions and Future Directions** **89**

---

Conclusions 90

Future Directions 92

Figures 98

**References** **101**

---

**Curriculum Vitae** **114**

---

## List of Figures

**Figure 1.1:** Microtubule structure.

**Figure 1.2:** Stathmin binding tubulin.

**Figure 1.3:** Apoptosis signaling pathway.

**Figure 1.4:** p53's role in the cell.

**Figure 2.1:** Stathmin depletion from HCT116<sup>p53<sup>WT</sup></sup> and HCT116<sup>p53<sup>-/-</sup></sup> cell lines.

**Figure 2.2:** Stathmin is required for survival of HCT116<sup>p53<sup>-/-</sup></sup> cells.

**Figure 2.3:** Restoring p53 in HeLa cells.

**Figure 2.4:** Restoring p53 rescues HeLa cells from stathmin-depletion induced death.

**Figure 2.5:** Stathmin-depletion induced cell death likely occurs via apoptosis.

**Figure 2.6:** Depleting both p53 and stathmin from normal human fibroblast (HFFs) cells leads to cell death

**Figure 2.7:** Stathmin depletion from HCT116<sup>p53<sup>-/-</sup></sup> cells delays G2 of the cell cycle.

**Figure 2.8:** Stathmin depletion from HeLa cells delays G2 of the cell cycle.

**Figure 3.1:** Stathmin depletion from HeLa cells increases MT stability only when p53 is absent.

**Figure 3.2:** Depolymerizing MTs with nocodazole allows cells to escape the G2 delay in both HeLa and HCT116<sup>p53<sup>-/-</sup></sup> cells.

**Figure 3.3:** Stathmin truncations can be expressed in HeLa cells in the presence of siRNA against the 5'UTR region of stathmin mRNA.

**Figure 3.4:** Stathmin truncations change MT polymer at the cell periphery.

**Figure 3.5:** Over-expression of truncated stathmin can rescue the cells from a G2 delay following depletion of endogenous stathmin.

**Figure 3.6:** Stathmin depletion does not increase p27<sup>kip1</sup> localization in the nucleus.

**Figure 3.7:** Models for how stathmin depletion in p53 null cells leads to a G2 delay.

**Figure 3.8:** Stathmin depletion from HCT116<sup>WT-p53</sup> and HCT116<sup>p53<sup>-/-</sup></sup> cells increases MT stability only when p53 is absent.

**Figure 3.9:** Nocodazole depolymerizes MTs in HeLa cells.

**Figure 3.10:** Mitotic index increases when cells are treated with nocodazole independent of stathmin depletion.

**Figure 4.1:** Depletion of stathmin leads to G2 delay followed by apoptosis only in p53 lacking cells.

**Figure 4.2:** Following the G2 delay, cells slip into the next cell cycle before activating apoptosis.

**Figure 4.3:** Flow chart of core enzymes involved in mitotic entry.

## List of Abbreviations

$\alpha$ -tb – alpha tubulin

$\beta$ -tb – beta tubulin

$\gamma$ -tb – gamma tubulin

$\gamma$ TuRCs – gamma tubulin ring complexes

tb – tubulin

AcTb – acetylated tubulin

MT – microtubules

STMN - stathmin

MAP – microtubule associated proteins

MTOC – microtubule-organizing center

EB1 – end binding protein 1, localizes to plus ends of growing MT tips

Noc - Nocodazole

DMSO - Dimethyl sulfoxide

PARP – poly (ADP-ribose) polymerase

## **Abstract**

Control of cell proliferation is greatly diminished in cancer cells. In order to understand how to prevent the uncontrolled proliferation of cancer cells, it is first important to understand how cells normally control proliferation. Stathmin, a microtubule regulatory protein, is over-expressed in many cancers and required for survival of several cancer lines. In a study of breast cancer cell lines, Alli et al. (*Oncogene*. 26:1003-12) proposed that stathmin is required for survival of cells lacking p53, but this hypothesis was not tested directly. Here we tested their hypothesis by examining cell survival in cells depleted of stathmin, p53 or both proteins. Comparing HCT116 colon cancer cell lines differing in TP53 genotype, stathmin depletion resulted in significant cell cycle delay and death only in cells lacking p53. As a second experimental system, we compared the effects of stathmin depletion from HeLa cells, which normally lack detectable levels of p53 due to expression of the HPV E6 protein. Stathmin depletion caused a large percentage of HeLa cells to both delay in the cell cycle and then die via apoptosis. Restoring p53, by depletion of HPV E6, rescued HeLa cells from stathmin-depletion induced delay and death. The stathmin-dependent survival of cells lacking p53 was not confined to cancerous cells because both proteins were required for survival of normal human fibroblasts.

P53 and stathmin depletion leads to a G2 cell cycle delay, however, it is still unclear as to why we see this synergy. We hypothesize that stathmin depletion relays a signal via stabilization of the microtubule cytoskeleton, specifically in cells lacking p53.

Alternatively, stathmin could have a function separate from its microtubule regulatory activity, and loss of this additional function could lead to cell cycle delay. As a test of our hypothesis, we examined whether microtubule stability is greatest in cells lacking both stathmin and p53. Results showed that HeLa cells depleted of both stathmin and p53 showed a large increase in both acetylated microtubule content (a marker of microtubule stability) and rate of microtubule nucleation. Restoring p53 in stathmin-depleted cells reduces both the amount of acetylated microtubules and the microtubule nucleation rate. To further test the link between stathmin depletion in cells lacking p53 and microtubules, the microtubule network was manipulated by either nocodazole-dependent depolymerization or by restoring the microtubule network to control levels by over-expressing stathmin truncations (full-length stathmin or stathmin  $\Delta$ 101-149). Both of these treatments allowed cells to escape the G2 delay, while over-expression of a stathmin truncation that does not affect the microtubule array (stathmin  $\Delta$ 5-25) did not affect the G2 delay.

Our results demonstrate that stathmin is required for cell survival in cells lacking p53, suggesting that stathmin depletion could be used therapeutically to induce a G2 cell cycle delay and apoptosis in tumors without functional p53. Our results also indicate that the interphase microtubule cytoskeleton is a novel target for control of cell proliferation, particularly for the greater than 50% of human cancers that lack p53 because of either inactivating mutations or viral infection. Together the results described in this dissertation could lead to new methods to treat and kill cancer cells that specifically lack p53, while leaving healthy cells relatively unaffected.

## **Chapter 1: Introduction**

Researchers have been trying to find a cure for cancer for decades. The American Cancer Society estimates cancers affect 11.7 million people in the United States alone (in 2007), but to date treatments have many side effects and are not effective against certain types of cancers. On a cellular level, cancers can and do have mutations to genes encoding many different proteins that affect numerous cellular pathways. Cancer cells that lack the p53 protein, for example, are among the most malignant and lethal, and account for about fifty percent of all human cancers (Wallace-Brodeur and Lowe, 1999). These types of cancer cells can no longer repair damaged DNA, or send apoptotic signals if the damage is beyond repair.

Alli et al (2007) and others have suggested that depleting stathmin from cells lacking p53 can lead to apoptosis, bypassing the natural role of p53 in apoptotic signaling. However, apoptotic death by stathmin depletion is only correlated with p53 status; it is not yet clear whether p53 must be absent for stathmin depletion to induce cell death. If the Alli et al (2007) hypothesis is correct, how does stathmin depletion accomplish the reactivation of the apoptotic-signaling pathway? Could stathmin's effects on the microtubule network, and therefore the microtubule network itself, be important in this signaling pathway? By answering these questions we can open up new avenues for possible advancements in finding novel targets for cancer therapies. These questions are addressed in this dissertation. The following sections introduce the critical cellular components and processes studied during the dissertation research.

## **Cytoskeleton**

Actin filaments (F-actin), intermediate filaments (IF), and microtubules (MTs) make up the cytoskeleton of a eukaryotic cell. These components work together to affect and establish many of the cell's characteristics, including maintaining its shape, creating polarity, and allowing motility. Although these filaments work together to form the whole of the cytoskeleton network, each has its own specific responsibilities in the cell. MTs in particular are responsible for cell division, vesicle trafficking, and cell movement via flagella. These processes all require the MT arrays within the cell to be both dynamic and static, depending on the function to which each array is being used. The nucleation (formation) rates and relative dynamics must therefore be controlled at all times. Microtubule-associating proteins (MAPs) function to create, maintain, and destroy the various MT arrays that are present in the cell in order to regulate the dynamics.

## **Microtubule Structure**

The structure of a microtubule is an essential part of what allows these filaments to function as they do in cells. Each filament is made of thirteen protofilaments that are noncovalently linked together to form the microtubule (Desai and Mitchison, 1997). These protofilaments connect together to form a hollow tube (Aldaz et al., 2005) with a 25nm diameter, and a 14nm gap in the center (Figure 1.1a). The tubulin dimer's ability to form longitudinal, as well as lateral bonds (Meurer-Grob et al., 2001; Nogales, 2000), and its unique shape gives the filament its sturdy (McGrath, 2006), yet flexible characteristic that makes it optimal for producing arrays that can bend but not break (Figure 1.1a).

Each protofilament is made of heterodimers of alpha tubulin ( $\alpha$ -tb) and beta tubulin ( $\beta$ -tb) that connect together in a head-to-tail fashion to form the protofilament (Meurer-Grob et al., 2001). Although they are never found in their monomeric form, both  $\alpha$ -tb and  $\beta$ -tb have a molecular weight of approximately 50 kDa, and are 451 and 442 amino acids in length, respectively (McKean et al., 2001).

### **Microtubule Dynamics**

The heterodimeric properties of these filaments allow for them to have polarity. In this case, the  $\alpha$ -tb is exposed at the “minus” end, while the  $\beta$ -tb is exposed at the “plus” end (Mitchison, 1993). Polarity forms because of the head to tail alignment of the dimers. The GTP bound to  $\alpha$ -tb is trapped in the heterodimer and is therefore non-exchangeable and unable to hydrolyze. The GTP on the  $\beta$ -tb, on the other hand, is able to rapidly hydrolyze GTP to GDP making the dimer’s connection with the other heterodimers unstable (Mitchison, 1993; Nogales et al., 1998). It is the  $\beta$ -tb bound GTP that gives MTs their dynamic nature. This fragile stability is what allows for the rapid dissociation of these structures. As long as a GTP is bound to  $\beta$ -tb, each protofilament will remain straight and stiff (Meurer-Grob et al., 2001). When GTP is hydrolyzed to GDP at the MT tip, the protofilament begins to bend and the protofilaments fray apart (Figure 1.1b). The loss of tb-GTP allows for the lateral connections to be disturbed causing the filament to depolymerize (Aldaz et al., 2005). In order to prevent this depolymerization, the tubulin subunits that are most recently added retain their GTP and form a “GTP cap” (Erickson and O'Brien, 1992). The GTP that is not at the end of the filament can be hydrolyzed, while the presence of a GTP cap at the plus end of the MT allows each protofilament to

remain in a straight conformation trapping the rest of the MT together despite the reduced strength of the lateral bonds between protofilaments (Figure 1.1c). Without this cap, the MT is no longer stable and cannot grow longer. Therefore, polymerization can only occur in the presence of the GTP cap. Tubulin subunits are added and lost from the plus end of the MT much faster than they are from the minus end (Moritz et al., 1995; Vorobjev et al., 1999). The gain and loss of a GTP cap is what allows the MT to quickly shift from a growth phase to a shortening phase and vice versa, in a process known as dynamic instability (Mitchison and Kirschner, 1984). The loss of the protective GTP cap leads to a rapid switch between growth and shortening, known as a catastrophe. A rescue event can occur if the MT stops shortening and begins to grow again. The exact mechanism of how these switches occur is not well understood. All that is known is that the GTP cap must be reformed if growth is to occur and must be lost for shortening to begin.

### **Assembly of Microtubules**

Microtubules can self-assemble at a slow rate *in vitro* depending on tubulin concentration. However, this process produces very unstable microtubules. Tubulin starts to polymerize into small fragments, but cannot remain in a polymerized form until the polymer becomes larger and more stable. Once a stable protofilament starts to form, which can take a long time, elongation can finally occur. After elongation begins, MTs quickly move towards a state where the proportion of free tubulin to MT polymer is constant. In animal cells, the assembly of MTs is not a spontaneous process unless tubulin concentration is high

enough; therefore growing MTs usually require other proteins to assemble properly (Moritz et al., 1995).

*In vivo*, assembly needs to be much more controlled and nucleation needs to be much faster. For this to happen, minus ends of MTs are bound to  $\gamma$ -tubulin ring complexes ( $\gamma$ TuRCs).  $\gamma$ -tubulin ring complexes are packed together in a highly organized complex called a microtubule organizing center (MTOC). The MTOC contains  $\gamma$  TuRC,  $\gamma$  tubulin ( $\gamma$ -tb), a pair of centrioles, and many additional proteins (Desai and Mitchison, 1997; Dictenberg et al., 1998). The MTOC forms a scaffold, where rapid MT nucleation occurs, since the dimers polymerize from the  $\gamma$  TuRC, and MTs radiate out into the cell. In mitosis, a centrosome (a MTOC) is at each spindle pole and allows MTs to radiate into the center and capture chromosomes. Nucleation sites orient the dynamic plus end away from nucleation sites, while the minus end is always anchored to this site (Becker and Cassimeris, 2005). In the life of any MT, multiple catastrophes and rescues events can frequently occur (Komarova et al., 2002).

The MT network plays an important role in vesicle and chromosome trafficking in the cell as well. The MT network is involved in transporting cargo into and out of the cell. Microtubule motor proteins, such as kinesin and dynein, attach to MTs and walk along the filament with its attached cargo (Hirokawa and Takemura, 2004; Vershinin et al., 2008). This cargo is then shuttled throughout the cell until it reaches its destination where the cargo is released from the motor protein.

The formation of a microtubule network throughout the cell also allows for MTs to play an essential role in cellular signaling. Acetylation, for instance, is a marker of more stable MTs and leads to greater binding of kinesin motors. These acetylated MTs are both remarkably stable and significantly less dynamic than other MTs. The increased affinity of motors to acetylated MTs leads to a higher level of selective transport of vesicles throughout the cell (Bulinski, 2007; Reed et al., 2006). Polyglutamylation of  $\alpha$ -tubulin was proposed to be important in the interaction of tubulin with MAPs (Edde et al., 1990; Kann et al., 2003). Other modifications such as detyrosination, phosphorylation, and polyglucylation are suggested to play a role in stabilizing MTs (Gundersen et al., 1984; Lin et al., 2002). Such post-translational modifications are also suggested to allow signals to be sent throughout the cell. This signaling function could be accomplished by using the MTs as a scaffold from which other proteins can bind or be transported along the MT in order to propagate the signal (Bulinski, 2007; Larsson et al., 1999).

### **Microtubule Associated Proteins (MAPs)**

Microtubule associated proteins (MAPs) are used to regulate assembly and either stabilize or destabilize the growing MT depending on the type of MAP that is active (Desai and Mitchison, 1997). The activity states of these proteins determine the turnover rate of a given MT. There are two general MAPs, those that stabilize MTs and those that destabilize them. Certain MAPs act to destabilize MTs by binding to tubulin dimers, sequestering them away from the growing MTs, while other types of destabilizing MAPs can bind to the tip of growing protofilaments and halt dynamics and promote catastrophes. MAPs can also act by binding along the side of the MT, both stabilizing

and cross linking them, or they can bind at the tips of the MTs promoting polymerization and further growth. The more stabilizing MAPs that are present on a MT, the longer the MT will grow. Many MAPs are activated or deactivated based on their phosphorylation state (Cassimeris and Spittle, 2001). MAP phosphorylation sites allow for a conformational change in the protein depending on whether the site is phosphorylated or not.

Drugs, such as paclitaxel (Taxol), can also stabilize the MT cytoskeleton. Taxol stabilizes MTs and leads to accumulation of polymer in the cell, preventing the completion of mitosis, resulting in a block during M phase. If the cell cycle is not allowed to continue, the cell will eventually begin apoptosis (Donaldson et al., 1994; Gascoigne and Taylor, 2009).

### **Stathmin/Oncoprotein 18**

Stathmin/Oncoprotein 18 (STMN) is a MAP that destabilizes MTs (Belmont and Mitchison, 1996; Cassimeris and Spittle, 2001). This 18 kDa (149 amino acid) protein functions to both sequester tubulin and promote catastrophes (Howell et al., 1999b; Larsson et al., 1999). *In vitro*, at a pH of 6.8, stathmin binds and sequesters two tubulin dimers (Figure 1.2) forming a T2S complex and removes tubulin from the polymer-forming tubulin pool (Cassimeris, 2002). While at a higher pH (7.5), stathmin promotes catastrophes possibly by attaching to a growing MT end (Howell et al., 1999a). Truncated versions of this protein show that the N-terminal sequence of stathmin is important for catastrophe promoting function. While the C-terminal sequence is

responsible for sequestering tubulin (Clement et al., 2005; Howell et al., 1999a; Howell et al., 1999b). Larsson et al (1999) showed that the C-terminal sequence activity of the stathmin protein is not required to disrupt the MT network in cells.

Stathmin is active in its unphosphorylated state. However, stathmin has four serine residues (S16, S25, S38, and S63) that can be phosphorylated (Cassimeris, 2002). The tubulin binding efficiency *in vitro* of this MAP decreases with the addition of phosphate groups and is completely off during mitosis when it is fully phosphorylated (Larsson et al., 1997; Larsson et al., 1995). Phosphorylation at serine 16 and 63 causes stathmin to bind weakly to tubulin. Phosphorylation at these sites suppresses stathmin to a much greater extent than at serine 25 and 38 (Cassimeris, 2002). PKA, MAP kinases, and CDKs are just a few of the kinases that are responsible for phosphorylating stathmin (Cassimeris and Spittle, 2001; Gradin et al., 1998; Marklund et al., 1996).

Along with its role in MT destabilization, stathmin is also involved in cell signaling, however, with the exception of crosstalk with actin via MTs (Wittmann et al., 2004), this signaling is not well understood. Despite the fact that little is known about this signaling function, it has been suggested that these signals play a pivotal role in both the cell cycle and cell differentiation (Sobel, 1991). Stathmin has been shown to be a target of numerous signal cascades which lead to phosphorylation of stathmin, allowing both cell division and differentiation to occur (Sobel, 1991).

Recently stathmin has been shown to have additional sources of regulation that do not involve phosphorylation. P27<sup>Kip1</sup>, a cyclin dependent kinase (CDK) inhibitor (Baldassarre et al., 2005), and STAT3, a transcription factor (Ng et al., 2006), have been shown to bind to stathmin's C-terminal amino acids (Baldassarre et al., 2005; Ng et al., 2006). Binding of STAT3 to stathmin has been shown to block the ability of stathmin to bind and destabilize MTs (Ng et al., 2006). The CKI, p27<sup>Kip1</sup> also binds stathmin's C-terminus and inhibits its MT destabilizing activity (Baldassarre et al., 2005). The binding of these proteins to stathmin suggests stathmin may play a greater role in signal transduction than was originally thought. Both p27<sup>Kip1</sup> and STAT3 have also been implicated in tumor cell migration and therefore have important roles in metastasis and cancer progression (Baldassarre et al., 2005; Ng et al., 2006).

Stathmin is overexpressed in many cancers. This phenotype exists in leukemia (Melhem et al., 1997), lymphoma (Nylander et al., 1995), multiple carcinomas (Kouzu et al., 2006; Nakashima et al., 2006; Nishio et al., 2001; Yuan et al., 2006), adenocarcinoma (Chen et al., 2003; Friedrich et al., 1995), prostate cancer (Mistry et al., 2005), breast cancer (Bieche et al., 1998; Brattsand, 2000), and ovarian cancer (Price et al., 2000). Because stathmin is associated with so many cancers, stathmin targeted treatments have started to be considered for cancer therapies (Kouzu et al., 2006; Mistry et al., 2005). Cancers where stathmin is overexpressed have a high malignancy phenotype, which leads to generally poor prognosis (Chen et al., 2003; Mistry et al., 2005).

The removal of stathmin from cells (or animals, such as mice) leads to organisms whose cell cycles seem normal throughout development. At the cellular level, transient removal of stathmin leads to an increase in MT concentration (Holmfeldt et al., 2006; Howell et al., 1999b; Ringhoff and Cassimeris, 2009b; Sellin et al., 2008). However, mice where stathmin has been knocked out produce viable embryos that mature and reproduce relatively normally (Schubart et al., 1996). Although mice develop normally without stathmin, an age-dependent axonopathy of the central and peripheral nervous system does occur (Liedtke et al., 2002). Stathmin also plays an essential role in regulating innate and learned fear in these mice (Shumyatsky et al., 2005), indicating that stathmin participates non-redundantly in spinal neuronal processes, but these processes are not sufficient to compromise viability in knockout mice.

Recent research has shown that while the removal of stathmin from healthy cells has no effect on the cell cycle, the removal of stathmin from certain cancer cell lines leads to cell death within as little as 24-48 hours (Alli et al., 2007; Mistry et al., 2005; Wang et al., 2007; Zhang et al., 2006). In each study, a slowing of cell proliferation rate was observed prior to apoptosis, but the literature shows conflicting evidence over whether it is a G1 or G2/M block. In either case, it has also been shown that this cell cycle block leads to an increase in apoptosis (Alli et al., 2007; Mistry et al., 2005; Zhang et al., 2006). While the removal of stathmin causes apoptosis in some cancer cell lines, other cancer lines have shown no such phenotype. Alli et al (2007) compared seven breast cancer cell lines differing in p53 status. The five cancer lines that lacked functional p53 showed an increase in cells with 4N DNA content and induction of apoptosis when stathmin was

depleted. However, these cancer cell lines have numerous other differences that could make them more susceptible to apoptosis due to stathmin depletion. Also one of the plus-p53 cell lines that did not die, MCF7, has a mutation in caspase 3, which would prevent apoptosis in this cell line. A successful knockdown of stathmin in cells with wild type p53 was not included in their study. Therefore, while it has been hypothesized that decreased stathmin level leads to apoptosis only in cells lacking p53, this hypothesis has not been tested directly (Alli et al., 2007). We tested this hypothesis using matched cancer cell lines that only differ in their p53 status (Chapter 2).

### **Cell Cycle**

In order for cells to grow and divide, they must proceed through the cell cycle. During the cell cycle certain events, like chromosomal duplication, must happen at specific places at specific times. Because of this, the processes of the cell cycle must be highly controlled. In its simplest form the cell cycle consists of two stages: interphase, where the cell grows and replicates its DNA, and mitosis, where the cell divides creating two identical daughter cells. Interphase consists of two gap (growth) phases, G1 and G2, which occur on either side of S phase, where DNA is replicated. In order to transition from one stage to another, many conditions or checkpoints must be met. The main controls of the cell cycle are a set of proteins called cyclins and cyclin-dependent kinases (CDKs). During the cell cycle, the cyclin proteins fluctuate in abundance and depending on which cyclins are present, at any given time, they allow the cell to proceed from one stage to another by interacting with CDKs to phosphorylate a wide array of proteins involved in each step of the cycle. (Morgan, 1997)

For stathmin-depleted cells, the focus is primarily on the transition from G2 to M phase of the cell cycle. Here, cyclin B levels rise significantly following DNA replication. Cyclin B binds CDK1, but is quickly made inactive by the inhibitory phosphorylation placed on CDK1, by Wee1, at two specific sites on the protein (Thr14 and Tyr15). To further control the activity of CDK1, CAK adds an additional phosphorylation at Thr167, priming the complex for activation as soon as the inhibitory phosphorylation is removed. These phosphorylation events prevent entrance in mitosis until the cell is ready, the environment is favorable, and all the DNA has been replicated. When all these checkpoints have been reached the inhibitory phosphorylation of CDK1 is reversed by the activity of Cdc25, which removes the phosphorylation and inactivates Wee1 activity, thereby activating the CDK1/cyclin B complex. This kinase activation allows for the phosphorylation of many mitotic proteins and drives progression into mitosis. If these checkpoints are not met the cell cycle will fail to progress until all necessary conditions have been met and satisfied. (Morgan, 1997)

### **Apoptosis**

Organisms need their cells to be able to sacrifice themselves for the benefit of the whole organism. Cells have developed a way to commit suicide or programmed cell death if their lack of health endangers the cells around it. This process, apoptosis, involves complex pathways that terminate the cell if the damage cannot be repaired. Cells have developed two specific mechanisms to transmit this death signal, an intrinsic and an extrinsic pathway.

In the intrinsic pathway, DNA damage or absence of survival signals, such as growth factor or hormone, lead to the start of apoptosis. As an example, if DNA damage is sensed by p53, the p53 protein is then activated. P53 is activated by its release from MDM2, which is phosphorylated in response to the damage. P53 then functions as a transcription factor and promotes the transcription of Bcl-2 proteins (such as Bax and Bad), which move to the mitochondria and disrupt its membrane. This causes the mitochondria to release cytochrome c. Cytochrome c binds with Apaf-1 and procaspase 9 to form the apoptosome, the formation of this complex leads to the cleavage of procaspase 9 into the functional component Caspase 9. Caspase 9 starts a cascade that activates caspase 3. Caspase 3 releases CAD from the ICAD-CAD protein complex. CAD enters the nucleus and with the help of poly ADP ribose polymerase (PARP), which is cleaved by caspase 3, cleaves DNA and causes the cell to die (Figure 1.3b). (Elmore, 2007)

In the extrinsic pathway, an external source activates the apoptotic pathway. As an example, a FAS ligand, released from a neighboring cell, binds to the FAS receptor of the apoptotic cell. The binding of the FAS ligand activates the receptor, which recruits and binds FADD. This transmembrane protein complex cleaves procaspase 8 into the protein's active form, caspase 8. Caspase 8 then activates caspase 3, which then follows the same pathway as the intrinsic pathway leading to cellular death (Figure 1.3a). (Elmore, 2007)

Cancer cells must avoid apoptosis to survive and proliferate. In order to survive, the pathways that would normally activate apoptosis in response to chromosomal defects and other cellular damage must be blocked (Elmore, 2007). For example, cells with a mutation in p53 are more likely to proliferate because p53 normally halts the cell cycle until DNA damage is repaired (Elledge, 1996). Therefore without functional p53, cells pass through the cell cycle even if there is significant damage to the DNA, allowing mutations to accumulate (Elledge, 1996).

### **P53: a DNA damage checkpoint protein**

The tumor suppressor, p53, is a protein that responds to DNA damage. When the protein is functioning normally, in a healthy cell, p53 is quickly bound to MDM2 and ubiquitinated and destroyed by the cell keeping its levels low (Caspari, 2000; Kelly and Brown, 2000). However, if DNA damage occurs, a serine/threonine kinase (ATM or ATR) phosphorylates p53 (at serine 15) causing it to release from MDM2 and results in increased p53 levels (Caspari, 2000). P53 then acts by initiating a pathway that stalls the cell cycle until repairs have been made or apoptosis begins. If DNA has not yet been replicated (G1), once p53 is released it binds to the regulatory region of the p21 gene (Ahn et al., 1999). This acts as a transcription factor, which leads it to increase the concentration of p21 (a cyclin dependent kinase inhibitor) protein in the cell (Figure 1.4). P21 acts by binding to an active cyclin/CDK complex and prevents it from advancing the cell cycle by causing a G1 arrest (Elledge, 1996; Kelly and Brown, 2000). If the damage cannot be repaired, the cell will enter apoptosis, leading to cell death (Caspari, 2000).

In about fifty percent of cancers, p53 is malfunctioning in some way (Caspari, 2000; Hollstein et al., 1991). Whether it is destroyed, sequestered, or just non-functional via a mutation, the inability of p53 to do its job can lead to numerous additional mutations or severe chromosomal alterations if the DNA is damaged. Mutations in p53 can prevent it from releasing from MDM2 or making it otherwise ineffective. The human papillomavirus, specifically, uses two viral proteins (E6 and E7 respectively) to sequester the host cell's p53 and Rb, another protein that can halt the cell cycle. The HPV E6 protein binds to p53 and targets it for ubiquitination and destruction, thus reducing p53 concentration to a very low level. Koivosalo et al (2005; 2006) showed that by utilizing RNA interference against the E6 protein, it is possible to restore p53 in HeLa cells.

Cells lacking functional p53 can no longer stop the cell cycle which leads to the damaged DNA being passed to the next generation before it can be repaired (Elledge, 1996). Cancers lacking p53 are some of the worst and have poor prognosis (Wallace-Brodeur and Lowe, 1999). The reason for this poor prognosis is because once the DNA damage checkpoint is bypassed it leads to genomic instability and more mutations thereby causing the mutation rate to increase exponentially (Elledge, 1996).

### **Dissertation Summary**

Chapter 2 explores whether or not the removal of stathmin from cancer cells only kills cancers that have a malfunctioning p53. We showed that stathmin depletion both causes a G2 delay and apoptosis in a p53-independent manner. We tested this by using two model systems; the first was a set of matched cancer cell lines, HCT116<sup>WTp53</sup> and

HCT116<sup>p53<sup>-/-</sup></sup>, in which one member lacks functional p53. As a second system, we restored p53 to HeLa cells to see if we could reverse the phenotype. Both models confirmed that both stathmin and p53 must be depleted for cells delay in G2 of the cell cycle and initiate apoptosis.

Experiments in chapter 3 addresses stathmin's specific role in the cell cycle delay pathway and determined if this signaling uses the microtubule network or stathmin's other binding partners, p27<sup>kip1</sup> and STAT3. We showed that there is a significant difference in the MT networks of cancer cells where stathmin was depleted when p53 was absent, when compared to the depletion of either protein alone. By destabilizing the MT network, we determined that changes to the MT cytoskeleton can bypass stathmin's role in the pathway and that MTs are therefore required for the signal to be relayed. Using truncated versions of the stathmin protein, we further confirmed that stathmin relays a cell cycle delay signal using the MTs and that p27<sup>kip1</sup> and/or STAT3 play little role, if any, in this signaling.

**Figures:**

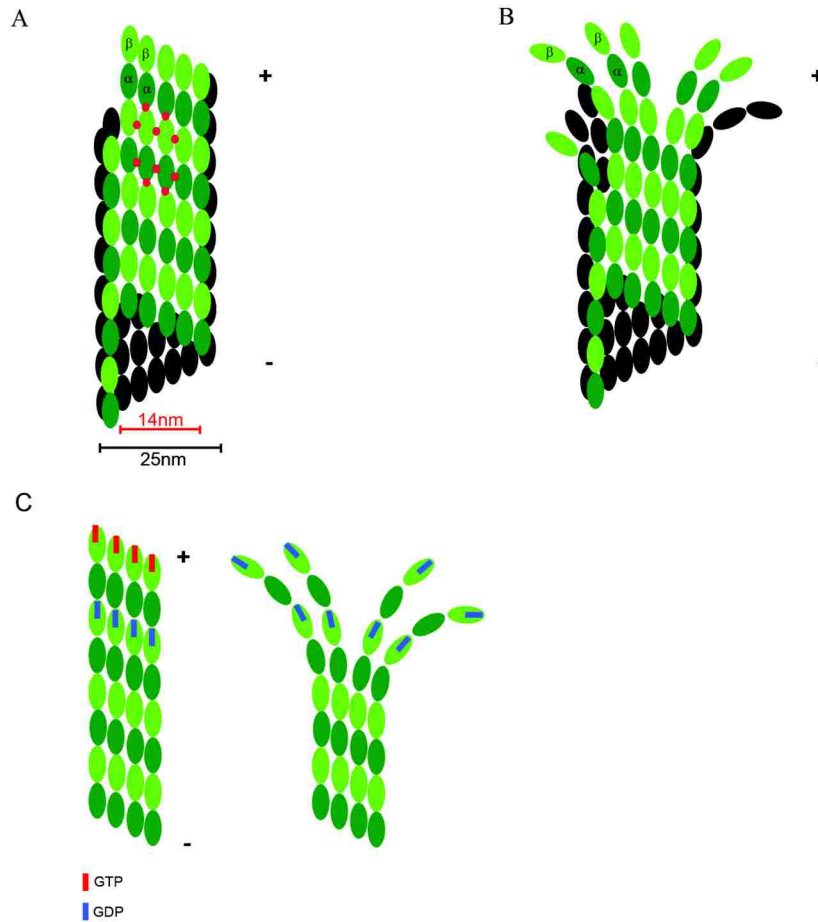


Figure 1.1: Microtubule structure. (A) A MT forms when 13 protofilaments align laterally to form a hollow tube. Red dots represent the lateral and longitudinal bonds between adjacent tubulin dimers. (B) When bonds between adjacent protofilaments are disturbed the MT frays and begins to lose stability. (C) The loss of bonds associated with a fraying MT is due to the loss of the GTP-cap that is found on the end of a growing MT. When the GTP is hydrolyzed to GDP, the MT begins to depolymerize.

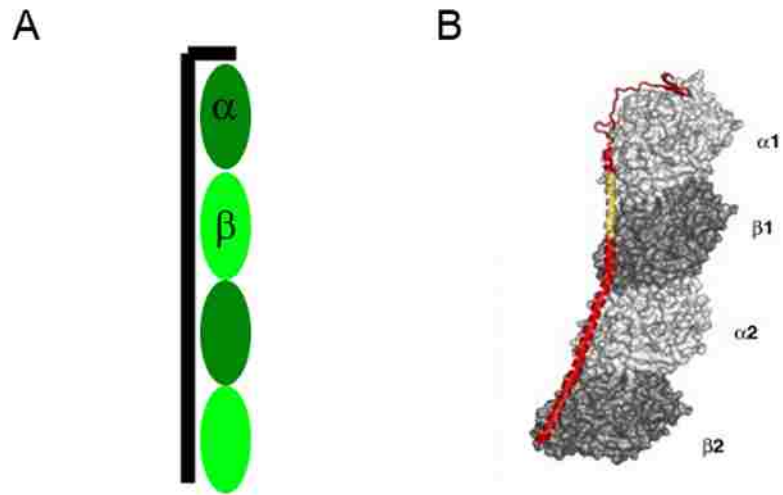


Figure 1.2: Stathmin binding tubulin. (A) A model of stathmin (black) binding to two tubulin heterodimers forming a T2S complex, thereby sequestering tubulin away from polymerizing MTs. (B) A 3.5 Å resolution X-ray crystal structure of the stathmin domain of the related protein, RB3, binding to two tubulin heterodimers (Steinmetz, 2007).

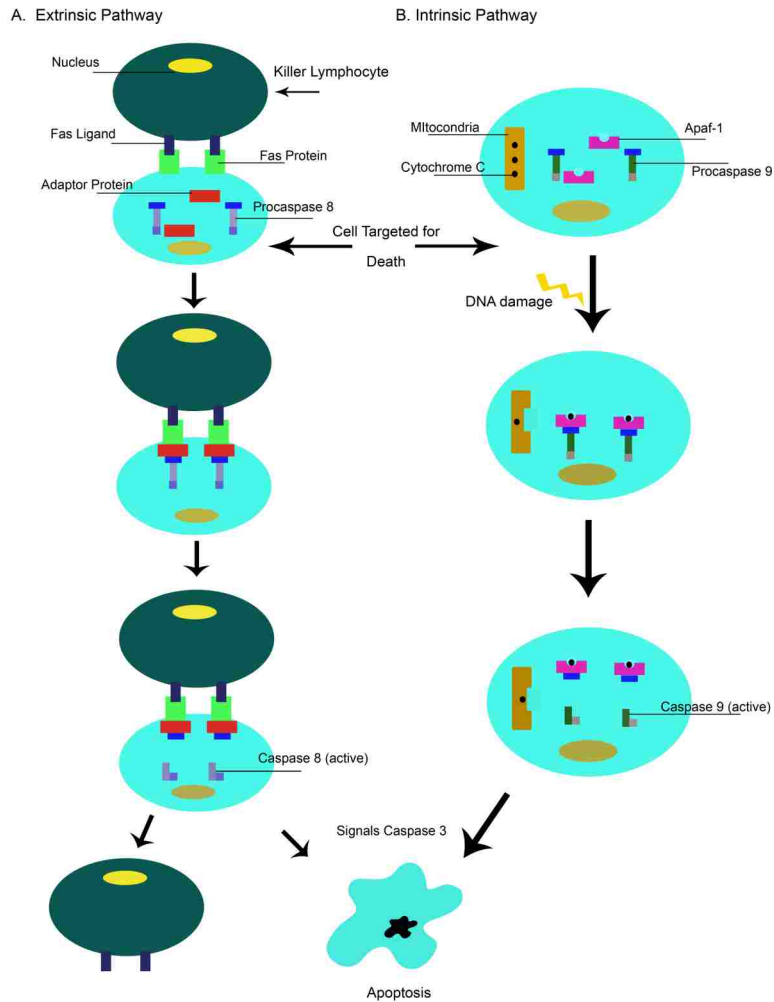


Figure 1.3: Apoptosis signaling pathway. (A) The extrinsic apoptotic pathway begins when an external source signals a cell to die. A signal enters the cell via cell-cell communication. The signal causes procaspase 8 to be cleaved to form caspase 8, which starts a signal cascade leading to apoptosis. (B) The intrinsic apoptotic pathway begins when an internal signal is detected (such as DNA damage). This signal leads the eventual disturbance of the mitochondrial inner membrane causing the release of cytochrome c. Cytochrome c forms a complex with procaspase 9 and Apaf-1, which causes the cleavage of procaspase 9 to caspase 9. Caspase 9 starts a signaling cascade leading to apoptosis.

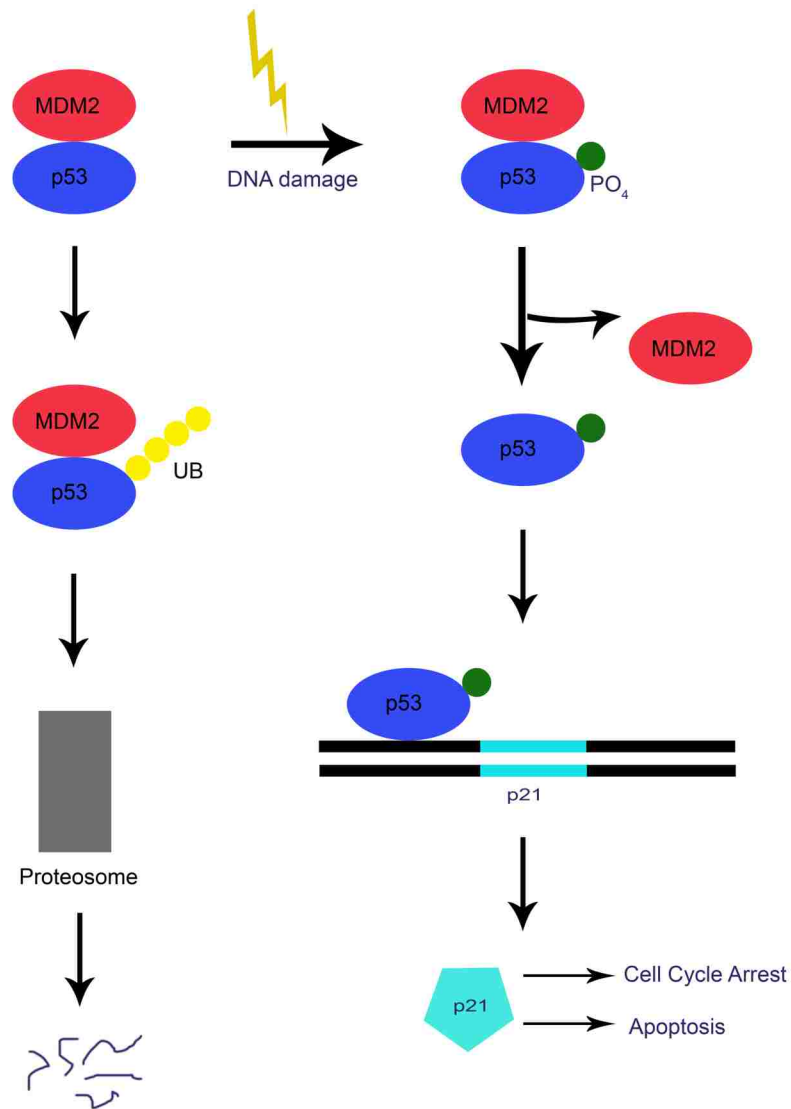


Figure 1.4: p53's role in the cell. Under normal conditions, p53 is immediately bound by MDM2 and marked for destruction by ubiquitin. This ubiquitinated protein is sent to the proteasome where it is degraded. When DNA damage occurs p53 is phosphorylated and released from mdm2. p53 then moves to the nucleus where it acts as a transcription factor for many different genes (p21 is shown as an example). These genes cause cell cycle arrest while DNA damage is repaired or can cause the cell to begin apoptosis.

## **Chapter 2**

**Stathmin/Oncoprotein 18, a microtubule regulatory protein, is required  
for survival of both normal and cancer cell lines lacking the tumor  
suppressor, p53**

## Introduction

Microtubules are dynamic polymers of  $\alpha/\beta$  tubulin dimer subunits that contribute to a number of cell processes including chromosome movement and mitosis. Several successful chemotherapies, including paclitaxel and vinblastine, are thought to act by targeting microtubules or their tubulin subunits, disrupting mitotic spindle function, activating the spindle assembly checkpoint and inducing cell death (Jordan and Kamath, 2007; Rieder and Maiato, 2004; Weaver and Cleveland, 2005). While microtubules have been a successful target for chemotherapy development (Jordan and Kamath, 2007), accessory proteins that regulate microtubule assembly and disassembly are also targets for novel chemotherapeutics (Bhat and Setaluri, 2007; Chin and Herbst, 2006). Of these regulatory proteins, stathmin/oncoprotein 18, a microtubule destabilizing protein, has received attention recently as a potential target for cancer therapy (Kouzu et al., 2006; Mistry et al., 2005; Rana et al., 2008).

Stathmin is overexpressed in many cancers including leukemia (Melhem et al., 1997), lymphoma (Nylander et al., 1995), oral squamous-cell (Kouzu et al., 2006), adenoid cystic (Nakashima et al., 2006), lung (Nishio et al., 2001), and hepatocellular carcinomas (Yuan et al., 2006), adenocarcinoma (Chen et al., 2003; Friedrich et al., 1995), prostate cancer (Mistry et al., 2005), sarcomas (Belletti et al., 2008), glioma (Ngo et al., 2007), breast cancer (Bieche et al., 1998; Brattsand, 2000), and ovarian cancer (Price et al., 2000). Cancers where stathmin is overexpressed have been shown to have a high malignancy phenotype, which leads to generally poor prognosis, supporting the use of

stathmin expression as a biomarker for cancer stage progression (Chen et al., 2003; Mistry et al., 2005).

While stathmin level may serve as a biomarker in many cancers, several studies have demonstrated that stathmin depletion may also have therapeutic value; in a number of cancer cell lines stathmin depletion results in cell cycle arrest and apoptosis. Mistry et al. (Mistry et al., 2005) found that expression of anti-stathmin ribozymes depleted stathmin and resulted in apoptosis in the androgen-independent prostate cancer cell line LNCaP. Depletion of stathmin by siRNA or shRNA in HeLa cells (Zhang et al., 2006), osteosarcoma cell lines (Wang et al., 2007) and several breast cancer cell lines (Alli et al., 2007) also demonstrated reduced cell proliferation and apoptosis after stathmin reduction. In contrast to these cancer cell lines, stathmin knockout mice are viable (Schubart et al., 1996). These results have raised interest in stathmin reduction as a potential cancer therapy, possibly active only in cancerous cells.

It is currently not known why even partial stathmin depletion is sufficient to induce apoptosis in several cancer cell lines. Most studies have indicated that stathmin depletion results in a G2/M block (Mistry et al., 2005; Wang et al., 2009; Zhang et al., 2006), but normally stathmin is inactivated by phosphorylation at entry into mitosis (Larsson et al., 1997; Larsson et al., 1995; Marklund et al., 1996) and does not have a detectable microtubule destabilizing activity during mitosis (Ringhoff and Cassimeris, 2009b). These latter data strongly suggest that stathmin depletion does not lead to apoptosis by inducing a mitotic block. An alternative mechanism was suggested by Alli et al. (Alli et

al., 2007), who noted that those cell lines requiring stathmin for survival also expressed mutant p53. This intriguing hypothesis was not tested directly because Alli et al. (Alli et al., 2007) were unable to deplete stathmin from cell lines expressing wildtype p53. Further complicating analysis, some of the breast cancer cell lines used by Alli et al. (Alli et al., 2007) have additional mutations targeting other tumor suppressor genes, including Rb and PTEN (DeGraffenried et al., 2004; Wang et al., 1993).

Here we used several experimental systems to test whether stathmin is specifically required for survival of those cells lacking p53. First, we compared cell proliferation and death after stathmin depletion from matched colon cancer cell lines (HCT116) differing in p53 genotype. As an alternate approach, we restored p53 to HeLa cells by depletion of the human papillomavirus (HPV) E6 protein, which normally binds p53 and marks it for destruction. Finally, we depleted stathmin and/or p53 from normal human foreskin fibroblasts (HFF cells) to address whether stathmin is specifically required for cancer cell survival. We found that stathmin is required for the survival of both cancerous and non-cancerous derived cell lines, but only in the absence of p53. In cells lacking both stathmin and p53, cells arrest or delay at G2 of the cell cycle.

## **Methods**

### Cell Culture:

Cells were grown at 37°C in a humidified atmosphere of 5% CO<sub>2</sub>. HCT116 and HFF cells were grown in DMEM (GIBCO) supplemented with 3.7g/L sodium bicarbonate, 1X

antibiotic/antimycotic (Sigma), 1% sodium pyruvate, and 10% fetal bovine serum (FBS) (GIBCO-Invitrogen). HeLa cells were grown in MEM (GIBCO) supplemented with 2.2g/L sodium bicarbonate, 1X antibiotic/antimycotic, and 10% FBS.

#### Drugs:

Doxorubicin was added to cells to induce DNA damage and stabilize p53, facilitating its detection by western blot. When used, doxorubicin (0.5  $\mu$ M) was added to cells for the last 24 hours of an experimental treatment. Doxorubicin was never used in experiments to measure cell proliferation or cell death. Some cells were treated with the caspase inhibitor, Z-VAD-FMK (10  $\mu$ M; Sigma-Aldrich) or DMSO as a vehicle control. Z-VAD-FMK was added to cells 24 hours prior to any other treatment and remained for the duration of the experiment.

#### RNA interference and shRNA transfections:

RNA interference (RNAi) was achieved using GeneSilencer reagents following the manufacturer's protocol. Cells were grown on 35 mm dishes for 1-2 days before the addition of siRNA. Cells were serum starved 30 minutes pre-transfection and 4 hours post-transfection to improve transfection efficiency. RNAi oligonucleotides (Dharmacon) used included: SMTN1 (Op18-443), 5'- CGUUUGCGAGAGAAGGAUAdtdt-3' (Holmfeldt et al., 2007) and HPV E6 (18E6-385), 5'- CUAACACUGGGUUAUCAAdtdt-3' (Koivusalo et al., 2005). SiGlo Risc-Free siRNA (Dharmacon) was used as a control siRNA sequence for these experiments. A stathmin shRNA plasmid and control plasmid were obtained from Superarray Bioscience

Corporation and used to confirm results from siRNA. Cells were grown similarly to those treated with RNAi except that Fugene 6 was used to transfect cells with shRNA plasmids. The shRNA (manufacturer's #4) used recognizes 607-627 of exon 4 of the stathmin gene. Some cells were also transfected with TransSilent empty vector or TransSilent p53 shRNA plasmids (Panomics;(Giono and Manfredi, 2007)) using Fugene 6 (Piehl and Cassimeris, 2003; Warren et al., 2006).

Cell growth and death measurements:

Cells were grown for 1-5 days post-transfection with siRNA or shRNA, trypsinized, stained with Trypan Blue (0.4%) and counted using a hemocytometer. Cell viability was assessed by Trypan Blue exclusion. Live and dead cells were counted, averaged and pooled for 3 separate experiments for each cell line and treatment. Data shown are means  $\pm$  standard deviations.

Groups of cells were also followed over time by plating cells on grid-etched coverslips attached to the bottoms of 35 mm dishes (MatTek Corporation). Cells were plated and incubated for 24 hrs before transfection of siRNAs. Cells were allowed to grow for an additional 24 hrs and then observed using a 20X objective on an inverted microscope (Nikon TE2000E) equipped with phase contrast optics and MetaVu image acquisition software. Ten grid squares were chosen randomly and images were acquired from these squares each day for up to 5 days. Three separate imaging time course experiments were performed and representative images are shown in Figures 2.1 and 2.3.

Statistical analysis of cell counts, including those determined after immunofluorescent staining (below), were performed using Paired t-tests in Microsoft Excel or GraphPad Software ([www.graphpad.com/quickcalcs/ttest1.cfm](http://www.graphpad.com/quickcalcs/ttest1.cfm)).

Indirect Immunofluorescence and confocal microscopy:

Cells were fixed and imaged as described previously (Piehl and Cassimeris, 2003).

Primary antibodies used were mouse monoclonal  $\alpha$ -tubulin (B512; Sigma-Aldrich), rabbit anti-TPX2 (Garrett et al., 2002) (Gift from Duane Compton, Dartmouth Medical School), rabbit anti-cyclin B<sub>1</sub> (Sigma-Aldrich), rabbit anti-phospho-CDK1 (Tyr 15) (Cell Signaling Technology) and mouse anti-cleaved PARP (ASP214) (Cell Signaling Technology). Goat anti-mouse or rabbit Alexa Fluor 488 or 563 (Invitrogen) were used as the secondary antibodies in these experiments. Confocal microscopy was used to image stained cells as described previously (Warren et al., 2006). Images were acquired using a 40X/1.3NA objective. Image stacks were converted to maximum intensity projections, exported as TIFF files and assembled using Photoshop.

Protein Isolation and Western Blotting:

Soluble cell extracts were prepared for SDS-polyacrylamide gel electrophoresis as described previously (Ringhoff and Cassimeris, 2009b). Protein concentrations were measured by Bradford assay (Bradford, 1976). Membranes were probed and imaged as previously described (Ringhoff and Cassimeris, 2009b) using primary antibodies mouse anti-p53 (Vision Bio Systems), rabbit anti-stathmin (Sigma-Aldrich), or rabbit anti-actin (Sigma-Aldrich) followed by goat anti-mouse or rabbit horseradish peroxidase-linked

IgG (Sigma-Aldrich). Protein depletions were estimated by comparison of western blot signals to those generated by serial dilution of the control-treated cell lysate.

## **Results**

### **Depletion of stathmin from HCT116 colon cancer cell lines**

To test directly whether p53 is required for survival of cells depleted of stathmin, we used HCT116 colon cancer cell lines differing in TP53 genotype. The HCT116<sup>p53<sup>-/-</sup></sup> line was developed by knocking out both copies of the TP53 gene from the parental HCT116 line (HCT116<sup>WTp53</sup>; (Bunz et al., 1998)). We first examined the extent and time course of stathmin depletion after siRNA transfection, compared to cells transfected with siGlo, a non-targeting control siRNA (Dharmacon). For HCT116<sup>p53<sup>-/-</sup></sup> cells, stathmin was depleted by approximately 75% within 24 hours after transfection and remained low for 5 days (Figure 2.1A). We found that stathmin depletion was more difficult in HCT116<sup>WTp53</sup>, consistent with a previous study of breast cancer cell lines (Alli et al., 2007). By 72 hrs after siRNA transfection, stathmin protein level was reduced by approximately 50% in HCT116<sup>WTp53</sup> (Figure 2.1B). Stathmin level often returned at later time points (not shown), but a second siRNA transfection at 72 hours kept the stathmin level low at day 5 (time after the first transfection, Figure 2.1B) and up to 7 days after the initial transfection (not shown). These results demonstrate that stathmin can be successfully knocked down in HCT116 matched cell lines.

### **Stathmin is required for cell survival in HCT116 cells lacking p53**

The HCT116 cell lines were depleted of stathmin using the conditions described above and were observed for up to five days post-siRNA transfection to observe the effect of stathmin depletion on cell proliferation and death. First, we followed living cells by imaging the same regions of coverslips over a 4 - 5 day time course. For HCT116<sup>WTp53</sup> cells, either expressing stathmin or depleted of stathmin, cell density increased over time, reaching near confluency by day 4 - 5 (Figure 2.1C). The same growth characteristics were observed for the HCT116<sup>p53<sup>-/-</sup></sup> cell line transfected with a control siRNA. In contrast, depletion of stathmin from the HCT116<sup>p53<sup>-/-</sup></sup> line significantly reduced the increase in cell number over time (Figure 2.1C).

Following living cells over time suggested that stathmin depletion slowed cell proliferation and/or led to cell death only in the HCT116<sup>p53<sup>-/-</sup></sup> cell line. To examine cell growth and death more directly, we measured both cell proliferation, by counting the number of living cells, and cell death, by counting the percentage of trypan blue positive cells over a 5 day time course. HCT116 cells expressing wildtype p53 and depleted of stathmin proliferated at a slower rate than cells transfected with a control RNA (solid lines, Figure 2.2A). Although the stathmin depleted HCT116<sup>WTp53</sup> cells grew more slowly, they remained viable, as measured by trypan blue exclusion (Figure 2.2B). Stathmin depletion from HCT116<sup>p53<sup>-/-</sup></sup> cells showed very slow proliferation over a 5 day time course (Figure 2.2A, see also Figure 2.1C) and these cells died at a much greater rate than HCT116<sup>WTp53</sup> cells depleted of stathmin, or either of the HCT116 cell lines transfected with a control RNA (Figure 2.2B). There was a high variability in the percentage of dead cells in HCT116<sup>p53<sup>-/-</sup></sup> cells depleted of stathmin, as seen by the large

standard deviations. At this time we do not know the reason for the inter-experiment variability. To confirm that the difference in means was significant, we compared the mean percentages of dead cells for control and stathmin-depleted cells within each HCT116 cell line at the 5 day time point. The difference in the mean percentage of dead cells in HCT116<sup>p53<sup>-/-</sup></sup> control and stathmin-depleted cells was highly significant ( $p < 0.001$ ), while the means were not significantly different in HCT116<sup>WTp53</sup> cells and HCT116<sup>WTp53</sup> cells depleted of stathmin. Taken together, these results provide strong evidence that stathmin is required for cell survival only in cells lacking p53, but the differences in time course of stathmin knockdown in cells differing in TP53 genotype complicates analysis.

### **Restoration of p53 in HeLa cells rescues cells from stathmin-depletion induced death**

To further test whether stathmin is required for survival of cells lacking p53, we used HeLa cells, which are wildtype for the TP53 gene, but fail to maintain p53 protein level because they stably express the human papillomavirus (HPV) E6 protein. The HPV E6 protein binds p53 and marks it for destruction (Koivusalo et al., 2005). The ability to deplete the HPV E6 protein by RNAi (Koivusalo et al., 2005) provides a mechanism to restore p53 in HeLa cells, allowing comparison of cells depleted of stathmin in the presence and absence of p53.

We first confirmed the results of Koivusalo et al (Koivusalo et al., 2005) that E6 depletion restores p53 in HeLa cells. Where noted, cells were treated with the DNA-damaging agent doxorubicin for the 24 hours prior to gel sample preparation to stabilize

p53 and enhance its detection. As shown in Figure 2.3A, HeLa cells have a very low level of p53, even after doxorubicin treatment. Depletion of E6 by siRNA results in a significant increase in p53 level, which is also detectable in cells depleted of both stathmin and E6 (Figure 2.3A).

Stathmin was also readily depleted from HeLa cells, as shown in Figure 2.3B. At 72 hours after siRNA transfection, stathmin was reduced by at least 75%, independent of whether cells were also depleted of E6 (p53 restored). Stathmin level was also reduced, although to a lesser extent, in cells depleted only of E6. In this latter case, reduced stathmin level may reflect the ability of p53 to negatively regulate stathmin expression when p53 level is transiently increased (Ahn et al., 1999; Johnsen et al., 2000).

We next examined cell density over time, similar to the experiments performed with HCT116 cell lines. Stathmin depletion from HeLa cells reduced the increase in cell number over time observed in control-siRNA treated cells (Figure 2.3C). Restoring p53 (E6 depletion), in the absence or presence of stathmin depletion, resulted in slower cell growth compared to control cells, but not nearly as significant an inhibition as that observed in stathmin depleted HeLa cells (Figure 2.3C). We then measured both cell proliferation (live cell number over time) and the percent dead cells (trypan blue positive) for these experimental conditions. Figure 2.4 shows that stathmin depletion from HeLa cells (lacking p53) resulted in both reduced cell proliferation and a large increase in the percentage of dead cells. Comparison of mean percentages of dead cells at day 5 showed that stathmin depletion significantly increased the percentage of dead cells over that

measured in control siRNA treated cells ( $p < 0.001$ ). Treatment of cells with siRNA to deplete both stathmin and HPV E6 (restoring p53) reversed the effects of stathmin depletion alone; cells showed proliferation rates and percentages of dead cells comparable to control-treated or HPV E6 siRNA-treated cells. Finally, we confirmed the siRNA results by transfecting cells with a plasmid encoding an shRNA directed against a different sequence in the stathmin mRNA (see Methods). As shown in Figure 2.4 C for cells examined 72 hours after transfection, shRNA depletion of stathmin significantly increased the percentage of dead cells, compared to cells transfected with a control plasmid. Together with the results from HCT116 cell lines, these results provide strong evidence that stathmin is required for cell survival only in the absence of p53.

In the above experiments, we used trypan blue exclusion as a simple assay to differentiate living and dead cells. It is likely that stathmin depletion results in death by apoptosis, as others have demonstrated previously (Alli et al., 2007; Mistry et al., 2005; Wang et al., 2009; Zhang et al., 2006). To confirm that cells die via apoptosis we examined whether stathmin-depletion induced cell death was inhibited by the caspase inhibitor Z-VAD-FMK. As expected, Z-VAD-FMK significantly blocked the death of HeLa cells depleted of stathmin (Figure 2.5A,B). Stathmin depleted cells treated with Z-VAD-FMK also showed cell proliferation rates intermediate between control-treated and stathmin-siRNA treated cells. In additional experiments, we found increased levels of cleaved poly-ADP ribose polymerase (PARP) in stathmin-depleted HCT116<sup>p53<sup>-/-</sup></sup> cells (Figure 2.5C,D), but not in stathmin-depleted HCT116<sup>WTp53</sup> cells. These results confirm

previous results of others (Alli et al., 2007; Mistry et al., 2005; Wang et al., 2009; Zhang et al., 2006) that stathmin depletion initiates apoptotic death in cells lacking p53.

### **Depletion of p53 and stathmin from non-cancerous cells leads to cell death**

The experiments above, along with previous results of others (Alli et al., 2007; Mistry et al., 2005; Zhang et al., 2006), demonstrated that stathmin depletion from cancer cell lines results in cell death by apoptosis. We next asked whether non-cancerous cells also require stathmin for survival using human foreskin fibroblasts (HFF) as a model non-cancerous cell line. To deplete p53 from these cells, we transfected cells with a plasmid for expression of an shRNA targeting p53 (Giono and Manfredi, 2007). A successful knockdown of both stathmin and p53 was achieved using RNAi and shRNA respectively (Figure 2.6A, B). A 50% knockdown of stathmin was seen as early as day 3 and continued to approximately 75% knockdown by day 5. By day 2, p53 showed a significant knockdown as well. Note that the only cells treated with doxorubicin were those used to prepare gel samples for p53 detection (as noted in Figure 2.6B). Depletion of stathmin or p53 alone did not inhibit cell proliferation rate and did not increase cell death compared to cells transfected with control siRNA or the empty vector used for shRNA delivery (Figure 2.6C, D). Interestingly, however, depleting both stathmin and p53 together resulted in significant cell death ( $p < 0.001$  at day 5) and a lack of cell proliferation (Figure 2.6C, D). These data demonstrate that stathmin is required for cell survival in both human cancerous and non-cancerous cell lines lacking p53.

### **Cells arrest in G2 of the Cell Cycle prior to Apoptosis**

Both the over-expression of wildtype p53 (Johnsen et al., 2000) and the absence of p53 (Sur et al., 2009) have been shown to cause cell cycle arrest, at least under some experimental conditions. To address whether stathmin depletion leads to a unique cell cycle arrest that is dependent upon p53 status, we examined cell cycle distributions in HCT116 matched cells depleted of stathmin and HeLa cells depleted of stathmin, HPV E6 (restoring p53) or both proteins. Others have previously followed DNA levels and identified a G2/M cell cycle arrest after stathmin depletion in cancer-derived cell lines (Alli et al., 2007; Mistry et al., 2005), but these studies measured DNA content and cannot differentiate between G2 and M phases. Therefore, we used an alternative protocol, by staining fixed cells with antibodies to TPX2 (present in the nuclei of S and G2 cells and bound to the mitotic spindle microtubules in M phase (Brito and Rieder, 2006)), Cyclin B (present in the cytoplasm of G2 cells and associated with the mitotic spindle until anaphase onset during M phase (Clute and Pines, 1999)), and CDK1 phosphorylated on Tyr15 (Phospho-CDK1(Y15); inhibitory phosphorylation on CDK1 present during G2 and removed at entry into mitosis (Borgne and Meijer, 1996)). Cells were co-stained with antibodies to tubulin (Figure 2.7 and 2.8), allowing visual classification of cells in M phase. Using these staining conditions and counting all cells within multiple images, we found that HCT116<sup>p53<sup>-/-</sup></sup> cells depleted of stathmin showed a significant ( $p < 0.05$ ) increase in non-mitotic cells staining positively for TPX2 (Figure 2.7A, B) or Cyclin B (Figure 2.7C, D) 48 hours post transfection. This result was most pronounced in TPX2 stained samples. The mitotic index was approximately equal among the two HCT116 lines whether stathmin was depleted or not.

We then extended these staining protocols to HeLa cells. Depletion of stathmin from HeLa cells also increased the percentage of non-mitotic TPX2 positive cells (Figure 2.8 A,B) and concomitantly significantly decreased the percentage of cells not recognized as TPX2 positive. Untreated HeLa cells, cells treated with a non-targeting siRNA or depleted of E6 to restore p53 showed a much smaller percentage of non-mitotic cells staining positive for TPX2. As a second marker for cells in G2, we also stained HeLa cells with antibodies recognizing phospho-CDK1(Y15), one of the two inhibitory phosphorylations holding CDK1 inactive until entry into M phase (Borgne and Meijer, 1996). Consistent with results from TPX2 staining, HeLa cells depleted of stathmin showed a significant increase ( $p < 0.05$ ) in non-mitotic cells stained positive for phospho-CDK1(Y15) (Figure 2.8 C,D). Cells depleted of E6 or of E6 and stathmin did not show significant changes in the percentage of non-mitotic, phospho-CDK1(Y15) positive cells. We confirmed these results by transfecting HeLa cells with a control plasmid or a plasmid expressing an shRNA directed against stathmin and again found an increase in non-mitotic phospho-CDK1(Y15) positive cells in stathmin-depleted cells (Figure 2.8E). From these data, it is evident that stathmin depletion disrupts cell cycle progression, leading to an increase in cells positive for G2 markers, but only in the absence of p53. Given that others have reported a G2/M block in stathmin depleted cells, based on analysis of DNA content, and our results indicate a G2 block, it most likely that cells are blocked or delayed in G2, prior to entry into mitosis. Depletion of either stathmin or p53 alone is not sufficient to delay progression through the cell cycle.

## Discussion

In the results presented here we demonstrated that stathmin is required for the survival of cell lines lacking p53, whether those lines are derived from cancerous or normal tissues. Stathmin depletion from HCT116<sup>p53<sup>-/-</sup></sup> and HeLa cells showed significantly reduced proliferation rates and an increased percentage of dead cells, while depletion of stathmin had little effect on the viability of HCT116<sup>WTp53</sup> cells or of HeLa cells expressing p53. These observations were not confined to cancer-derived cell lines since normal human fibroblasts (HFFs) also required stathmin for proliferation and survival, but only in the absence of p53. For both HCT116<sup>WTp53</sup> and HPV E6-depleted HeLa cells, stathmin depletion slowed cell proliferation somewhat, but did not result in cell death and did not impose a cell cycle block. Our results provide direct support for the model proposed by Alli et al. (Alli et al., 2007), demonstrating that stathmin is required for survival in cells lacking p53.

Several groups have previously reported slowing of cell proliferation and cell death after stathmin depletion, but these studies did not address a stathmin requirement for cell survival in non-cancerous cells. Zhang et al. (Zhang et al., 2006) developed a method for expression of stathmin shRNA driven by the survivin promoter, limiting shRNA expression to those cells expressing survivin. Since normal differentiated cells do not express survivin, it is unclear whether the survivin promoter would be active, and thus expressing stathmin shRNA, in the endothelial cells used as controls. Alli et al. (Alli et al., 2007) were unable to deplete stathmin from breast cancer lines expressing p53,

making it unclear whether stathmin was required for survival of these cells. Wang et al. (Wang et al., 2007) and Mistry et al. (Mistry et al., 2005) examined stathmin depletion in cancer cell lines and did not test stathmin's requirement for survival of non-cancerous cells.

Our finding that stathmin and p53 depletions from normal human fibroblasts results in significantly reduced cell proliferation and increased cell death contrasts with the reported viability of mice with both copies of the stathmin and p53 genes knocked out (Schubart et al., 1996). It is possible that these mice compensate through increased or decreased expression of other proteins allowing normal development and survival in these mice.

### **Stathmin and p53 are required for cell cycle progression**

To address why stathmin is required for cell survival only in cells lacking p53, we examined cell cycle distributions in HCT116 cell lines depleted of stathmin and in HeLa cells expressing stathmin and p53, either protein alone, or depleted of both proteins. We found that cells depleted of both stathmin and p53 show a delay in G2 (based on staining for TPX2, cyclin B, phospho-CDK1(Y15) and tubulin) while others have reported a G2/M delay in cancer cells depleted of stathmin (Alli et al., 2007; Mistry et al., 2005; Wang et al., 2009; Zhang et al., 2006). As discussed above, we think it is likely that cells depleted of stathmin and p53 are blocked in G2, prior to entry into mitosis. It is interesting that induced expression of p53 both represses stathmin expression and induces

a G2/M block (Johnsen et al., 2000). Thus, it is likely that the levels of stathmin and p53, rather than simply their presence or absence, contribute to G2/M cell cycle progression.

It is not yet clear why both stathmin and p53 are required for cell cycle progression through G2 or for entry into M phase. Stathmin is phosphorylated during mitosis, resulting in loss of its microtubule destabilizing activity (Holmfeldt et al., 2006; Larsson et al., 1997). Stathmin inactivation is required for proper assembly of the mitotic spindle (Holmfeldt et al., 2006; Larsson et al., 1997) and stathmin depletion does not impact microtubule formation in the spindle (Ringhoff and Cassimeris, 2009b). Because stathmin is normally turned off at entry into mitosis and is not required for spindle assembly, it is unlikely that stathmin depletion would prevent entry into mitosis by disrupting microtubule assembly and turnover.

Activation of p53, typically in response to DNA damage, primarily induces a G1 block, but a G2 block is also possible under some conditions (O'Connell and Cimprich, 2005). It is intriguing that many proteins functioning in the G2/M checkpoint, including p53, are associated with the centrosome (Wang et al., 2009) and we recently found that stathmin regulates microtubule nucleation from the centrosome during interphase (Ringhoff and Cassimeris, 2009b). These data suggest that depletion of both stathmin and p53 may influence either centrosome function or the function(s) of G2/M checkpoint proteins at the centrosome to cause a cell cycle delay during G2. An alternative model is also possible, where loss of p53 and stathmin impact separate pathways that together function synergistically to slow cell cycle progression.

A role for p53, or loss of p53, in regulating G2/M progression was also identified recently by comparing transcriptome differences between matched cell lines differing in p53 status, including the HCT116 colon cancer cells used here. Cells lacking p53 upregulated expression of genes functioning in G2/M and were sensitive to treatment with a Plk (polo-like kinase) inhibitor (Plk functions in G2 to M progression) (Sur et al., 2009). In terms of cell proliferation, stathmin depletion acts similarly to Plk inhibition, since each treatment slows proliferation of cells lacking p53. Stathmin is one target of Plk, but this phosphorylation inhibits stathmin's microtubule regulatory activity (Budde et al., 2001). Thus inhibiting Plk will keep stathmin in an active form, which could contribute to a G2/M block by preventing proper spindle assembly (Larsson et al., 1997; Larsson et al., 1995). It is not clear why stathmin depletion acts similarly to Plk inhibition to slow G2/M progression; possibly a balance of stathmin and p53 functions are necessary to pass through G2.

## **Conclusions**

Stathmin depletion is required for cell proliferation and survival of those cells lacking p53. Given that p53 is mutated in at least 50% of human cancers, mechanisms to specifically target these cells for death hold great promise in treatment of a wide range of cancers (Wiman, 2007). Although the cellular mechanism responsible is unknown, our data add stathmin depletion to the handful of strategies available to block proliferation of those cells lacking a functional p53. Given that nitrosoureas appear to target stathmin and

control glioma cell migration (Liang et al., 2008), these compounds may be useful agents to induce apoptosis in a mutant p53 background.

## Figures:

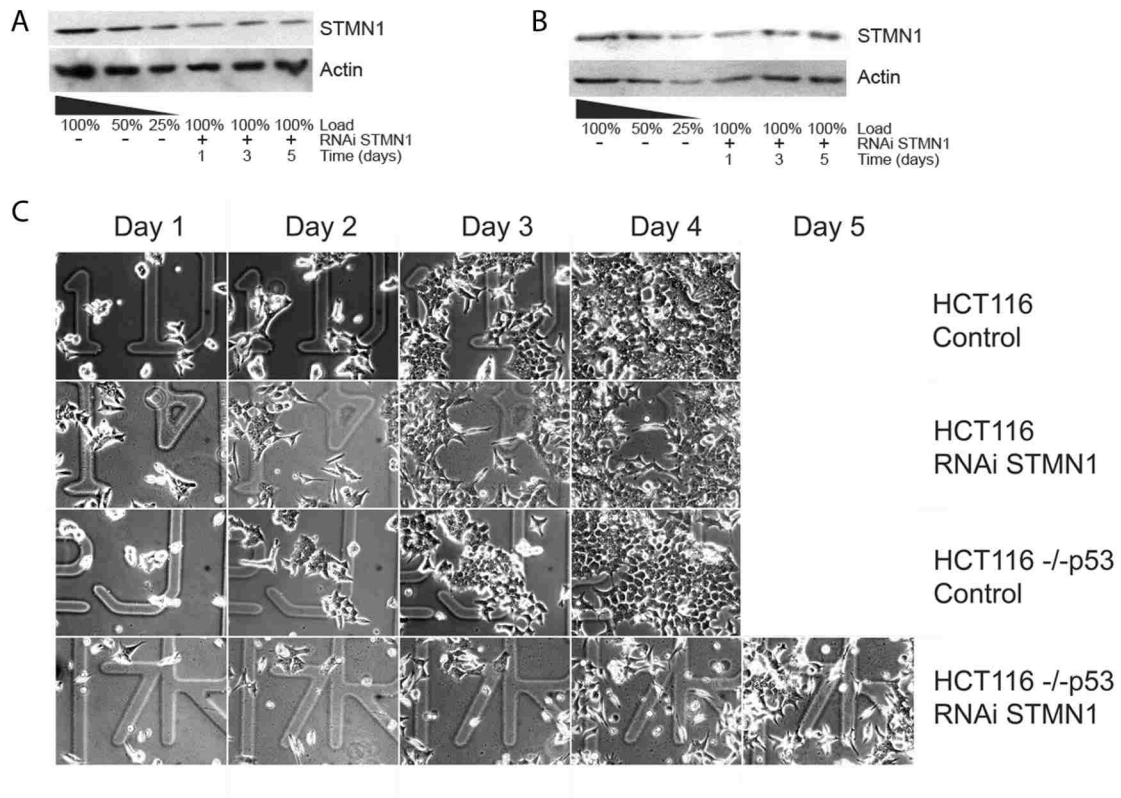


Figure 2.1: Stathmin depletion from HCT116<sup>p53WT</sup> and HCT116<sup>p53-/-</sup> cell lines. Matched lines of HCT116 cells differing in p53 genotype were treated with siRNA targeting stathmin. (A) Stathmin depletion from HCT116<sup>p53-/-</sup> cells was clearly detectable 24 hrs after transfection and stayed low for at least 5 days post transfection. (B) siRNA depletion of stathmin from HCT116<sup>WTp53</sup> cells. The sample shown at 5 days included a second siRNA transfection, 72 hrs after the initial siRNA transfection, which was necessary to keep stathmin level low. Samples at 1 and 3 days are from a single siRNA transfection. In both (A) and (B), the lysates from non-targeting siRNA treated cells were loaded in a dilution series to estimate the extent of depletion by stathmin siRNA. Blots were re-probed for actin as an indicator of equal loading between control (100% load)

and stathmin-depleted samples. (C) Low magnification phase contrast images of living cells acquired at the times given after transfection with control or stathmin siRNA. The same field is shown within an experimental condition over 4 - 5 days. HCT116<sup>p53<sup>-/-</sup></sup> cells depleted of stathmin remain relatively sparse over the time course while cells grow to near confluency in the other experimental conditions. Data shown are representative of 3 separate experiments.

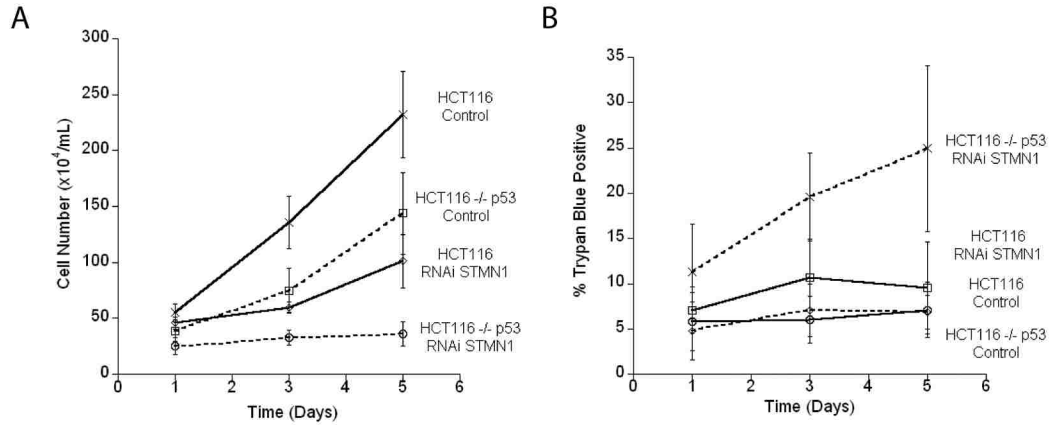


Figure 2.2: Stathmin is required for survival of HCT116<sup>p53-/-</sup> cells. HCT116 cell lines were treated with non-targeting control or stathmin RNAi. At the indicated time points, cells were trypsinized, incubated in Trypan Blue to identify dead cells, and numbers of living and dead cells counted. Cell proliferation rates (A) and the percentage of dead cells (B) represent the means of 3 independent experiments  $\pm$ SD.

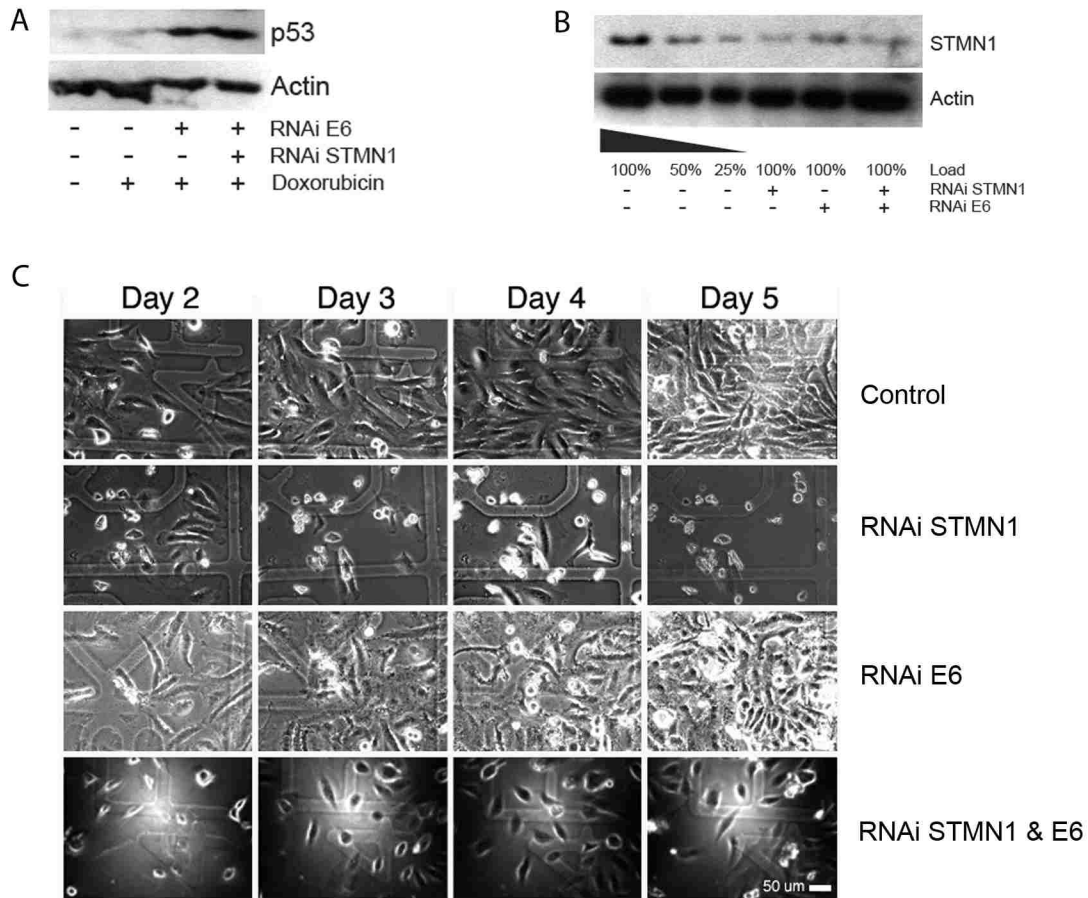


Figure 2.3: Restoring p53 in HeLa cells. (A) HeLa cells were treated with control or siRNA targeting HPV E6 for 72 hrs and exposed to 0.5  $\mu$ M doxorubicin for the final 24 hrs to induce DNA damage and stabilize p53, facilitating its detection by immunoblot. In control-treated HeLa cells, p53 is present at a very low level, even in the presence of doxorubicin. Depletion of HPV E6 restored p53. (B) HeLa cells were treated with siGlo control siRNA (or empty vector controls) or siRNAs targeting stathmin, HPV E6 or both mRNAs. Anti-stathmin immunoblot of cell lysates were collected 72 hrs after siRNA transfection. Stathmin was depleted by at least 75% after treatment with siRNA targeting stathmin or stathmin and HPV E6. Depletion of HPV E6 also caused a reduction in

stathmin level, possibly by p53-mediated repression of stathmin expression (Ahn et al., 1999; Johnsen et al., 2000). For both A and B, blots were re-probed for actin as a marker of equal loading between control (100%) and siRNA samples. (C) Low magnification phase contrast images of living cells acquired at the times given after transfection with control or siRNAs targeting stathmin, HPV E6 or both mRNAs. The same field is shown for each experimental condition over 4 - 5 days. HeLa cells depleted of E6 or stathmin and E6 grow slightly slower than control siRNA treated cells, while stathmin depleted cells show minimal growth. Data shown are representative of 3 separate experiments.

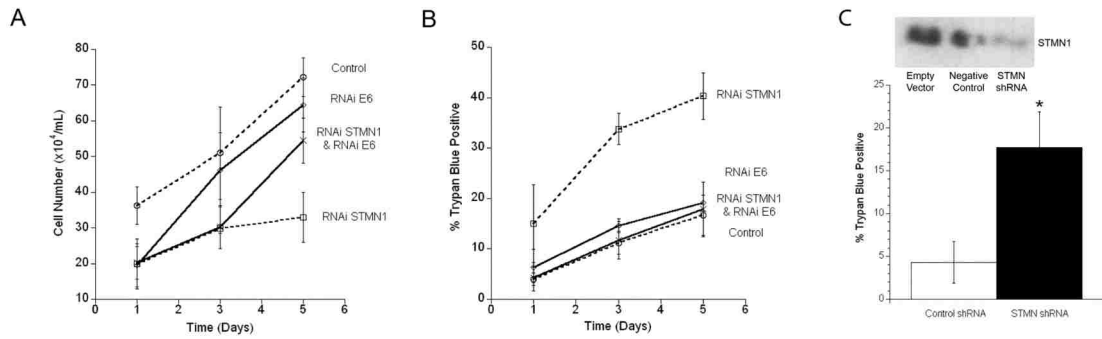


Figure 2.4: Restoring p53 rescues HeLa cells from stathmin-depletion induced death. Cell proliferation rates and the percentage of dead cells were measured as described in Figure 2.2. (A,B) Stathmin depletion slows cell proliferation and increases the percentage of dead (trypan blue positive) cells. Depletion of HPV E6 (restoring p53) alone or in combination with stathmin depletion does not lead to significant cell death. (C) Transfection of cells with an shRNA targeting stathmin resulted in stathmin depletion (top) and a significant increase in the percentage of dead cells at 72 hours post-transfection. Controls were transfected with the negative control plasmid provided by the manufacturer. \* denotes  $p < 0.05$ . All data represent the means of 3 independent experiments  $\pm$ SD.

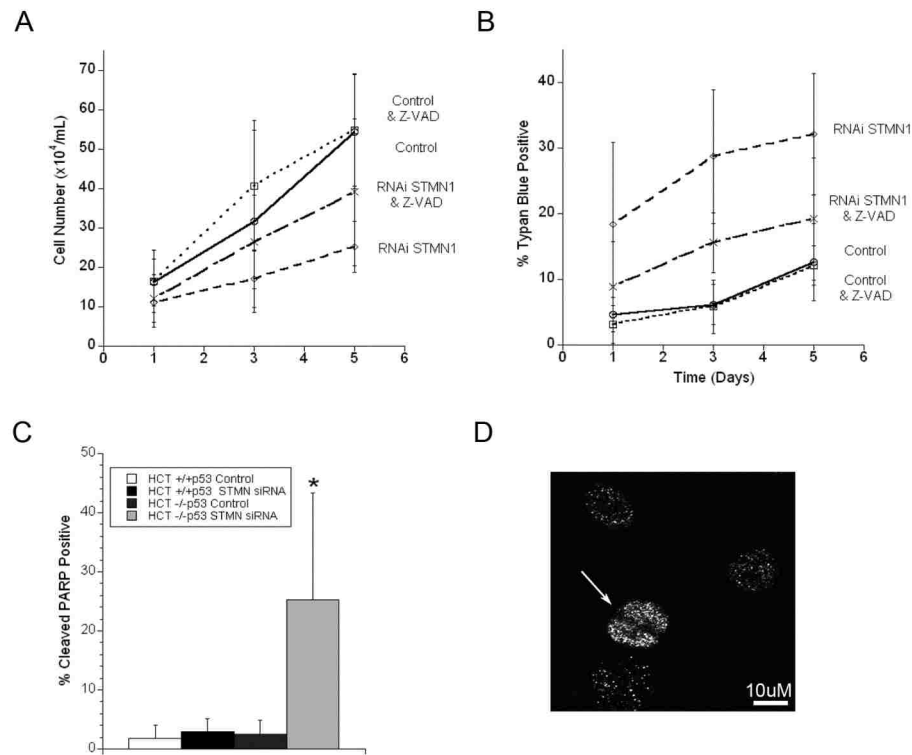


Figure 2.5: Stathmin-depletion induced cell death likely occurs via apoptosis. (A) The caspase inhibitor Z-VAD-FMK blocks stathmin-depletion induced cell death in HeLa cells. HeLa cells were treated with 10  $\mu$ m Z-VAD-FMK for 24 hrs prior to transfection with either siGlo control siRNA (or empty vector controls) or RNAi against stathmin. Plots of cell proliferation rates (A) and the percentage of dead cells (B) represent the means of three independent experiments  $\pm$ SD. (C) HCT116 matched cell lines were transfected with control or stathmin RNAi, fixed 72 hrs later and stained for cleaved PARP. The percentage of cells positive for cleaved PARP are plotted. Only HCT116<sup>p53-/-</sup> cells depleted of stathmin show a significant increase in cells positive for cleaved PARP. Data shown are the means  $\pm$  SD of 3 independent experiments and a total of  $\sim$ 200 cells

per treatment. (D) Representative image from HCT116<sup>p53<sup>-/-</sup></sup> cells depleted of stathmin and staining positive for cleaved PARP in the nucleus (arrow). Several weakly stained cells (counted as negative) are also included. Scale bar = 10  $\mu$ m.

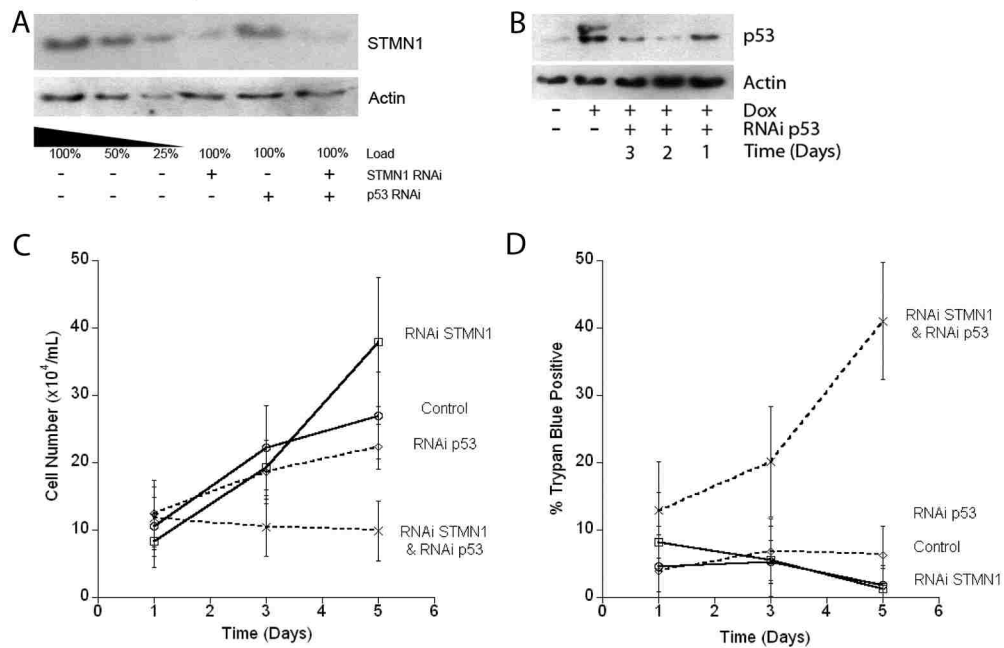


Figure 2.6: Depleting both p53 and stathmin from normal human fibroblast (HFFs) cells leads to cell death. HFF cells were transfected with TransSilent empty vector, p53 shRNA plasmid and/or siRNA targeting stathmin as indicated. (A) Anti-stathmin immunoblot from cell lysates were isolated 3 days after transfection. A knockdown of >75% was observed for both stathmin siRNA alone or when used in combination with shRNA against p53. (B) Anti-p53 immunoblot from cell lysates isolated at the times indicated. When present, doxorubicin was included for the final 24 hrs of incubation. The level of p53 is detectably reduced 1 day after shRNA transfection, but is more significantly depleted by 2-3 days after transfection. (C,D) Plots of HFF cell proliferation rates (C) and the percentage of dead cells (D) represent the means of 3 independent experiments  $\pm$ SD.

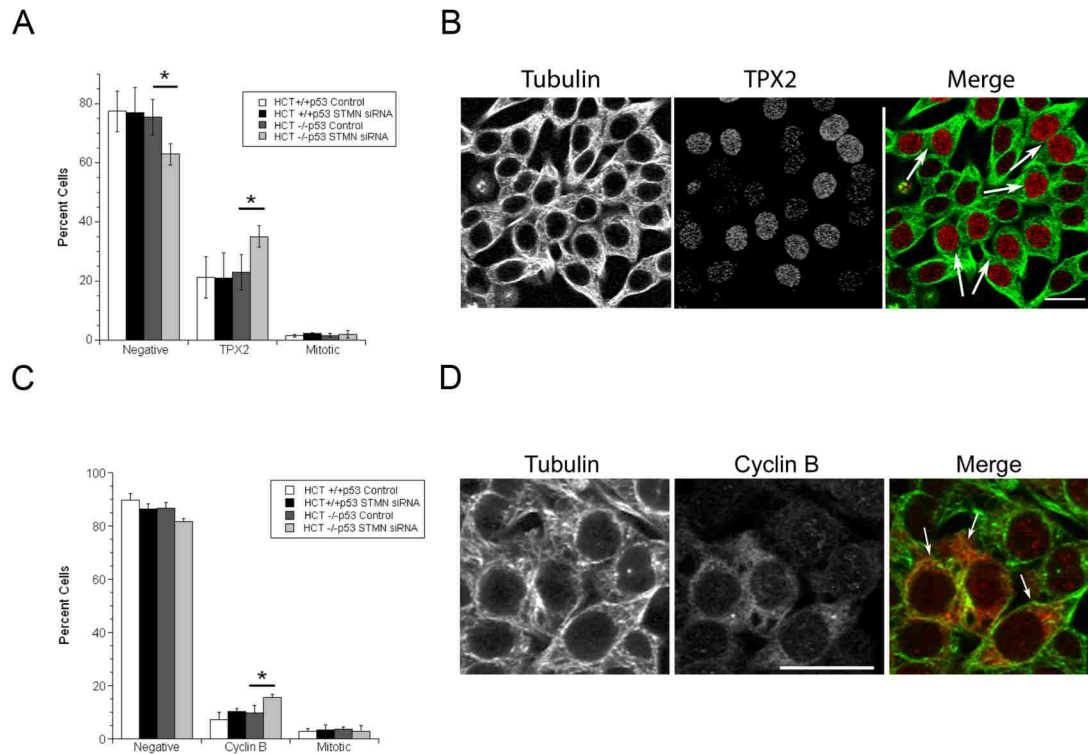


Figure 2.7: Stathmin depletion from HCT116<sup>p53-/-</sup> cells delays G2 of the cell cycle. Matched HCT116 cell lines were treated with either siGlo control siRNA or siRNA targeting stathmin mRNAs. (A, B) HCT116 cells were fixed 48 hrs after siRNA transfection and stained with antibodies against  $\alpha$ -tubulin (green in merged images) and TPX2 (red in merged images). TPX2 is present in S/G2 and M phases of the cell cycle (Brito and Rieder, 2006). The numbers of TPX2 positive, negative and mitotic cells were counted, and the percentage of cells in each group are shown in A. Images shown in (B) are from a representative field of cells transfected with stathmin siRNA. Negative cells were identified by their array of interphase microtubules and their lack of TPX2 staining. Cells in interphase staining positively for TPX2 were scored as positive. Mitotic cells

were identified by the presence of a mitotic spindle (tubulin staining). Scale bar = 25  $\mu$ m. (C,D) HCT116 cell lines were fixed 48 hrs after siRNA transfections and stained with antibodies against  $\alpha$ -tubulin (green in merged images) and cyclin B (red in merged images). Cytoplasmic cyclin B is a marker of G2 cells (Clute and Pines, 1999). The percentage of non-mitotic cyclin B positive and negative cells are shown in (C). Images shown in (D) are from representative cells fixed 48 hrs after stathmin siRNA transfection. Scale bar = 25  $\mu$ m. The data represent the means of 3 (C) or 4 (A) independent experiments, each including  $\sim$ 1000 cells  $\pm$ SD for each treatment group. \* denotes  $p < 0.05$ .

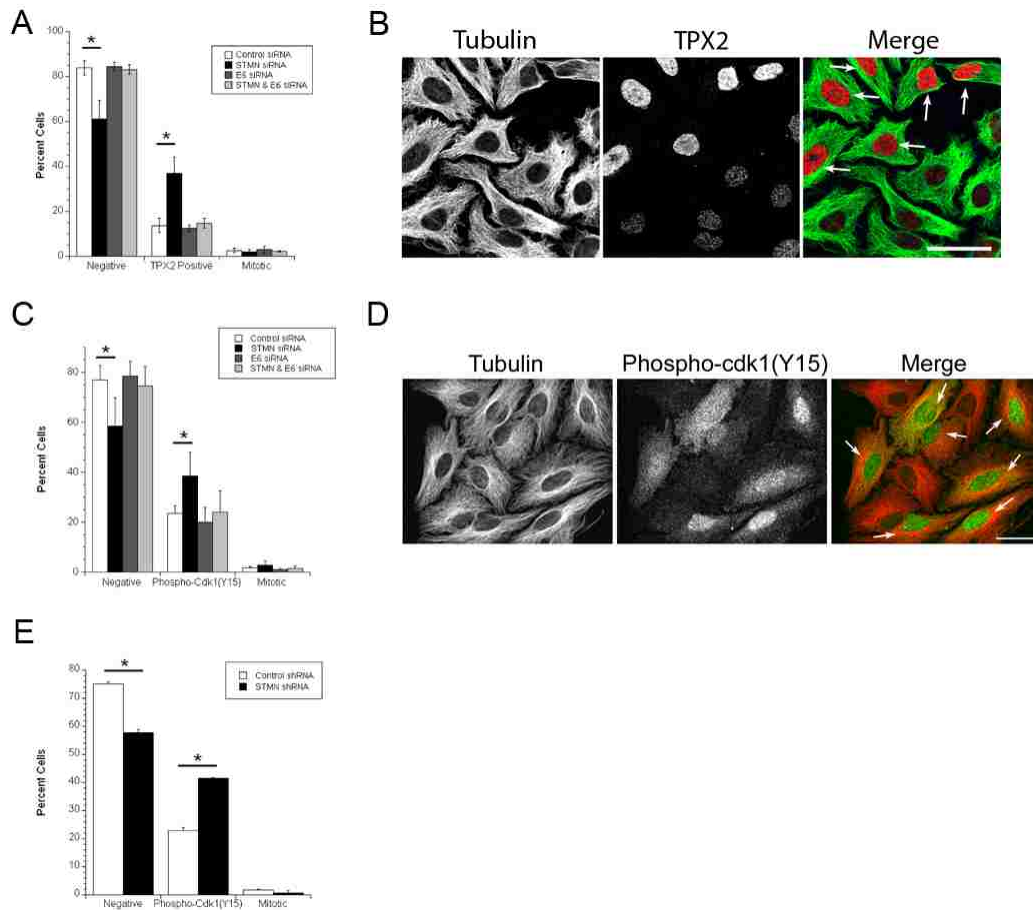


Figure 2.8: Stathmin depletion from HeLa cells delays G2 of the cell cycle. HeLa cells were transfected with either siGlo control siRNA or siRNA targeting stathmin, HPV E6 or both mRNAs. (A, B) HeLa cells were fixed and stained with antibodies against  $\alpha$ -tubulin (green in merged images) and TPX2 (red in merged images). Cells were then counted as described in Figure 2.7A, and the percent cells in each group are shown in Figure 2.8A. Images shown (B) are from representative cells fixed 48 hrs after siRNA transfections. Arrows in the merged image denote several TPX2 positive cells. Scale bar = 50  $\mu$ m. (C,D) HeLa cells were fixed and stained with antibodies against  $\alpha$ -tubulin (red

in merged images) and phospho-CDK1(Y15) (green in merged images; this inhibitory phosphorylation must be removed for entry into M phase). The percentage of non-mitotic cells staining positive for phospho-CDK1(Y15) is shown in (C). Representative images from phospho-CDK1(Y15) stained cells are shown in (D). Arrows in the merged image denote phospho-CDK1(Y15) positive cells. Scale bar = 50  $\mu$ m. (E) Depletion of stathmin by shRNA also increased the percentage of phospho-CDK1(Y15) positive non-mitotic cells at 48 hours after transfection. Each plot represents the mean of 3 independent experiments  $\pm$  SD including  $\sim$  1000 cells per treatment. \* denotes  $p < 0.05$ .

## **Chapter 3**

### **Increasing Stable Microtubules Leads to G2 Delay in Human Cell Lines**

#### **Lacking p53**

## **Introduction:**

Stathmin/Oncoprotein 18 is a microtubule (MT) destabilizing protein that is highly over-expressed in many cancers (Belletti et al., 2008; Bieche et al., 1998; Brattsand, 2000; Chen et al., 2003; Friedrich et al., 1995; Kouzu et al., 2006; Melhem et al., 1997; Nakashima et al., 2006; Ngo et al., 2007; Nishio et al., 2001; Nylander et al., 1995; Price et al., 2000; Yuan et al., 2006). We and others have recently shown that depleting stathmin in certain cancer cells leads to apoptosis (Alli et al., 2007; Carney and Cassimeris, 2010; Mistry et al., 2005; Wang et al., 2009; Zhang et al., 2006). While our results confirmed previous observations, we also showed that only when depleting both stathmin and p53, a tumor suppressor protein, do cells delay in G2 of the cell cycle and activate apoptosis. What is unknown, however, is whether it is the absence of stathmin's MT destabilizing activity that is causing the cells to delay during G2 and die, or whether it is the changes in stathmin's affects on its other known binding partners that are causing these detrimental phenotypes. Stathmin is best known as a MT destabilizer, but two other binding partners, the transcription factor STAT3 and the cyclin-dependent kinase inhibitor p27<sup>Kip1</sup>, could also be responsible for relaying signals downstream of stathmin depletion.

Because stathmin is a MT destabilizer, its reduction increases MT polymer (Holmfeldt et al., 2006; Howell et al., 1999a; Ringhoff and Cassimeris, 2009b; Sellin et al., 2008), inhibits MT dynamic turnover (Howell et al., 1999a; Howell et al., 1999b; Ringhoff and Cassimeris, 2009b), and increases MT nucleation from centrosomes (Ringhoff and

Cassimeris, 2009b). P53 also contributes to MT dynamics, although reduced p53 level has a relatively minor impact on MT dynamic turnover (Galmarini et al., 2003). To date, the effect of stathmin depletion on MT stability has only been measured in cells expressing p53 (Belletti et al.; Holmfeldt et al., 2007; Ringhoff and Cassimeris, 2009b) and it is not known whether reducing both stathmin and p53 levels will synergize to provide a more robust stabilization of the MT cytoskeleton. If MT stability acts downstream of stathmin depletion to slow G2 progression and induce apoptosis, then MT stability must be greatest when stathmin is depleted from cells expressing very low levels of p53.

Whether MT stability regulates cell cycle progression outside of M phase is controversial. Some have previously suggested that the MT cytoskeleton is necessary for interphase cell cycle progression, particularly G2 progression (Balestra and Jimenez, 2008; Blajeski et al., 2002; Rieder and Cole, 2000), but Uetake and Sluder (Uetake and Sluder, 2007) have argued that an interphase MT integrity checkpoint does not exist; rather it is the length of the previous mitosis that matters. It is possible that a MT-dependent interphase checkpoint is much more robust and detectable only in synergy with another factor, such as loss of p53. Alternatively, it is possible that stathmin level controls more than MT stability as discussed next.

Although stathmin's interactions with tubulin and MTs are well known, they are not the only proteins known to interact with stathmin. P27<sup>Kip1</sup>, a CDK inhibitor (Baldassarre et al., 2005), and STAT3, a transcription factor (Ng et al., 2006), have also been shown to

bind to stathmin's C terminal 50 amino acids (Baldassarre et al., 2005; Ng et al., 2006). Binding of STAT3 to stathmin has been shown to block stathmin's MT destabilizing activity (Ng et al., 2006). Stathmin depletion does not activate STAT3 (Ng et al., 2006) making it unlikely that stathmin depletion signals a cell cycle delay via STAT3 activation. The CKI, p27<sup>kip1</sup> also binds stathmin's C terminus and inhibits its MT destabilizing activity. p27<sup>kip1</sup> has recently been shown to cause a G2 delay in addition to its known function in G1 (Stacey, 2010). But, whether stathmin depletion could free cytoplasmic p27<sup>kip1</sup>, allowing it to enter the nucleus and inhibit cell cycle progression in G2 has not been tested, but such a scenario could generate the observed cell cycle delay.

Here we examine whether stathmin depletion relays a cell cycle inhibitory signal through stabilization of interphase MTs or through its other binding partners p27<sup>kip1</sup> and STAT3. We show that stathmin depletion induces greater MT stability in combination with negligible p53 levels. Additionally, MT depolymerization by incubation in nocodazole is sufficient to abrogate the G2 delay and push cells into mitosis. Finally, we show over-expression of either GFP-tagged full-length stathmin or stathmin  $\Delta$ 101-149 is sufficient to relieve the cell cycle delay. Each of these constructs is active as a MT destabilizer. In contrast, signaling via STAT3 or p27<sup>kip1</sup> would be reversed by expression of stathmin  $\Delta$ 5-25, and this was not observed. These results indicate that MT stability relays signals that can delay the cell cycle in G2.

## **Methods:**

#### Cell Culture:

Cells were grown at 37°C in a humidified atmosphere of 5% CO<sub>2</sub>. HeLa cells were grown in either MEM (GIBCO) supplemented with 2.2g/L sodium bicarbonate, 1X antibiotic/antimycotic (Sigma), and 10% fetal bovine serum (FBS) (GIBCO-Invitrogen), or DMEM (Sigma) supplemented with 1X antibiotic/antimycotic, 1% L-Glutamine (Sigma), and 10% FBS. HCT116<sup>p53<sup>-/-</sup></sup> cells were grown in the same DMEM as HeLa cells.

#### RNA Interference and Transient Transfection:

RNA interference (RNAi) was achieved using GeneSilencer reagents following the manufacturer's protocol. Cells were grown on 35 mm dishes for 1-2 days before the addition of siRNA. Cells were serum starved 30 minutes pre-transfection and 4 hours post-transfection to improve transfection efficiency. RNAi oligonucleotides (Dharmacon) used included: SMTN1 (Op18-443), 5'- CGUUUGCGAGAGAAGGAUAdtdt-3', (Holmfeldt et al., 2007) STMN1-5'-UTR (only when specified, removes only endogenous stathmin mRNA): 5'- CCCAGUUGAUUGUGCAGAAUU-3' and HPV E6 (18E6-385), 5'-CUAACACUGGGUUAUACAAAdtdt-3' (restores p53 by depleting the HPV E6 protein) (Koivusalo et al., 2005). SiGlo Risc-Free siRNA (Dharmacon) was used as a control siRNA sequence for these experiments.

For plasmid transfection, cells were grown similarly to those treated with RNAi except that Fugene 6 (Piehl and Cassimeris, 2003; Warren et al., 2006) or X-tremeGene HP was used to transfect cells with plasmids. Cells were transfected with EB1-GFP (Piehl and

Cassimeris, 2003) and stathmin-GFP (Ringhoff and Cassimeris, 2009b) as previously described (Piehl and Cassimeris, 2003) as well as with two new stathmin truncations (see next section).

#### DNA Constructs of Truncated Stathmin:

Stathmin truncations lacking either the N-terminus ( $\Delta$ 5-25) or the C-terminus ( $\Delta$ 101-149) were constructed using the pEGFP-N1 expression vector. Full-length stathmin-GFP (Ringhoff and Cassimeris, 2009b) was modified using PCR primers to remove the desired regions. Stathmin  $\Delta$ 5-25 was made in a two-step PCR reaction where the extreme N-terminal region (1-5) and the 25-149 region were amplified separately and then combined in the second reaction (using overhangs designed into the primers) to make a full length product where the 5-25 region was removed. In the first reaction, the primers used were: F1 (see below) and R2 to make the N-terminal region and F3 and R4 to make the 25-149 region. In the second reaction, the products from the previous reactions were combined with primers F1 and R4 to make the full-length truncated stathmin product. Stathmin  $\Delta$ 101-149 was made using a single PCR reaction using primers F1 and R5 to remove the C-terminus. Both of these products were then digested using BamHI and HindIII and ligated into the pEGFP-N1 expression vector. These new constructs were then verified using restriction digestions and sequencing.

#### Primers:

F1: 5'-GATCCCAAGCTTATGGCTTCT-3'

R2: 5'-TTCTTTTGACCGAGGATCAGAAGAAGCCAT-3'

F3: 5'-ATGGCTTCTTCTGATCCTCGGTCAAAGAA-3'

R4: 5'-TCCGGTGGATCCAAGTCAGCTTCAGTCTCGTC-3'

R5: 5'-TCCGGTGGATCCAATTTCTTCTTGCCATTTT-3'

Indirect immunofluorescence and confocal microscopy:

Cells were fixed, stained and imaged as described previously (Carney and Cassimeris, 2010; Piehl and Cassimeris, 2003; Ringhoff and Cassimeris, 2009b). Primary antibodies used were mouse anti-acetylated-tubulin (Clone 6-11B-1; Sigma-Aldrich), rabbit anti-TPX2 (Garrett et al., 2002) (Gift from Duane Compton, Dartmouth Medical School), rabbit anti-phospho-CDK1 (Tyr 15) (Cell Signaling Technology), and rabbit anti-p27 Kip1 (D69C12; Cell signaling Technology. Goat anti-mouse or rabbit Alexa Fluor 488 or 563 (Invitrogen) were used as the secondary antibodies in these experiments. Confocal microscopy was used to image stained cells as described previously (Carney and Cassimeris, 2010; Warren et al., 2006). Images were acquired using a 40X/1.3NA objective. Image stacks were converted to maximum intensity projections, exported as TIFF files and assembled using Photoshop. For all cell cycle markers, we counted interphase cells as stained or unstained, and did not count mitotic cells on most experiments.

Relative intensity was measured using MetaMorph software (Universal Imaging, Downington, PA). Cells were fixed and stained for  $\alpha$ -tubulin. Images were taken of microtubules at the cell periphery and then compared between the treatments.

#### Live Cell Imaging of EB1-GFP:

Confocal microscopy was used to image live cells as described previously (Warren et al., 2006). Using EB1-GFP (Piehl and Cassimeris, 2003; Warren et al., 2006) to measure nucleation rates, images were taken every 2 seconds for up to 2 minutes. EB1-GFP comets were counted as they emerged from the centrosome and used as a measure of nucleation rate.

#### Protein Isolation and Western Blotting:

Soluble cell extracts were prepared for SDS-polyacrylamide gel electrophoresis as described previously (Carney and Cassimeris, 2010). Protein concentrations were measured by Bradford assay (Bradford, 1976). Membranes were probed and imaged as previously described (Carney and Cassimeris, 2010) using primary antibodies rabbit anti-stathmin (Sigma-Aldrich or Cell Signaling Technology), mouse anti-acetylated-tubulin (Clone 6-11B-1; Sigma-Aldrich), or goat anti-GAPDH (Abcam) followed by goat anti-mouse or rabbit horseradish peroxidase-linked IgG (Sigma-Aldrich) or rabbit anti-goat IgG HRP (Abcam).

#### Statistics:

Statistical analysis of cell counts and intensity readings, including those determined after immunofluorescent staining (above), were performed using unpaired t-tests in Microsoft Excel or GraphPad Software ([www.graphpad.com/quickcalcs/ttest1.cfm](http://www.graphpad.com/quickcalcs/ttest1.cfm)).

## **Results:**

### **Microtubule stability and nucleation increase following stathmin depletion only when p53 is lacking.**

Stathmin depletion from cells lacking p53 results in a G2 cell cycle delay (Carney and Cassimeris, 2010; Caruso, V. and Cassimeris, unpublished), and restoring p53 is sufficient to abrogate this delay (Carney and Cassimeris, 2010). If stathmin depletion is relaying a signal via increased MT stability, we predict that interphase MT stability will be greatest when both stathmin and p53 are reduced. We tested this prediction using HeLa cells because we previously demonstrated that we could lower stathmin by siRNA and restore p53 by depleting the HPV E6 protein, which normally targets p53 for destruction in these cells (Carney and Cassimeris, 2010). We examined two characteristics of MTs that are known to change when stathmin is depleted: the levels of acetylated  $\alpha$ -tubulin, which serves as a marker of stable MTs (Belletti et al., 2008; Cambray-Deakin and Burgoyne, 1987; Perdiz et al.; Schulze et al., 1987), and centrosomal MT nucleation rate, which is dependent on stathmin level (Ringhoff and Cassimeris, 2009b).

In order to look for a change in the amount of stable MTs, we used the presence of acetylated tubulin as a marker. HeLa cells were depleted of either stathmin, HPV E6 (restoring p53), or both stathmin and HPV E6 and then allowed to grow for 72 hours post transfection (Carney and Cassimeris, 2010). Western blotting showed a significant rise in acetylated tubulin when stathmin is depleted alone, but not when p53 is restored (Figure

3.1A). When both stathmin and E6 are depleted, no significant change in acetylated tubulin level is observed (Figure 3.1A). Using confocal microscopy, we observe the same effect (Figure 3.1B). Only when stathmin is depleted from cells lacking p53 does the presence of acetylated tubulin increase. Restoring p53 reverses the effect of stathmin depletion on acetylated tubulin. We also observed an increase in the presence of acetylated tubulin in HCT116<sup>p53<sup>-/-</sup></sup> cells when stathmin was depleted; while HCT116 cells depleted of stathmin showed no change compared to control treated cells (Figure 3.8).

Experiments in mouse embryo fibroblasts derived from wild-type and stathmin knockout mice showed that stathmin knockout significantly increased the rate of MT nucleation from centrosomes with less dramatic effects on MT dynamic instability (Ringhoff and Cassimeris, 2009b). Therefore, we used MT nucleation as a measure of MT stability in HeLa cells depleted of stathmin to determine if there was a change in MT dynamics. To measure centrosomal MT nucleation rate we observed live cells expressing EB1-GFP (Piehl et al., 2004). Cells were depleted of stathmin, HPV E6, or both proteins and then allowed to grow for 24 hours. EB1-GFP plasmid was then transfected into the cells, which then continued to grow for an additional 48 hours. Using live cell imaging, MT nucleation rate was determined by observing the number of EB1 comets emerging from the centrosome per minute. Depletion of stathmin increased nucleation rate significantly compared to siGlo treated controls, while restoring p53 had no effect on MT nucleation rate compared to control levels (Figure 3.1C). Depletion of both stathmin and HPV E6 (restoring p53) caused nucleation rate to return to control levels. Taken together, these

data provide strong evidence that there is indeed an increase in MT stability when stathmin is depleted, but only in combination with negligible levels of p53.

**Removing MTs with nocodazole allows p53 null cells to escape the G2 block induced by stathmin depletion.**

The results shown above demonstrated that MT stability is increased significantly when both stathmin and p53 levels are very low, but do not address whether stathmin depletion induces a G2 delay via increased MT stability. To establish whether MT stability is necessary for the G2 delay in stathmin-depleted cells, we asked whether nocodazole-induced MT depolymerization could eliminate the cell cycle delay. Cells were grown for 40-48 hours post transfection with siRNA directed against stathmin and then incubated in 33 $\mu$ M nocodazole for 3 - 5 hours prior to fixation. After 3 - 5 hours of exposure to nocodazole, the MT network was depolymerized to near completion (Figure 3.9). Cells were also stained with several markers to identify cells in G2. Although MTs were no longer present, interphase and mitotic cells were still easily differentiated by cell morphology (not shown).

Consistent with our previous results (Carney and Cassimeris, 2010), HeLa cells depleted of stathmin showed about a 2 fold increase in the percent of interphase cells staining positively for TPX2, a protein expressed in the nucleus in late S and G2 (Brito and Rieder, 2006), when compared to control treated cells (Figure 3.2A). The percent of TPX2 positive cells returned to control levels when cells were also treated with nocodazole (Figure 3.2A). Using phospho-CDK1(Y15) (Borgne and Meijer, 1996), as a

second marker of G2 cells, we saw a similar effect, where nocodazole treatment reduced the percent of stathmin-depleted cells staining positive for this marker (Figure 3.2B). Although the percent of positively stained cells was not statistically significant between stathmin depleted cells treated with nocodazole or not, the results showed the same pattern as TPX2 localizations, where nocodazole reduces the percent of cells in G2. Cells that normally delay in G2 following stathmin depletion should proceed into mitosis after MT disruption by the addition of nocodazole. The previous counts considered only interphase cells. Therefore, we also measured the mitotic index and found as expected, nocodazole treatment also increased the mitotic index (Figure 3.10).

We repeated this experimental protocol, using HCT116<sup>p53-/-</sup> cells, as a second model system in which to test whether the removal of MTs was sufficient to bypass a stathmin-depletion induced G2 delay. Using TPX2 as a marker and following the same procedure as above, we saw a statistically significant increase in the percent of TPX2 positive interphase cells after stathmin depletion. This is consistent with our previous results using this marker in HCT116<sup>p53-/-</sup> cells (Carney and Cassimeris, 2010). Following the addition of nocodazole, stathmin depleted cells staining positive for TPX2 returned to a percentage of the total interphase population equivalent to controls (Figure 3.2C). Taken together, these data demonstrate that MT depolymerization is sufficient to abrogate a G2 cell cycle delay caused by stathmin depletion.

**Over-expression of truncated stathmin proteins, after the depletion of endogenous stathmin, can change whether the cells delay in G2 of the cell cycle.**

The above results support a model where increased MT stability relays a signal that delays cell cycle progression during G2. To confirm this conclusion, and to test whether either STAT3 or p27<sup>Kip1</sup> could contribute to signals generated by stathmin depletion, we examined whether expression of stathmin, or stathmin truncations, could alleviate the G2 delay. Plasmids for expression of GFP-tagged stathmin truncations were designed to delete either the N- ( $\Delta$ 5-25) or C- ( $\Delta$ 101-149) terminus (Figure 3.3A). The  $\Delta$ 5-25 truncation should not depolymerize MTs (Larsson et al., 1999), but should bind both STAT3 and p27<sup>Kip1</sup> (Baldassarre et al., 2005; Ng et al., 2006). The  $\Delta$ 101-149 truncation should depolymerize MTs (Larsson et al., 1999) but lacks the region necessary to bind STAT3 or p27<sup>Kip1</sup>. Truncations were expressed in cells and each was expressed at the correct molecular weight for a fusion protein with GFP (Figure 3.3B).

The microtubule cytoskeleton was then examined in cells over-expressing these truncations as well as full-length stathmin fused to GFP. Over-expression of either full length-stathmin or stathmin  $\Delta$ 101-149 caused a decrease in the MTs and this was most easily seen at the cell periphery. Image intensity measurements confirmed the decrease in MT polymer in these cells (Figure 3.4B). Expression of stathmin  $\Delta$ 5-25 did not change the MT network when compared to control treated cells (Figure 3.4). As expected based on previous results (Holmfeldt et al., 2006; Howell et al., 1999a; Ringhoff and Cassimeris, 2009b; Sellin et al., 2008), stathmin depletion increased the amount of MT polymer, as measured at the cell periphery (Fig 3.4A).

To knockdown endogenous stathmin mRNA while allowing expression of GFP-tagged proteins, an siRNA against the 5-UTR of endogenous stathmin was used. This siRNA was as effective as those targeting the coding sequence in reducing stathmin level (Figure 3.3B) and was also as effective in causing a G2 cell cycle delay (Figure 3.5). Following endogenous stathmin depletion, cells were transfected with plasmids for expression of GFP or GFP- fused to stathmin, stathmin  $\Delta$ 5-25, or stathmin  $\Delta$ 101-149. This method allowed depletion of endogenous stathmin, while all three stathmin versions were expressed (Figure 3.3B). These cells were allowed to grow for 48 hours after transfection before being fixed and stained.

Expression of GFP-tagged stathmin truncations were then used to test whether either protein could rescue the G2 delay caused by stathmin depletion. If MT stability is the critical signal relay downstream of stathmin depletion, then over-expression of stathmin-GFP or stathmin  $\Delta$ 101-149 should abrogate the delay, but expression of the stathmin  $\Delta$ 5-25 truncation should not change the delay.

Cells expressing stathmin-GFP and depleted of the endogenous protein, showed a reversal of the G2 delay and had a percentage of cells in G2 similar to control levels. Stathmin  $\Delta$ 5-25 expression did not change the percent of cells delayed in G2. Similar to stathmin depletion alone, this treatment had about a two-fold increase in the percent of TPX2 positive interphase cells when compared to controls. Over-expression of stathmin  $\Delta$ 101-149, on the other hand, resulted in a percentage of TPX2 positive interphase cells

similar to control cells and thus successfully rescued the cell cycle delay observed when stathmin is depleted (Figure 3.5A).

We observed a similar effect after these transfections when phospho-CDK1 was used as a marker of cells in G2. Cells that normally delay in G2 following stathmin depletion escaped the delay only when MTs were altered by the expression of either WT-stathmin or stathmin  $\Delta$ 101-149. As previously shown, when stathmin  $\Delta$ 5-25 is reintroduced, the percentage of interphase cells positive for phosphorylated CDK1 remains at an elevated level compared to control treated cells (Figure 3.5B). These results suggest that cells can only escape the G2 cell cycle delay when the MT network is depolymerized (using full-length stathmin or stathmin  $\Delta$ 101-149) following stathmin depletion.

Expression of stathmin truncations also allows us to establish what, if any, roles p27<sup>kip1</sup> and STAT3 might play in the cell cycle arrest that is observed following stathmin depletion. Both p27<sup>kip1</sup> and STAT3 bind to the C-terminus of stathmin (Baldassarre et al., 2005; Gao and Bromberg, 2006; Ng et al., 2006). If stathmin binding contributes to their localization in the cytoplasm, where they are inactive, then expression of full-length stathmin or stathmin  $\Delta$ 5-25 could bind and sequester either of these two proteins in the cytoplasm, preventing their nuclear entry. On the other hand, stathmin  $\Delta$ 101-149 would not be able to bind either p27<sup>kip1</sup> or STAT3 and they would be free to move to the nucleus and possibly delay the cell cycle. Figure 3.5 shows that this model is highly unlikely because our observations are directly opposite of what this model would propose.

Specifically, it is the expression of the  $\Delta$ 101-149 truncation that rescues the stathmin-depletion induced cell cycle delay and not the expression of the  $\Delta$ 5-25 truncation.

**p27<sup>kip1</sup> localization does not change when stathmin is depleted.**

As described above, stathmin has two identified binding partners in addition to tubulin that could contribute to a G2 cell cycle delay. Previous data from Ng et al (2006) showed that STAT3 is not activated following stathmin depletion and our results from expression of stathmin truncations further confirmed that stathmin depletion is not relaying signals via STAT3 activation. The expression of stathmin truncations and the rescue of a G2 cell cycle delay by the  $\Delta$ 101-149 truncation also did not support involvement of p27<sup>Kip1</sup>. To further exclude p27<sup>kip1</sup> involvement, we tested whether stathmin depletion activated p27<sup>Kip1</sup>, as measured by p27 localization to the nucleus. HeLa cells were depleted of stathmin for 48 hours after which they were fixed and stained for p27<sup>kip1</sup>. The protein showed no increase in the percent of interphase cells scored positive for nuclear p27<sup>Kip1</sup> after stathmin depletion (Figure 3.6). As a positive control, MG132 (a proteasome inhibitor) was used to stabilize p27<sup>kip1</sup> and this stabilization significantly increased the percentage of interphase cells scored positive for nuclear p27<sup>Kip1</sup>. Therefore, these results do not support a role for p27<sup>Kip1</sup> in mediating the G2 delay observed after stathmin depletion.

**Discussion:**

We explored the signal downstream of stathmin depletion sufficient to cause a G2 cell cycle delay and found that increased MT stability is the likely source of delayed cell cycle progression. In stathmin-depleted cells, MT depolymerization by nocodazole treatment was sufficient to abrogate the G2 cell cycle delay. These data indicate that MT stability acts downstream of stathmin depletion to cause the delay since depolymerizing MTs allows cell to escape into mitosis. Additional support for MT stability acting downstream of stathmin depletion comes from experiments to rescue the G2 delay by expression of stathmin truncations. Expression of GFP-tagged full-length stathmin or stathmin  $\Delta 101-149$ , after depletion of endogenous stathmin, both decreased MTs and reduced the population of cells in G2 to that measured in cells transfected with control siRNA. Over-expressing stathmin  $\Delta 5-25$ , which has no effect on MTs, however, did not affect the percentage of cells in G2. Taken together, these experiments also indicate that neither p27<sup>kip1</sup> nor STAT3, alternative binding partners of stathmin, is responsible for relaying a cell cycle delay downstream of stathmin depletion, since they bind to stathmin's C-terminus and over-expressing stathmin  $\Delta 101-149$  still rescues the delay. Instead, our results provide strong evidence that excess MT stability can delay the cell cycle during interphase. Based on these results, it is evident that a stathmin-dependent change in the MT network leads to a cell cycle delay and not an alternative function of stathmin's via its other binding partners, STAT3 and p27<sup>kip1</sup>.

The MT phenotypes, observed after lowering stathmin level, like increased nucleation rate and higher polymer level, have been shown in cells expressing p53 (Belletti et al.; Holmfeldt et al., 2007; Ringhoff and Cassimeris, 2009b), so why do we only see these

effects on MTs when both p53 and stathmin are depleted? Although we do observe slight increases in both nucleation rate and stable MTs when stathmin is depleted in p53-positive cells, they are not significant and are much lower than previously published results. The differences we observe here may be due to the fact that we are transiently restoring p53 thereby altering its level in the cell compared to other experiments where the cells constitutively express wild-type p53. Stathmin depletion changes the expression of many genes (Ringhoff and Cassimeris, 2009a), and these changes could differ in a p53-dependent fashion. These differences in gene expression may complicate comparisons. Taken together, these may account for the disparity we observe here.

While the depletion of stathmin leading to a G2 delay might seem logical because increased MT stability reduces the ability of a cell to form a spindle, this is not the case when cells are exposed to paclitaxel (Taxol). Although treatment with taxol has been shown to significantly increase mitotic duration due to a mitotic block (Gascoigne and Taylor, 2009), it does not change interphase duration (Uetake and Sluder, 2007). This differs greatly from what we see when stathmin is depleted, suggesting that the two cells differ in how they enter mitosis. In taxol treated cells, MTs reorganized uniquely leading to the formation of a bizarre state where nucleation sites accumulate at the cell periphery leading to improper spindle formation (Hornick et al., 2008). Since stathmin is turned off in mitosis due to phosphorylation of the protein (Larsson et al., 1997; Larsson et al., 1995), stathmin-depleted cells may not develop the odd phenotype associated with taxol treatment and delay in G2 until a proper spindle can form. Nguyen et al (1997) also observed an increase in interphase duration and a G2 delay when MAP4 (a MT stabilizer)

is over-expressed, further supporting the idea that stathmin depletion acts outside of mitosis and generates a more natural state of stability, since stathmin and MAP4 act antagonistically and therefore differently than taxol.

However, as we stated earlier, MT stability's role in regulating cell cycle progression outside of M phase has been controversial. Rieder and others suggested that the MT cytoskeleton is necessary for cell cycle progression through G2 in numerous cell types (Balestra and Jimenez, 2008; Blajeski et al., 2002; Rieder and Cole, 2000). They suggest the presence of "MT integrity checkpoint" which must be met before the cell can escape G2 and enter mitosis. Uetake and Sluder (2007) disagreed, instead suggesting that it is the length of the previous mitosis that matters. In their experiments, Uetake and Sluder used taxol to stabilize MTs and showed that there is no change in the interphase duration, however the unique MT phenotype resulting from taxol exposure could, however, be responsible for the observed effects. Unpublished data from our lab shows that depletion of stathmin has no effect on mitotic duration when compared to controls (Caruso, V. and Cassimeris, unpublished), indicating that our observed G2 delay is not the result of a previous slowed mitosis. Our results support the idea of a "MT integrity sensor" which monitors the state of the MT network before the cell can enter mitosis or slows the kinetics of mitotic entry during the transition from G2 to M.

The question still remains as to why the G2 delay only occurs when both stathmin and p53 are absent. Although loss of p53 only has a minor effect on MT dynamic turnover (Galmarini et al., 2003), p53 has been shown to localize to the centrosome (Tarapore and

Fukasawa, 2002). P53's localization to the centrosome turns out to be important in amplification of the centrosome itself (Fukasawa, 2008; Tarapore and Fukasawa, 2002). When p53 is absent, cells show an increase in both centrosome number and the rate of chromosome mis-segregation (Tarapore and Fukasawa, 2002). This change in centrosome structure could also account for the changes in MT dynamics observed by Galmarini et al (2003). If this is the case, any additional disruption to the MT network when p53 is absent, such as stathmin depletion, may intensify changes to MT dynamics including the stability of MTs thereby signaling the cell to stall the cell cycle. Previously, Ringhoff and Cassimeris (2009b) showed an increased nucleation at the centrosome in MEF cells where stathmin has been knocked out and for HeLa cells where stathmin had been depleted, we found this increased nucleation rate only when combined with negligible levels of p53. The ability of p53 and stathmin to impact centrosome structure or function may place centrosomes as the critical signal integrator. The increased MT stability and nucleation rate could also lead to both difficulties breaking down the MT array before the cell enters mitosis, as well as disruptions or alterations to signal transduction via MTs (discussed below).

### **Microtubule stability transduces signals to delay cells in G2.**

Before the cell can enter mitosis, the interphase MT array must break down and reorganize to form the mitotic spindle (Figure 3.7A). During prophase, centrosomes separate and astral arrays form with long MTs, as polymer level remains constant. A steep drop in polymer level occurs near the time of nuclear envelope breakdown despite a dramatic increase in nucleation (Zhai et al., 1996). This shift occurs rapidly and is

accomplished by disassembly of individual MTs from a change in dynamic instability favoring disassembly and by shuttling of MT bundles by cytoplasmic dynein toward the nuclear envelope (Rusan et al., 2002). Increased stability of MTs at this point would likely hinder the reorganization process. We hypothesize that delayed mitotic entry results from disrupted reorganization of the interphase MT array (Figure 3.7B), and may act as a physical signal to delay the cell cycle. However, increased stabilization of MTs may also affect other more conventional signaling pathways as well.

Microtubules' acting to relay signals is not a novel idea, but is an area that has not been well studied. MTs have been proposed to be involved in not only signaling to control the cell cycle and differentiation (Sobel, 1991), but they are also believed to be important in many other signal cascades (Gundersen and Cook, 1999). Therefore, changes to the MT network can drastically alter these signals affecting not only the cell cycle, but many other cell functions, as well. MTs are also known to sequester many proteins, including GEF-H1, an activator of RhoA (Chang et al., 2008), as well as to act as docks for other signaling scaffolds, such as those in MAPK pathway (Gundersen and Cook, 1999) and the glycolytic pathway (Durrieu et al., 1987; Knull and Walsh, 1992; Lehotzky et al., 1993; Vertessy et al., 1997). When stathmin is depleted and the amount of stable MTs increases, this changes the way such scaffolds function, by changing not only scaffolding but delivery, sequestration, and the release of many proteins that both directly and indirectly interact with the MTs (Gundersen and Cook, 1999) (Figure 3.7C).

The glycolytic pathway, for example, can also bring the absence of p53 back into the picture, since this protein has been shown to have some control over metabolic regulation (Maddocks and Vousden). When p53 is lacking the amount of glycolysis increases, promoting an amplification in the Warburg effect (high rate of aerobic glycolysis characteristic of cancer cells). The ability of the cell to adapt metabolically also decreases and as a result cells become more sensitive to metabolic stress (Maddocks and Vousden). Changes in MT stability, following stathmin depletion in p53 null cells, may provide additional stress, thereby activating stress pathways, leading to a delay in the cell cycle and apoptosis.

Although we are not sure of the exact downstream mechanism, it is clear that MT stability plays an important role in G2 progression and mitotic entry. It is also evident that the role of MTs is regulated in an unknown p53-dependent process in which it is likely that p53 suppresses the amount of stable MTs. If MT stability increases and p53 is no longer present to prevent it, the cell proceeds to delay in the cell cycle.

### **Conclusion:**

Stathmin depletion in p53 null cells leads to a significant increase in MT stability. This stability activates an as yet unknown signal pathway that leads to a cell cycle delay and although not studied here most likely apoptosis as well. This synergistic affect on the cell cycle when both p53 and stathmin are depleted could prove promising in the treatment on a wide array of cancers.

## Figures:

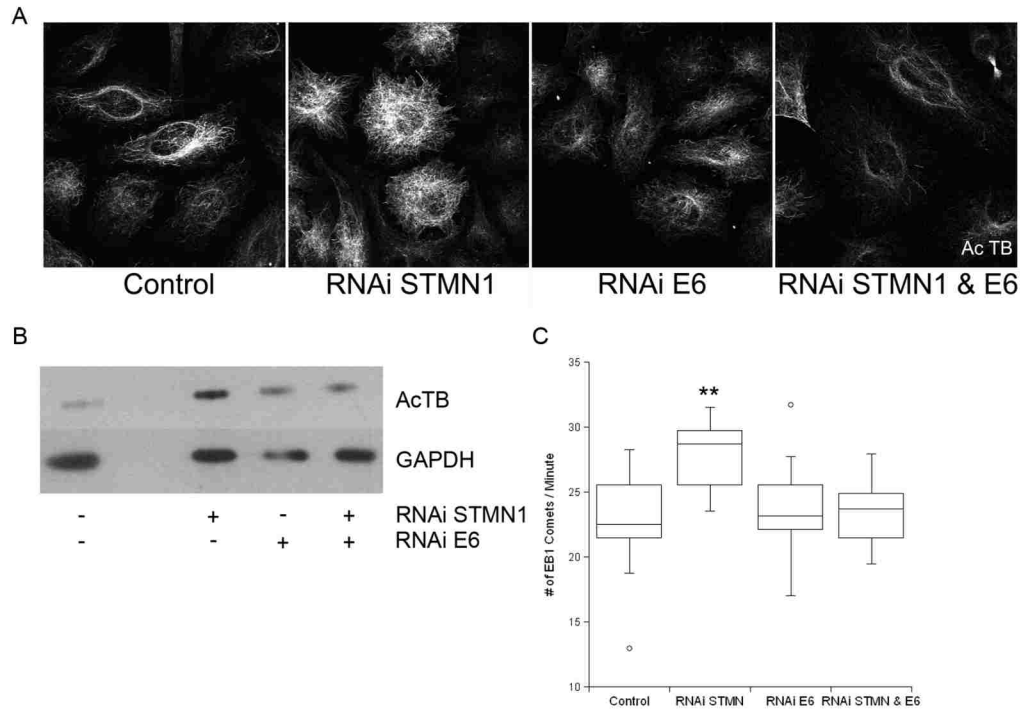


Figure 3.1: Stathmin depletion from HeLa cells increases MT stability only when p53 is absent. HeLa cells were transfected with siGlo control siRNA or siRNA targeting stathmin, HPV E6, or both mRNAs. (A) Cells were fixed 72 hrs after transfection and then stained with antibodies against acetylated tubulin. Representative images of each treatment are presented here. (B) Anti- acetylated tubulin immunoblot from cell lysates isolated 72 hrs after transfection. (C) MT nucleation rates were determined by transfecting HeLa cells with EB1-GFP 24 hrs after siRNA treatment. Live cell imaging at the centrosome was performed 48 hrs after EB1-GFP transfection. Images were used to count the number EB1 comets emerging from the centrosome per minute. Box plot represents the mean of 3 independent experiments. \*\*denotes  $p < 0.0001$ , °denotes outliers.

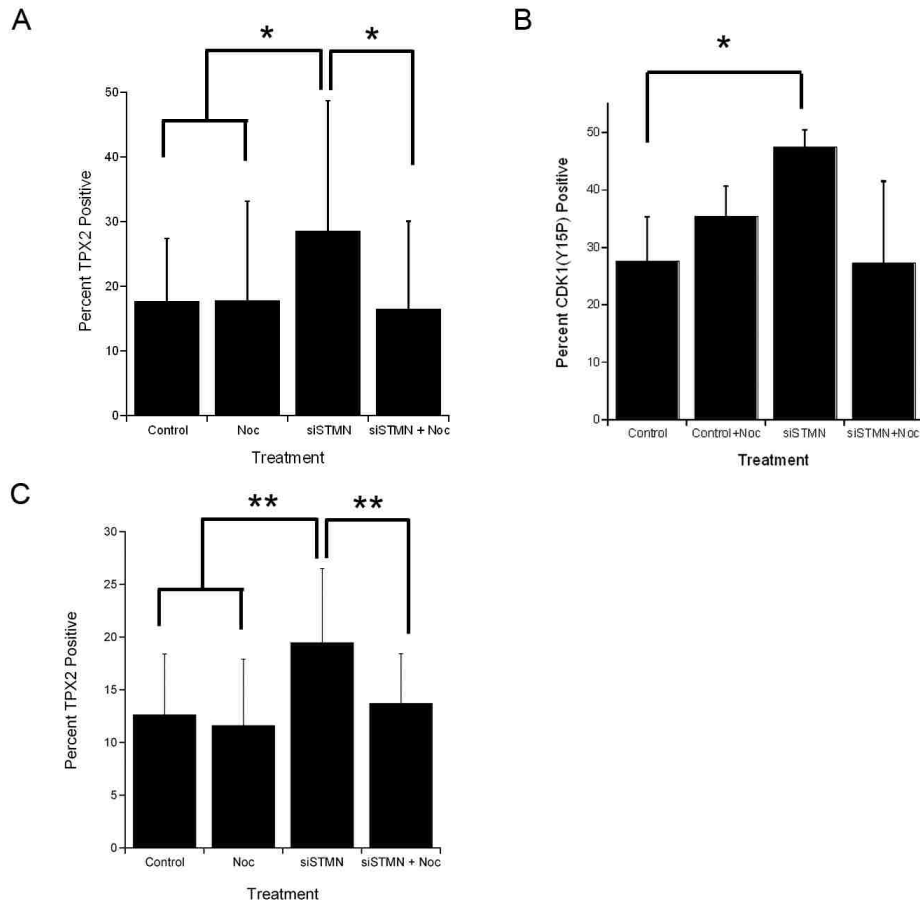


Figure 3.2: Depolymerizing MTs with nocodazole allows cells to escape the G2 delay in both HeLa and HCT116<sup>p53<sup>-/-</sup></sup> cells. Cells were transfected with either siGlo control siRNA or siRNA targeting stathmin mRNA. 40-48 hrs after transfection, cells were treated with DMSO, as a control, or 33 $\mu$ M nocodazole for 3-5 hrs before fixation and staining. (A) HeLa cells were stained with antibodies against  $\alpha$ -tubulin and TPX2. The numbers of TPX2 positive and negative cells were counted, and the percentage of interphase cells staining positive are shown in A. (B) HeLa cells were stained with antibodies against  $\alpha$ -tubulin and phospho-CDK1(Y15). The numbers of phospho-CDK1(Y15) positive and negative cells were counted, and the percentage of interphase cells staining positive are shown in B. (C) HCT116<sup>p53<sup>-/-</sup></sup> cells were stained with

antibodies against  $\alpha$ -tubulin and TPX2. The numbers of TPX2 positive and negative cells were counted, and the percentage of interphase cells staining positive are shown in C. Each plot represents the mean of 3 independent experiments  $\pm$  SD. \*denotes  $p < 0.01$  and \*\*denotes  $p < 0.001$ .

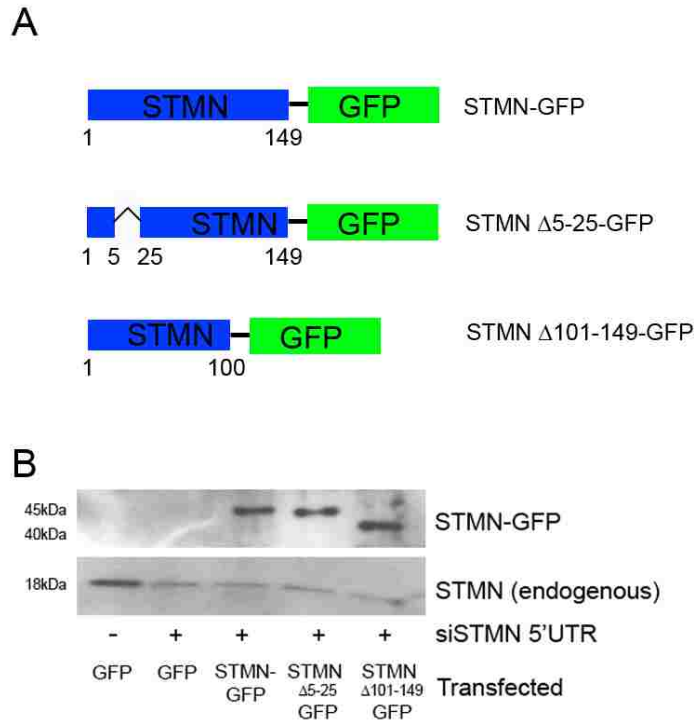


Figure 3.3: Stathmin truncations can be expressed in HeLa cells in the presence of siRNA against the 5'UTR region of stathmin mRNA. (A) Represents the three stathmin-GFP fusion proteins designed for these experiments. (B) Cells were treated with either siGLO control siRNA or siRNA against the 5'UTR region of stathmin mRNA, to deplete only the endogenous stathmin. Ten minutes after siRNA treatment cells were transfected with either GFP or one of the three stathmin-GFP fusion proteins. Anti-stathmin immunoblots from cell lysates were isolated 72 hrs after the second round of transfection. In order to get a successful blot, two stathmin antibodies were used separately because the Sigma stathmin antibody recognizes the extreme C-terminus, and will not recognize all the truncations, while the Cell Signaling stathmin antibody (binds around S38) failed to recognize endogenous stathmin, but was able to recognize all the truncations.

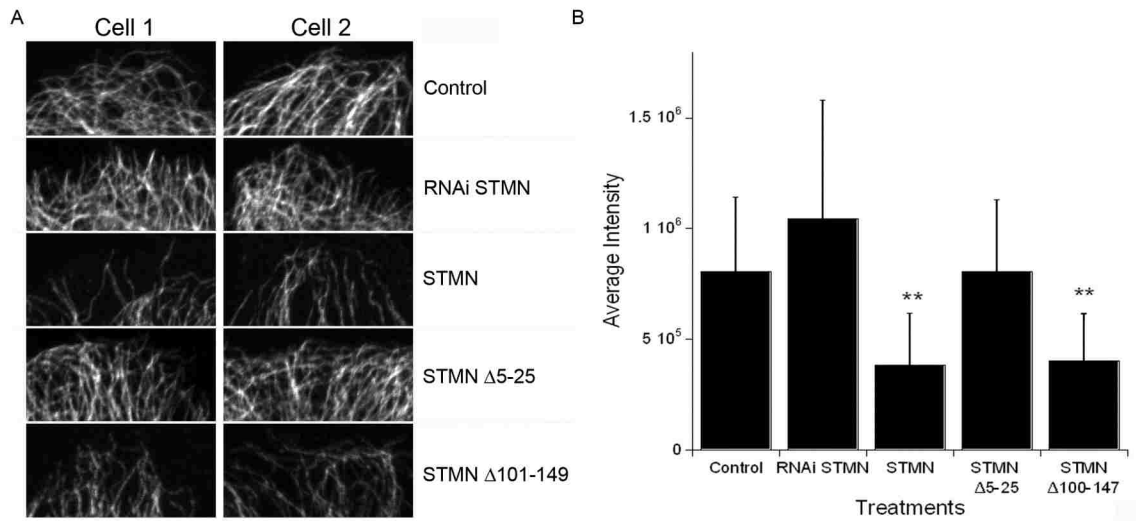


Figure 3.4: Stathmin truncations change MT polymer at the cell periphery. Cells were transfected with GFP, one of three stathmin GFP fusion proteins, or siRNA against stathmin mRNA. (A) Cells were fixed 72 hrs after transfection and then stained with antibodies against  $\alpha$ -tubulin. GFP expressing cells were imaged at the cell periphery in order to discern differences in MT polymer. Representative images of two cells transfected with each construct are shown in A. (B) Relative intensity data was collected from all images using Metamorph software. Each plot represents the mean of 2 independent experiments  $\pm$  SD, consisting of >10 cells for each treatment. \*\* denotes  $p < 0.005$ .

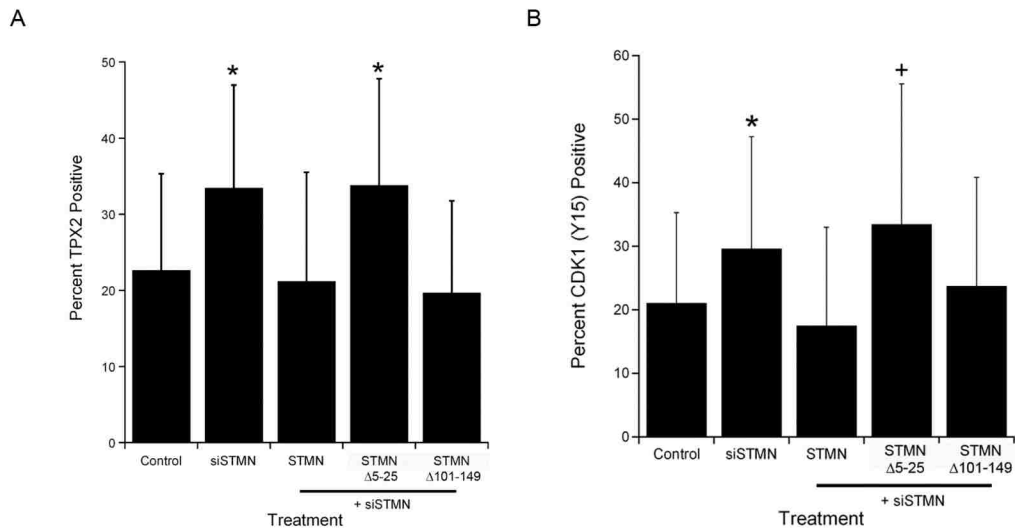


Figure 3.5: Over-expression of truncated stathmin can rescue the cells from a G2 delay following depletion of endogenous stathmin. Cells were transfected with either siGLO control siRNA or siRNA against the 5'UTR region of stathmin mRNA. Ten minutes after siRNA treatment cells were transfected with either GFP or one of the three stathmin-GFP fusion proteins before fixation and staining. (A) HeLa cells were stained with antibodies against  $\alpha$ -tubulin and TPX2. The numbers of TPX2 positive and negative cells were counted, and the percentage of interphase cells staining positive are shown in A. (B) HeLa cells were stained with antibodies against  $\alpha$ -tubulin and phospho-CDK1(Y15). The numbers of phospho-CDK1(Y15) positive and negative cells were counted, and the percentage of interphase cells staining positive are shown in B. Each plot represents the mean of 3 (A) or 4 (B) independent experiments  $\pm$  SD. \*denotes  $p < 0.05$  and +denotes  $p < 0.055$ .

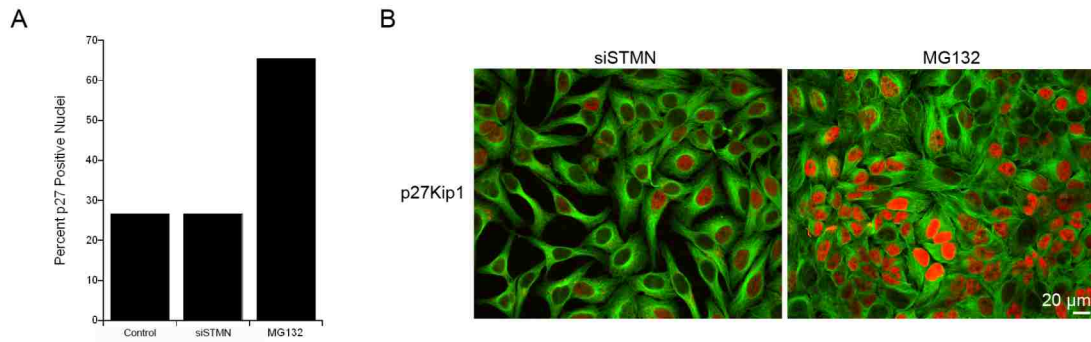


Figure 3.6: Stathmin depletion does not increase p27<sup>Kip1</sup> localization in nucleus. HeLa cells were transfected with either siGlo control siRNA or siRNA targeting stathmin mRNAs. 40-48 hrs after transfection, cells were fixed and stained. As a positive control, cells were treated with MG132 (5 $\mu$ M), a proteasome inhibitor, for 5-6 hrs before fixation. Cells were stained with antibodies against  $\alpha$ -tubulin and p27<sup>Kip1</sup>. (A) The numbers of p27<sup>Kip1</sup> positive and negative cells were counted, and the percentage of interphase cells staining positive are shown in A. (B) Images shown are from a representative field of cells transfected with stathmin siRNA or the drug MG132. The plot above represents one of two independent experiments, representing >200 cells per condition.

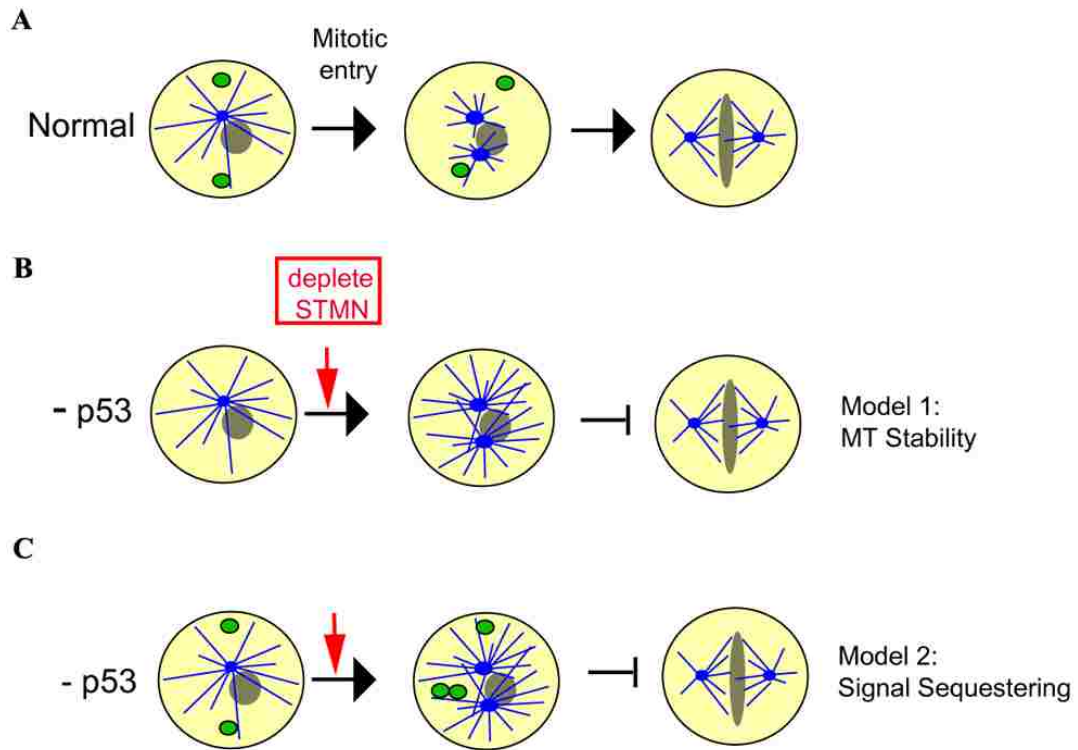


Figure 3.7: Models for how stathmin depletion in p53 null cells leads to a G2 delay. (A) Under normal conditions, the cell can depolymerize its MTs and form a proper spindle allowing entry into mitosis. However, stathmin depletion in p53 null cells leads to a G2 delay in a yet unknown mechanism. (B) After stathmin depletion, cells could have an inability to properly depolymerize their MT arrays and successfully progress into mitosis. (C) Depleting stathmin could, on the other hand, cause a disruption of cellular signaling (in this case a change in the ratio of free/bound protein).

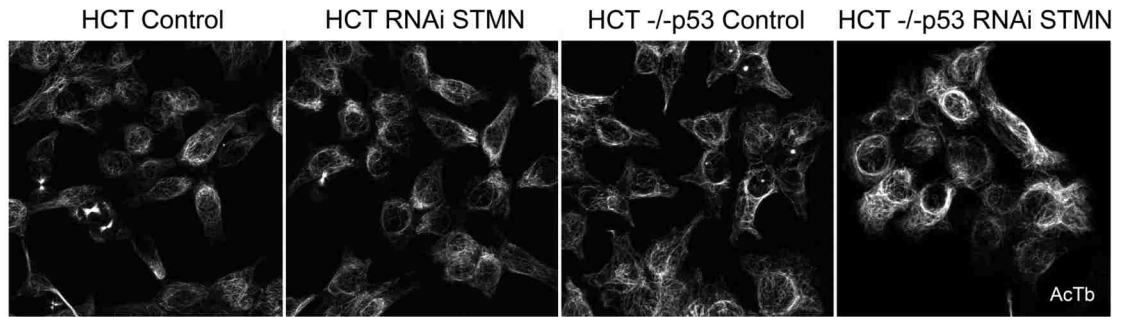


Figure 3.8: Stathmin depletion from HCT116<sup>wt-p53</sup> and HCT116<sup>p53-/-</sup> cells increases MT stability only when p53 is absent. HCT116 cells were transfected with siGlo control siRNA or siRNA targeting stathmin mRNA. Cells were fixed 72 hrs after transfection and then stained with antibodies against acetylated tubulin. Representative images of each treatment are presented here.

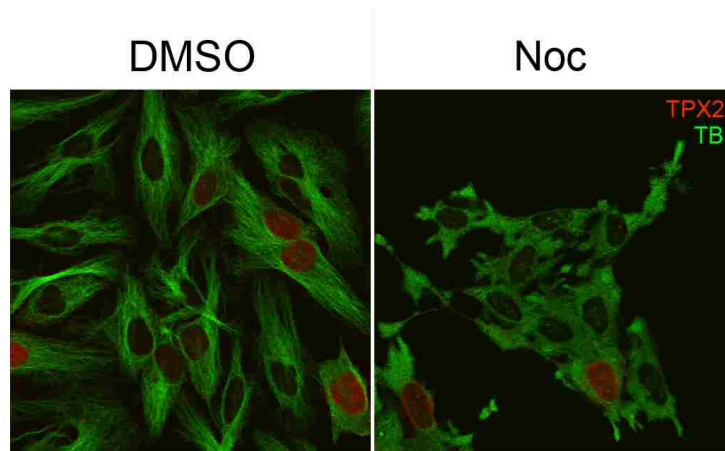


Figure 3.9: Nocodazole depolymerizes MTs in HeLa cells. Cells were treated with either DMSO or 33 $\mu$ M nocodazole for 3-5 hrs before fixation and staining. HeLa cells were stained with antibodies against  $\alpha$ -tubulin and TPX2. This treatment is sufficient to depolymerize MTs in these cells. These are representative images of a field of cells for each treatment.

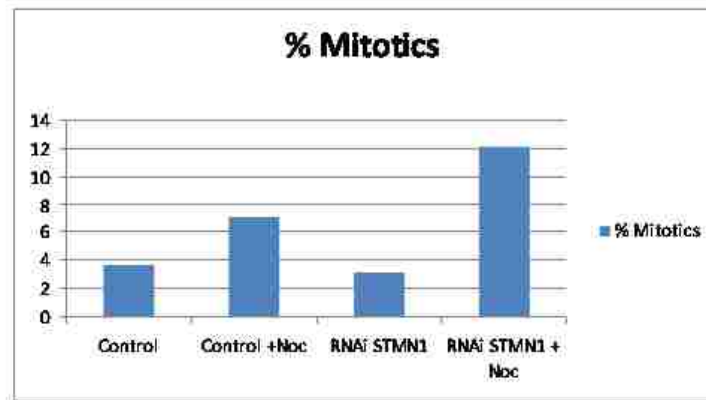


Figure 3.10: Mitotic index increases when cells are treated with nocodazole independent of stathmin depletion. Cells were transfected with either siGlo control siRNA or siRNA targeting stathmin mRNA. 40-48 hrs after transfection, cells were treated with DMSO or 33 $\mu$ M nocodazole for 3-5 hrs before fixation and staining. (A) HeLa cells were stained with propidium iodide (PI) and mitotic index was determined.

## **Chapter 4**

### **Conclusions and Future Directions**

## Conclusions

Stathmin has been known to play key roles in MT dynamics. Stathmin's functions in regulating dynamic instability (Holmfeldt et al., 2002; Howell et al., 1999a), tubulin sequestering (Howell et al., 1999b), and MT polymer content (Holmfeldt et al., 2007) are well established. Stathmin has also been shown to be highly over-expressed in many cancers (Belletti et al., 2008; Bieche et al., 1998; Brattsand, 2000; Chen et al., 2003; Friedrich et al., 1995; Kouzu et al., 2006; Melhem et al., 1997; Mistry et al., 2005; Ngo et al., 2007; Nishio et al., 2001; Nylander et al., 1995; Price et al., 2000; Yuan et al., 2006) which constitute some of the most malignant and hardest to treat cancers. Only recently has stathmin been shown to have a role in cell cycle delay and apoptosis (Alli et al., 2007; Mistry et al., 2005; Wang et al., 2009; Zhang et al., 2006). However, although Alli et al proposed the involvement of p53 in these pathways, it had not been tested directly. Here I tested Alli et al's hypothesis directly (chapter 2) and determined how such a pathway might function (chapter 3).

In chapter 2, I showed that only cells lacking both p53 and stathmin activate a G2 cell cycle delay and die via apoptosis, similar to what Alli et al (2007) hypothesized. While the knockdown of either protein alone showed a slight slowing of the cell cycle, this type of depletion does not lead to a delay or apoptosis (Carney and Cassimeris, 2010). Restoring p53 to cells that normally lack a functional copy of the protein rescued both the delay and the apoptosis that is observed in their p53 lacking counterparts (Carney and Cassimeris, 2010). This is the case for both cancer cell lines tested (HeLa and HCT116),

as well as a non-cancerous primary cell line (HFF). Stathmin depletion could prove to be very effective as a means of selectively targeting for death only cells that have an absent or nonfunctional p53. As a siRNA-based therapy, depletion of stathmin would allow for treatment of cancers lacking p53 that normally have a poor prognosis and are relatively hard to treat (Wallace-Brodeur and Lowe, 1999). While depletion of stathmin would kill p53 null cells, it would be able to leave the surrounding cells relatively unaffected since depletion of stathmin from healthy cells not only fails to activate apoptosis (Carney and Cassimeris, 2010), but those same healthy cells can still grow and proliferate normally without the presence of stathmin (Schubart et al., 1996). However, siRNA-based treatments are thus far unsuccessful or not optimal in animal models (Higuchi et al., 2010; Kim et al., 2009). Identifying the pathway where stathmin knockdown acts therefore could lead to other potential targets where it may be easier to design treatments until siRNA technology improves. Which begs the question, what about stathmin's depletion in these p53 null cells is leading to both the G2 delay and apoptosis?

Chapter 3 answers how stathmin depletion leads to a cell cycle delay. In the third chapter of this dissertation, I showed that it is the affect stathmin depletion has on MT stability that leads cells to stall in G2. By depolymerizing or simply lowering the amount of stable MTs back to control levels, I was able to successfully alleviate the G2 delay that is normally associated with stathmin depletion in cells lacking p53 (Carney and Cassimeris, 2010). Based on our results, I was also able to eliminate p27<sup>kip1</sup> and STAT3, stathmin's other binding partners, as participating in delaying the cells in G2 since their involvement would have yielded the opposite results. Changes in MT stability are less significant

when p53 is restored, supporting the idea that depletion of stathmin and p53 leads to a greater change in the MT network.

The results above are consistent with what is observed with other known chemotherapies. For instance, paclitaxel causes tumor cell death in mitosis due to an inability to both rearrange the MT array and progress through the cell cycle (Xiao et al., 2006). However, unlike paclitaxel, which leads to a cell cycle block in mitosis (Rieder and Maiato, 2004) and eventual apoptosis, the depletion of stathmin initiates a cell cycle delay in G2 (Carney and Cassimeris, 2010). In order to determine both what MT stability is effecting, as well as, what pathways are leading the cell to delay will need more experimentation.

## **Future Directions**

In chapter 2, I demonstrated that stathmin depletion in the absence of p53 leads to both a G2 delay and apoptosis, but I did not test how, or if, these two outcomes are connected. Two days after stathmin depletion a significant increase in the population of G2 cells was observed, which begins to drop as cells proceed to day three (Carney, B. and Cassimeris, unpublished). On the other hand, apoptosis does not reach a significant level until three days after stathmin depletion (Carney and Cassimeris, 2010). Based on this time line of events, I assume that cells begin to delay in G2 24-48 hours after stathmin depletion and only after this delay is apoptosis initiated. Cell death only occurs when p53 and stathmin are both depleted and leads to a model (Figure 4.1) where stathmin depletion increases

MT stability causing a G2 delay before activating apoptosis. Evidence from Sur et al (2009) supports the model that a G2 delay is followed by apoptosis. Using an inhibitor against a G2 cell cycle activator, polo-like kinase 1, they showed that cells lacking p53 were more sensitive to death after a stress that follows the arrest. For simplicity in chapter 3, I decided to look at only the G2 delay, but these same experiments should be able to determine if apoptosis is linked to MT stability and if apoptosis follows the G2 delay. By using stathmin truncations, one could look at longer time course experiments to see if manipulating MTs allows cells to escape apoptosis, as well as the delay. A short-term MT depolymerization, with nocodazole, to alleviate a G2 delay could possibly address whether the G2 delay and apoptosis are linked. Unpublished data from our lab (Cassimeris, L., unpublished) shows that cells can slip out of G2 and into the next cell cycle prior to apoptosis (Figure 4.2). Synchronizing cells before stathmin depletion could increase the number of cells delayed in G2. After the delay is established, adding nocodazole will allow cells to progress into mitosis. In order for cells to continue into the next cell cycle, nocodazole must be washed out shortly afterwards (3-5 hours). Bypassing this delay should not change whether cells activate apoptosis if the two are not linked, but will allow cells to continue to grow and proliferate for a longer period of time if there is a link between the processes.

Similar to the Sur et al (2009) experiments discussed above, hindering progression into M phase by using inhibitors against proteins that control the G2/M transition could determine if there is a link between the processes of G2 delay and apoptosis that I observe here. Assuming the block created using such inhibitors could be reversed, this

arrest would mimic the affect of stathmin depletion on cell cycle progression. If the processes of G2 delay and apoptosis are linked, then cells should begin apoptosis assuming the cell cycle delay is equivalent to the one induced when stathmin is depleted.

If the G2 delay and apoptosis are not linked it would suggest that in the absence of p53 and stathmin more then one pathway is activated. These pathways would likely be initiated in a similar manner (increased stable MTs) but lead to distinct downstream phenotypes. If this is in fact the case determining what signals are activating each branch of the pathway would be the next logical step.

After determining if there is a link between the G2 delay and apoptosis, one could go about testing the models discussed in chapter 3. For instance, in order to test if the signal to delay and/or kill the cells is relayed through an inability to breakdown the MT array, live cell imaging of stathmin depleted cells can be used. Using a fluorescent marker of cell cycle progression, one could observe the duration required for MT disassembly in stathmin-depleted cells, compared to control treated cells. If the rate of MT disassembly does not change, it is likely that the G2 delay is occurring prior to the breakdown of the interphase MT array and may be caused by the signal sequestering model instead of due to an inability to breakdown the MT array.

Another possible involvement of the MT array would be if the increase in acetylated MTs that was observed functions as a signal itself. Acetylation of MTs changes the way certain motors and other proteins bind to the MTs and therefore may be responsible for

the phenotypes observed when stathmin is depleted in cells lacking p53. To test this model, one could change the state of MT acetylation by over-expressing the proteins that deacetylate MTs (HDAC6) (Warren and Cassimeris, 2007). By artificially decreasing acetylation of MTs, but leaving them otherwise stable, one could test if the delay in G2 and apoptosis is due to the acetylation or just the presence of stable MTs. If a delay is present when acetylation is removed it would suggest the involvement of the sequestering model independent of MT acetylation state.

In order to determine players that may act as signals on MTs, it would also be beneficial to determine what signals are initiating the cell cycle delay observed in stathmin-depleted p53 null cells. Determining the pathway could narrow down potential connections between cell cycle delay and increased MT stability. One pathway that is already being tested in our lab is the Rho dependent pathway that drives mitotic entry (Figure 4.3). Preliminary data from the lab (Caruso, V. and Cassimeris, unpublished) shows a significant decrease in the level of phosphorylation of three important players in this pathway, Aurora A, PLK1, and PAK1, when stathmin is depleted in p53 null cells. In contrast, Wee1 and signals from the DNA damage pathway (Chk1) remain unchanged. The decrease in activation of enzymes downstream of RhoA supports the Rho pathway as a possible link between MT stability and cell cycle delay. Activators of this pathway that bind to MTs, like GEF-H1 (which is inactive when bound), are therefore possible candidates that are causing the G2 delay. Once we determine possible links between cell cycle delay and MT stability, they can be tested directly by altering their levels in the cell without depleting stathmin. It would also be beneficial to observe if the phosphorylation

states of these proteins change in the presence of p53. Restoring p53 to these cells would allow us to see if a p53-dependent pathway is also involved. In the presence of p53, no delay occurs. Thus the decrease in the phosphorylation states of proteins, such as Aurora A, are unlikely to occur. Since these experiments are being done in HeLa cells, one could utilize the HPV E6 siRNA to restore p53 and observe if there is a difference in the phosphorylation states of proteins in the Rho pathway when p53 is present. If a connection is found between MT stability, p53, and this signaling pathway it would suggest a change in MT scaffolding, sequestering, or delivery is responsible for the cell cycle delay and apoptosis that is observed.

So far, most of the experiments discussed here look at pathways associated with stathmin's effects on MTs, but it is important to remember that p53 is also involved in this synergy. In a normal cell, p53 has been shown to interact with both stathmin and MAP4 by down-regulating their transcription when p53 is active (Ahn et al., 1999). Although, this interaction between p53 and stathmin only occurs when p53 is active, it still shows that these proteins can function together. To better understand the synergy observed here it would be beneficial to further explore this interaction. Perhaps, p53 and stathmin have a yet unknown association whether direct, or indirect, that can explain the phenotype observed here. Examining p53's roles in transcription, at the centrosome, and in metabolism may allow us to determine what about p53 mutation is leading to the synergy.

One such pathway leading to a cell cycle delay that I discussed in chapter 3 was glycolysis. We already know that due to the Warburg effect the amount of glycolysis increases and the rate of oxidative phosphorylation decreases when p53 is lacking (Maddocks and Vousden). Coupling that to changes in microtubule scaffolding due to stathmin depletion could cause a failure in glycolysis leading to a starvation state and may promote cell cycle delay and/or apoptosis. This model should be relatively easy to test due to an increase in anaerobic metabolism even in the presence of oxygen. This increases the amount of lactic acid produced by the cell (Delgado et al., 2010) thereby increasing its presence in the media. By collecting the media, lactic acid levels can be compared and it can be determined if there is a decrease when stathmin is depleted in p53 lacking cells compared to cells with stathmin or p53. If a significant change in lactic acid levels is observed, then this pathway may also be involved. Obviously, additional experiments would be necessary to test a metabolic model for synergy between stathmin and p53 reduction.

Once we determine which pathways are involved and how the signal is relayed, we can determine better ways to activate the same pathways in cancer cells leading to cell death. My research should provide a good starting point in this process and may lead to improvements in cancer treatment in the future.

**Figures:**

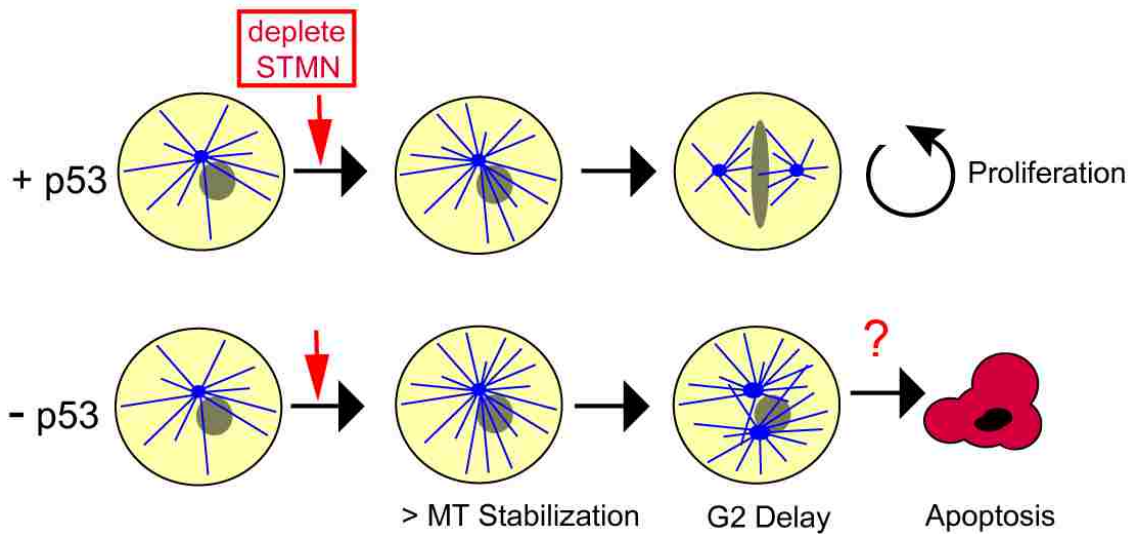


Figure 4.1: Depletion of stathmin leads to G2 delay followed by apoptosis only in p53 lacking cells. This is a proposed model of how increasing MT stability can lead to apoptosis. We know that increased stability leads to a G2 delay only when p53 is lacking and that it is only about 72 hours after stathmin depletion that cells begin to activate apoptosis. But we still do not know if apoptosis follows the delay or if it is activated in a different pathway. Based on the timing of events this pathway seems most likely.

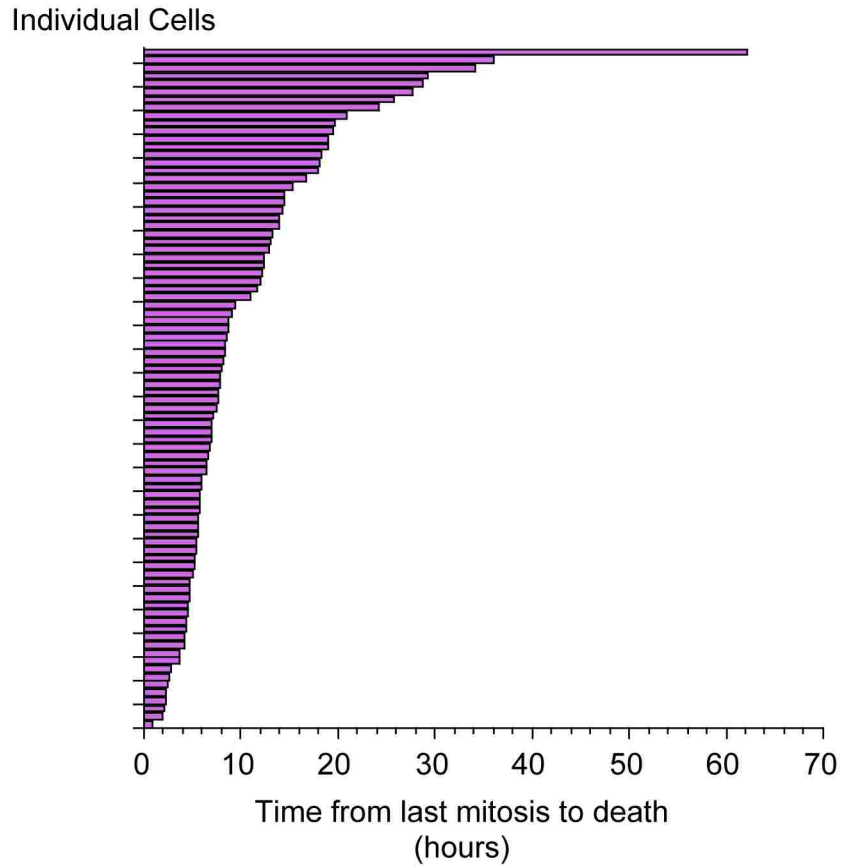


Figure 4.2: Following the G2 delay, cells slip into the next cell cycle before activating apoptosis. This graph tracks individual cells to determine how long after the previous mitosis it is before they die. Based on data from Kulartz and Kipper (2004) it appears that a majority of the cells die in G1 or S phase of the following cell cycle, assuming the cell cycle continues at the normal rate even though these cells never enter the next mitosis.

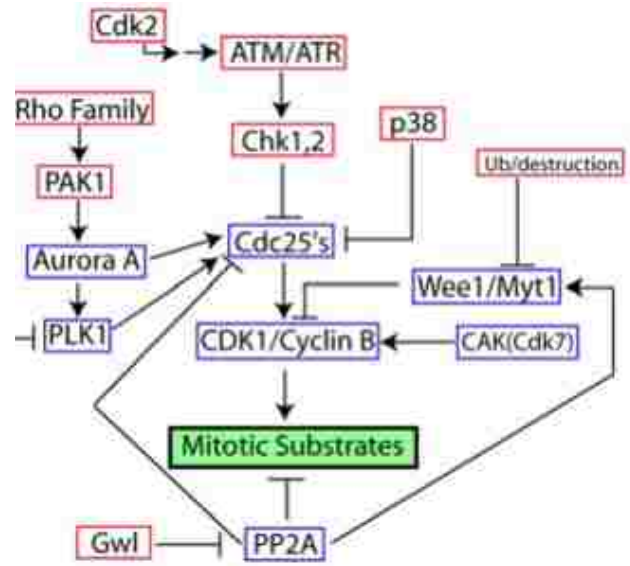


Figure 4.3: This flow chart shows the core enzymes involved in mitotic entry. Based on preliminary data, the Rho family of enzymes is a likely link between the mitotic stability and G2 delay we observe when p53 is lacking based on significant decrease in the phosphorylation (activation) states of its downstream targets, PAK1, Aurora A, and PLK1.

## References:

- Ahn, J., M. Murphy, S. Kratowicz, A. Wang, A.J. Levine, and D.L. George. 1999. Down-regulation of the stathmin/Op18 and FKBP25 genes following p53 induction. *Oncogene*. 18:5954-8.
- Aldaz, H., L.M. Rice, T. Stearns, and D.A. Agard. 2005. Insights into microtubule nucleation from the crystal structure of human gamma-tubulin. *Nature*. 435:523-7.
- Alli, E., J.M. Yang, and W.N. Hait. 2007. Silencing of stathmin induces tumor-suppressor function in breast cancer cell lines harboring mutant p53. *Oncogene*. 26:1003-12.
- Baldassarre, G., B. Belletti, M.S. Nicoloso, M. Schiappacassi, A. Vecchione, P. Spessotto, A. Morrione, V. Canzonieri, and A. Colombatti. 2005. p27(Kip1)-stathmin interaction influences sarcoma cell migration and invasion. *Cancer Cell*. 7:51-63.
- Balestra, F.R., and J. Jimenez. 2008. A G2-phase microtubule-damage response in fission yeast. *Genetics*. 180:2073-80.
- Becker, B.E., and L. Cassimeris. 2005. Cytoskeleton: microtubules born on the run. *Curr Biol*. 15:R551-4.
- Belletti, B., M.S. Nicoloso, M. Schiappacassi, S. Berton, F. Lovat, K. Wolf, V. Canzonieri, S. D'Andrea, A. Zucchetto, P. Friedl, A. Colombatti, and G. Baldassarre. 2008. Stathmin activity influences sarcoma cell shape, motility, and metastatic potential. *Mol Biol Cell*. 19:2003-13.
- Belletti, B., I. Pellizzari, S. Berton, L. Fabris, K. Wolf, F. Lovat, M. Schiappacassi, S. D'Andrea, M.S. Nicoloso, S. Lovisa, M. Sonogo, P. Defilippi, A. Vecchione, A. Colombatti, P. Friedl, and G. Baldassarre. p27kip1 controls cell morphology and motility by regulating microtubule-dependent lipid raft recycling. *Mol Cell Biol*. 30:2229-40.
- Belmont, L.D., and T.J. Mitchison. 1996. Identification of a protein that interacts with tubulin dimers and increases the catastrophe rate of microtubules. *Cell*. 84:623-31.

- Bhat, K.M., and V. Setaluri. 2007. Microtubule-associated proteins as targets in cancer chemotherapy. *Clin Cancer Res.* 13:2849-54.
- Bieche, I., S. Lachkar, V. Becette, C. Cifuentes-Diaz, A. Sobel, R. Lidereau, and P.A. Curmi. 1998. Overexpression of the stathmin gene in a subset of human breast cancer. *Br J Cancer.* 78:701-9.
- Blajeski, A.L., V.A. Phan, T.J. Kottke, and S.H. Kaufmann. 2002. G(1) and G(2) cell-cycle arrest following microtubule depolymerization in human breast cancer cells. *J Clin Invest.* 110:91-9.
- Borgne, A., and L. Meijer. 1996. Sequential dephosphorylation of p34(cdc2) on Thr-14 and Tyr-15 at the prophase/metaphase transition. *J Biol Chem.* 271:27847-54.
- Bradford, M.M. 1976. A rapid and sensitive method for the quantitation of microgram quantities of protein utilizing the principle of protein-dye binding. *Anal Biochem.* 72:248-54.
- Brattsand, G. 2000. Correlation of oncoprotein 18/stathmin expression in human breast cancer with established prognostic factors. *Br J Cancer.* 83:311-8.
- Brito, D.A., and C.L. Rieder. 2006. Mitotic checkpoint slippage in humans occurs via cyclin B destruction in the presence of an active checkpoint. *Curr Biol.* 16:1194-200.
- Budde, P.P., A. Kumagai, W.G. Dunphy, and R. Heald. 2001. Regulation of Op18 during spindle assembly in *Xenopus* egg extracts. *J Cell Biol.* 153:149-58.
- Bulinski, J.C. 2007. Microtubule modification: acetylation speeds anterograde traffic flow. *Curr Biol.* 17:R18-20.
- Bunz, F., A. Dutriaux, C. Lengauer, T. Waldman, S. Zhou, J.P. Brown, J.M. Sedivy, K.W. Kinzler, and B. Vogelstein. 1998. Requirement for p53 and p21 to sustain G2 arrest after DNA damage. *Science.* 282:1497-501.
- Cambray-Deakin, M.A., and R.D. Burgoyne. 1987. Acetylated and detyrosinated alpha-tubulins are co-localized in stable microtubules in rat meningeal fibroblasts. *Cell Motil Cytoskeleton.* 8:284-91.

- Carney, B.K., and L. Cassimeris. 2010. Stathmin/oncoprotein 18, a microtubule regulatory protein, is required for survival of both normal and cancer cell lines lacking the tumor suppressor, p53. *Cancer Biol Ther.* 9:699-709.
- Caspari, T. 2000. How to activate p53. *Curr Biol.* 10:R315-7.
- Cassimeris, L. 2002. The oncoprotein 18/stathmin family of microtubule destabilizers. *Curr Opin Cell Biol.* 14:18-24.
- Cassimeris, L., and C. Spittle. 2001. Regulation of microtubule-associated proteins. *Int Rev Cytol.* 210:163-226.
- Chang, Y.C., P. Nalbant, J. Birkenfeld, Z.F. Chang, and G.M. Bokoch. 2008. GEF-H1 couples nocodazole-induced microtubule disassembly to cell contractility via RhoA. *Mol Biol Cell.* 19:2147-53.
- Chen, G., H. Wang, T.G. Gharib, C.C. Huang, D.G. Thomas, K.A. Shedden, R. Kuick, J.M. Taylor, S.L. Kardia, D.E. Misek, T.J. Giordano, M.D. Iannettoni, M.B. Orringer, S.M. Hanash, and D.G. Beer. 2003. Overexpression of oncoprotein 18 correlates with poor differentiation in lung adenocarcinomas. *Mol Cell Proteomics.* 2:107-16.
- Chin, G.M., and R. Herbst. 2006. Induction of apoptosis by monastrol, an inhibitor of the mitotic kinesin Eg5, is independent of the spindle checkpoint. *Mol Cancer Ther.* 5:2580-91.
- Clement, M.J., I. Jourdain, S. Lachkar, P. Savarin, B. Gigant, M. Knossow, F. Toma, A. Sobel, and P.A. Curmi. 2005. N-terminal stathmin-like peptides bind tubulin and impede microtubule assembly. *Biochemistry.* 44:14616-25.
- Clute, P., and J. Pines. 1999. Temporal and spatial control of cyclin B1 destruction in metaphase. *Nat Cell Biol.* 1:82-7.
- DeGraffenried, L.A., L. Fulcher, W.E. Friedrichs, V. Grunwald, R.B. Ray, and M. Hidalgo. 2004. Reduced PTEN expression in breast cancer cells confers susceptibility to inhibitors of the PI3 kinase/Akt pathway. *Ann Oncol.* 15:1510-6.
- Delgado, T., P.A. Carroll, A.S. Punjabi, D. Margineantu, D.M. Hockenbery, and M. Lagunoff. 2010. Induction of the Warburg effect by Kaposi's sarcoma herpesvirus

- is required for the maintenance of latently infected endothelial cells. *Proc Natl Acad Sci U S A*. 107:10696-701.
- Desai, A., and T.J. Mitchison. 1997. Microtubule polymerization dynamics. *Annu Rev Cell Dev Biol*. 13:83-117.
- Dictenberg, J.B., W. Zimmerman, C.A. Sparks, A. Young, C. Vidair, Y. Zheng, W. Carrington, F.S. Fay, and S.J. Doxsey. 1998. Pericentrin and gamma-tubulin form a protein complex and are organized into a novel lattice at the centrosome. *J Cell Biol*. 141:163-74.
- Donaldson, K.L., G.L. Goolsby, and A.F. Wahl. 1994. Cytotoxicity of the anticancer agents cisplatin and taxol during cell proliferation and the cell cycle. *Int J Cancer*. 57:847-55.
- Durrieu, C., F. Bernier-Valentin, and B. Rousset. 1987. Binding of glyceraldehyde 3-phosphate dehydrogenase to microtubules. *Mol Cell Biochem*. 74:55-65.
- Edde, B., J. Rossier, J.P. Le Caer, E. Desbruyeres, F. Gros, and P. Denoulet. 1990. Posttranslational glutamylation of alpha-tubulin. *Science*. 247:83-5.
- Elledge, S.J. 1996. Cell cycle checkpoints: preventing an identity crisis. *Science*. 274:1664-72.
- Elmore, S. 2007. Apoptosis: a review of programmed cell death. *Toxicol Pathol*. 35:495-516.
- Erickson, H.P., and E.T. O'Brien. 1992. Microtubule dynamic instability and GTP hydrolysis. *Annu Rev Biophys Biomol Struct*. 21:145-66.
- Friedrich, B., H. Gronberg, M. Landstrom, M. Gullberg, and A. Bergh. 1995. Differentiation-stage specific expression of oncoprotein 18 in human and rat prostatic adenocarcinoma. *Prostate*. 27:102-9.
- Fukasawa, K. 2008. P53, cyclin-dependent kinase and abnormal amplification of centrosomes. *Biochim Biophys Acta*. 1786:15-23.
- Galmarini, C.M., K. Kamath, A. Vanier-Viorner, V. Hervieu, E. Peiller, N. Falette, A. Puisieux, M. Ann Jordan, and C. Dumontet. 2003. Drug resistance associated with loss of p53 involves extensive alterations in microtubule composition and dynamics. *Br J Cancer*. 88:1793-9.

- Gao, S.P., and J.F. Bromberg. 2006. Touched and moved by STAT3. *Sci STKE*. 2006:pe30.
- Garrett, S., K. Auer, D.A. Compton, and T.M. Kapoor. 2002. hTPX2 is required for normal spindle morphology and centrosome integrity during vertebrate cell division. *Curr Biol*. 12:2055-9.
- Gascoigne, K.E., and S.S. Taylor. 2009. How do anti-mitotic drugs kill cancer cells? *J Cell Sci*. 122:2579-85.
- Giono, L.E., and J.J. Manfredi. 2007. Mdm2 is required for inhibition of Cdk2 activity by p21, thereby contributing to p53-dependent cell cycle arrest. *Mol Cell Biol*. 27:4166-78.
- Gradin, H.M., N. Larsson, U. Marklund, and M. Gullberg. 1998. Regulation of microtubule dynamics by extracellular signals: cAMP-dependent protein kinase switches off the activity of oncoprotein 18 in intact cells. *J Cell Biol*. 140:131-41.
- Gundersen, G.G., and T.A. Cook. 1999. Microtubules and signal transduction. *Curr Opin Cell Biol*. 11:81-94.
- Gundersen, G.G., M.H. Kalnoski, and J.C. Bulinski. 1984. Distinct populations of microtubules: tyrosinated and nontyrosinated alpha tubulin are distributed differently in vivo. *Cell*. 38:779-89.
- Higuchi, Y., S. Kawakami, and M. Hashida. 2010. Strategies for in vivo delivery of siRNAs: recent progress. *BioDrugs*. 24:195-205.
- Hirokawa, N., and R. Takemura. 2004. Kinesin superfamily proteins and their various functions and dynamics. *Exp Cell Res*. 301:50-9.
- Hollstein, M., D. Sidransky, B. Vogelstein, and C.C. Harris. 1991. p53 mutations in human cancers. *Science*. 253:49-53.
- Holmfeldt, P., K. Brannstrom, S. Stenmark, and M. Gullberg. 2006. Aneugenic activity of Op18/stathmin is potentiated by the somatic Q18-->E mutation in leukemic cells. *Mol Biol Cell*. 17:2921-30.
- Holmfeldt, P., G. Brattsand, and M. Gullberg. 2002. MAP4 counteracts microtubule catastrophe promotion but not tubulin-sequestering activity in intact cells. *Curr Biol*. 12:1034-9.

- Holmfeldt, P., S. Stenmark, and M. Gullberg. 2007. Interphase-specific phosphorylation-mediated regulation of tubulin dimer partitioning in human cells. *Mol Biol Cell*. 18:1909-17.
- Hornick, J.E., J.R. Bader, E.K. Tribble, K. Trimble, J.S. Breunig, E.S. Halpin, K.T. Vaughan, and E.H. Hinchcliffe. 2008. Live-cell analysis of mitotic spindle formation in taxol-treated cells. *Cell Motil Cytoskeleton*. 65:595-613.
- Howell, B., H. Deacon, and L. Cassimeris. 1999a. Decreasing oncoprotein 18/stathmin levels reduces microtubule catastrophes and increases microtubule polymer in vivo. *J Cell Sci*. 112 ( Pt 21):3713-22.
- Howell, B., N. Larsson, M. Gullberg, and L. Cassimeris. 1999b. Dissociation of the tubulin-sequestering and microtubule catastrophe-promoting activities of oncoprotein 18/stathmin. *Mol Biol Cell*. 10:105-18.
- Johnsen, J.I., O.N. Aurelio, Z. Kwaja, G.E. Jorgensen, N.S. Pellegata, R. Plattner, E.J. Stanbridge, and J.F. Cajot. 2000. p53-mediated negative regulation of stathmin/Op18 expression is associated with G(2)/M cell-cycle arrest. *Int J Cancer*. 88:685-91.
- Jordan, M.A., and K. Kamath. 2007. How do microtubule-targeted drugs work? An overview. *Curr Cancer Drug Targets*. 7:730-42.
- Kann, M.L., S. Soues, N. Levilliers, and J.P. Fouquet. 2003. Glutamylated tubulin: diversity of expression and distribution of isoforms. *Cell Motil Cytoskeleton*. 55:14-25.
- Kelly, T.J., and G.W. Brown. 2000. Regulation of chromosome replication. *Annu Rev Biochem*. 69:829-80.
- Kim, S.S., H. Garg, A. Joshi, and N. Manjunath. 2009. Strategies for targeted nonviral delivery of siRNAs in vivo. *Trends Mol Med*. 15:491-500.
- Knull, H.R., and J.L. Walsh. 1992. Association of glycolytic enzymes with the cytoskeleton. *Curr Top Cell Regul*. 33:15-30.
- Koivusalo, R., E. Krausz, H. Helenius, and S. Hietanen. 2005. Chemotherapy compounds in cervical cancer cells primed by reconstitution of p53 function after short interfering RNA-mediated degradation of human papillomavirus 18 E6 mRNA:

- opposite effect of siRNA in combination with different drugs. *Mol Pharmacol.* 68:372-82.
- Koivusalo, R., A. Mialon, H. Pitkanen, J. Westermarck, and S. Hietanen. 2006. Activation of p53 in cervical cancer cells by human papillomavirus E6 RNA interference is transient, but can be sustained by inhibiting endogenous nuclear export-dependent p53 antagonists. *Cancer Res.* 66:11817-24.
- Komarova, Y.A., I.A. Vorobjev, and G.G. Borisy. 2002. Life cycle of MTs: persistent growth in the cell interior, asymmetric transition frequencies and effects of the cell boundary. *J Cell Sci.* 115:3527-39.
- Kouzu, Y., K. Uzawa, H. Koike, K. Saito, D. Nakashima, M. Higo, Y. Endo, A. Kasamatsu, M. Shiiba, H. Bukawa, H. Yokoe, and H. Tanzawa. 2006. Overexpression of stathmin in oral squamous-cell carcinoma: correlation with tumour progression and poor prognosis. *Br J Cancer.* 94:717-23.
- Kulartz, M., and R. Knippers. 2004. The replicative regulator protein geminin on chromatin in the HeLa cell cycle. *J Biol Chem.* 279:41686-94.
- Larsson, N., U. Marklund, H.M. Gradin, G. Brattsand, and M. Gullberg. 1997. Control of microtubule dynamics by oncoprotein 18: dissection of the regulatory role of multisite phosphorylation during mitosis. *Mol Cell Biol.* 17:5530-9.
- Larsson, N., H. Melander, U. Marklund, O. Osterman, and M. Gullberg. 1995. G2/M transition requires multisite phosphorylation of oncoprotein 18 by two distinct protein kinase systems. *J Biol Chem.* 270:14175-83.
- Larsson, N., B. Segerman, B. Howell, K. Fridell, L. Cassimeris, and M. Gullberg. 1999. Op18/stathmin mediates multiple region-specific tubulin and microtubule-regulating activities. *J Cell Biol.* 146:1289-302.
- Lehotzky, A., M. Telegdi, K. Liliom, and J. Ovadi. 1993. Interaction of phosphofructokinase with tubulin and microtubules. Quantitative evaluation of the mutual effects. *J Biol Chem.* 268:10888-94.
- Liang, X.J., Y. Choi, D.L. Sackett, and J.K. Park. 2008. Nitrosoureas inhibit the stathmin-mediated migration and invasion of malignant glioma cells. *Cancer Res.* 68:5267-72.

- Liedtke, W., E.E. Leman, R.E. Fyffe, C.S. Raine, and U.K. Schubart. 2002. Stathmin-deficient mice develop an age-dependent axonopathy of the central and peripheral nervous systems. *Am J Pathol.* 160:469-80.
- Lin, S.X., G.G. Gundersen, and F.R. Maxfield. 2002. Export from pericentriolar endocytic recycling compartment to cell surface depends on stable, detyrosinated (glu) microtubules and kinesin. *Mol Biol Cell.* 13:96-109.
- Maddocks, O.D., and K.H. Vousden. Metabolic regulation by p53. *J Mol Med.* 89:237-45.
- Marklund, U., N. Larsson, H.M. Gradin, G. Brattsand, and M. Gullberg. 1996. Oncoprotein 18 is a phosphorylation-responsive regulator of microtubule dynamics. *Embo J.* 15:5290-8.
- McGrath, J.L. 2006. Microtubule mechanics: a little flexibility goes a long way. *Curr Biol.* 16:R800-2.
- McKean, P.G., S. Vaughan, and K. Gull. 2001. The extended tubulin superfamily. *J Cell Sci.* 114:2723-33.
- Melhem, R., N. Hailat, R. Kuick, and S.M. Hanash. 1997. Quantitative analysis of Op18 phosphorylation in childhood acute leukemia. *Leukemia.* 11:1690-5.
- Meurer-Grob, P., J. Kasparian, and R.H. Wade. 2001. Microtubule structure at improved resolution. *Biochemistry.* 40:8000-8.
- Mistry, S.J., A. Bank, and G.F. Atweh. 2005. Targeting stathmin in prostate cancer. *Mol Cancer Ther.* 4:1821-9.
- Mitchison, T., and M. Kirschner. 1984. Dynamic instability of microtubule growth. *Nature.* 312:237-42.
- Mitchison, T.J. 1993. Localization of an exchangeable GTP binding site at the plus end of microtubules. *Science.* 261:1044-7.
- Morgan, D.O. 1997. Cyclin-dependent kinases: engines, clocks, and microprocessors. *Annu Rev Cell Dev Biol.* 13:261-91.
- Moritz, M., M.B. Braunfeld, J.W. Sedat, B. Alberts, and D.A. Agard. 1995. Microtubule nucleation by gamma-tubulin-containing rings in the centrosome. *Nature.* 378:638-40.

- Nakashima, D., K. Uzawa, A. Kasamatsu, H. Koike, Y. Endo, K. Saito, S. Hashitani, T. Numata, M. Urade, and H. Tanzawa. 2006. Protein expression profiling identifies maspin and stathmin as potential biomarkers of adenoid cystic carcinoma of the salivary glands. *Int J Cancer*. 118:704-13.
- Ng, D.C., B.H. Lin, C.P. Lim, G. Huang, T. Zhang, V. Poli, and X. Cao. 2006. Stat3 regulates microtubules by antagonizing the depolymerization activity of stathmin. *J Cell Biol*. 172:245-57.
- Ngo, T.T., T. Peng, X.J. Liang, O. Akeju, S. Pastorino, W. Zhang, Y. Kotliarov, J.C. Zenklusen, H.A. Fine, D. Maric, P.Y. Wen, U. De Girolami, P.M. Black, W.W. Wu, R.F. Shen, N.O. Jeffries, D.W. Kang, and J.K. Park. 2007. The 1p-encoded protein stathmin and resistance of malignant gliomas to nitrosoureas. *J Natl Cancer Inst*. 99:639-52.
- Nguyen, H.L., S. Chari, D. Gruber, C.M. Lue, S.J. Chapin, and J.C. Bulinski. 1997. Overexpression of full- or partial-length MAP4 stabilizes microtubules and alters cell growth. *J Cell Sci*. 110 ( Pt 2):281-94.
- Nishio, K., T. Nakamura, Y. Koh, F. Kanzawa, T. Tamura, and N. Saijo. 2001. Oncoprotein 18 overexpression increases the sensitivity to vindesine in the human lung carcinoma cells. *Cancer*. 91:1494-9.
- Nogales, E. 2000. Structural insights into microtubule function. *Annu Rev Biochem*. 69:277-302.
- Nogales, E., S.G. Wolf, and K.H. Downing. 1998. Structure of the alpha beta tubulin dimer by electron crystallography. *Nature*. 391:199-203.
- Nylander, K., U. Marklund, G. Brattsand, M. Gullberg, and G. Roos. 1995. Immunohistochemical detection of oncoprotein 18 (Op18) in malignant lymphomas. *Histochem J*. 27:155-60.
- O'Connell, M.J., and K.A. Cimprich. 2005. G2 damage checkpoints: what is the turn-on? *J Cell Sci*. 118:1-6.
- Perdiz, D., R. Mackeh, C. Pous, and A. Baillet. The ins and outs of tubulin acetylation: more than just a post-translational modification? *Cell Signal*. 23:763-71.

- Piehl, M., and L. Cassimeris. 2003. Organization and dynamics of growing microtubule plus ends during early mitosis. *Mol Biol Cell*. 14:916-25.
- Piehl, M., U.S. Tulu, P. Wadsworth, and L. Cassimeris. 2004. Centrosome maturation: measurement of microtubule nucleation throughout the cell cycle by using GFP-tagged EB1. *Proc Natl Acad Sci U S A*. 101:1584-8.
- Price, D.K., J.R. Ball, Z. Bahrani-Mostafavi, J.C. Vachris, J.S. Kaufman, R.W. Naumann, R.V. Higgins, and J.B. Hall. 2000. The phosphoprotein Op18/stathmin is differentially expressed in ovarian cancer. *Cancer Invest*. 18:722-30.
- Rana, S., P.B. Maples, N. Senzer, and J. Nemunaitis. 2008. Stathmin 1: a novel therapeutic target for anticancer activity. *Expert Rev Anticancer Ther*. 8:1461-70.
- Reed, N.A., D. Cai, T.L. Blasius, G.T. Jih, E. Meyhofer, J. Gaertig, and K.J. Verhey. 2006. Microtubule acetylation promotes kinesin-1 binding and transport. *Curr Biol*. 16:2166-72.
- Rieder, C.L., and R. Cole. 2000. Microtubule disassembly delays the G2-M transition in vertebrates. *Curr Biol*. 10:1067-70.
- Rieder, C.L., and H. Maiato. 2004. Stuck in division or passing through: what happens when cells cannot satisfy the spindle assembly checkpoint. *Dev Cell*. 7:637-51.
- Ringhoff, D.N., and L. Cassimeris. 2009a. Gene expression profiles in mouse embryo fibroblasts lacking stathmin, a microtubule regulatory protein, reveal changes in the expression of genes contributing to cell motility. *BMC Genomics*. 10:343.
- Ringhoff, D.N., and L. Cassimeris. 2009b. Stathmin regulates centrosomal nucleation of microtubules and tubulin dimer/polymer partitioning. *Mol Biol Cell*. 20:3451-8.
- Rusan, N.M., U.S. Tulu, C. Fagerstrom, and P. Wadsworth. 2002. Reorganization of the microtubule array in prophase/prometaphase requires cytoplasmic dynein-dependent microtubule transport. *J Cell Biol*. 158:997-1003.
- Schubart, U.K., J. Yu, J.A. Amat, Z. Wang, M.K. Hoffmann, and W. Edelmann. 1996. Normal development of mice lacking metablastin (P19), a phosphoprotein implicated in cell cycle regulation. *J Biol Chem*. 271:14062-6.
- Schulze, E., D.J. Asai, J.C. Bulinski, and M. Kirschner. 1987. Posttranslational modification and microtubule stability. *J Cell Biol*. 105:2167-77.

- Sellin, M.E., P. Holmfeldt, S. Stenmark, and M. Gullberg. 2008. Global regulation of the interphase microtubule system by abundantly expressed Op18/stathmin. *Mol Biol Cell*. 19:2897-906.
- Shumyatsky, G.P., G. Malleret, R.M. Shin, S. Takizawa, K. Tully, E. Tsvetkov, S.S. Zakharenko, J. Joseph, S. Vronskaya, D. Yin, U.K. Schubart, E.R. Kandel, and V.Y. Bolshakov. 2005. stathmin, a gene enriched in the amygdala, controls both learned and innate fear. *Cell*. 123:697-709.
- Sobel, A. 1991. Stathmin: a relay phosphoprotein for multiple signal transduction? *Trends Biochem Sci*. 16:301-5.
- Stacey, D.W. 2010. Three Observations That Have Changed Our Understanding of Cyclin D1 and p27kip1 in Cell Cycle Control. *Genes & Cancer*. 1:1189-1199.
- Steinmetz, M.O. 2007. Structure and thermodynamics of the tubulin-stathmin interaction. *J Struct Biol*. 158:137-47.
- Sur, S., R. Pagliarini, F. Bunz, C. Rago, L.A. Diaz, Jr., K.W. Kinzler, B. Vogelstein, and N. Papadopoulos. 2009. A panel of isogenic human cancer cells suggests a therapeutic approach for cancers with inactivated p53. *Proc Natl Acad Sci U S A*. 106:3964-9.
- Tarapore, P., and K. Fukasawa. 2002. Loss of p53 and centrosome hyperamplification. *Oncogene*. 21:6234-40.
- Uetake, Y., and G. Sluder. 2007. Cell-cycle progression without an intact microtubule cytoskeleton. *Curr Biol*. 17:2081-6.
- Vershinin, M., J. Xu, D.S. Razafsky, S.J. King, and S.P. Gross. 2008. Tuning microtubule-based transport through filamentous MAPs: the problem of dynein. *Traffic*. 9:882-92.
- Vertessy, B.G., F. Orosz, J. Kovacs, and J. Ovadi. 1997. Alternative binding of two sequential glycolytic enzymes to microtubules. Molecular studies in the phosphofructokinase/aldolase/microtubule system. *J Biol Chem*. 272:25542-6.
- Vorobjev, I.A., V.I. Rodionov, I.V. Maly, and G.G. Borisy. 1999. Contribution of plus and minus end pathways to microtubule turnover. *J Cell Sci*. 112 ( Pt 14):2277-89.

- Wallace-Brodeur, R.R., and S.W. Lowe. 1999. Clinical implications of p53 mutations. *Cell Mol Life Sci.* 55:64-75.
- Wang, N.P., H. To, W.H. Lee, and E.Y. Lee. 1993. Tumor suppressor activity of RB and p53 genes in human breast carcinoma cells. *Oncogene.* 8:279-88.
- Wang, R., K. Dong, F. Lin, X. Wang, P. Gao, S.H. Wei, S.Y. Cheng, and H.Z. Zhang. 2007. Inhibiting proliferation and enhancing chemosensitivity to taxanes in osteosarcoma cells by RNA interference-mediated downregulation of stathmin expression. *Mol Med.* 13:567-75.
- Wang, Y., P. Ji, J. Liu, R.R. Broaddus, F. Xue, and W. Zhang. 2009. Centrosome-associated regulators of the G(2)/M checkpoint as targets for cancer therapy. *Mol Cancer.* 8:8.
- Warren, J.C., and L. Cassimeris. 2007. The contributions of microtubule stability and dynamic instability to adenovirus nuclear localization efficiency. *Cell Motil Cytoskeleton.* 64:675-89.
- Warren, J.C., A. Rutkowski, and L. Cassimeris. 2006. Infection with replication-deficient adenovirus induces changes in the dynamic instability of host cell microtubules. *Mol Biol Cell.* 17:3557-68.
- Weaver, B.A., and D.W. Cleveland. 2005. Decoding the links between mitosis, cancer, and chemotherapy: The mitotic checkpoint, adaptation, and cell death. *Cancer Cell.* 8:7-12.
- Wiman, K.G. 2007. Restoration of wild-type p53 function in human tumors: strategies for efficient cancer therapy. *Adv Cancer Res.* 97:321-38.
- Wittmann, T., G.M. Bokoch, and C.M. Waterman-Storer. 2004. Regulation of microtubule destabilizing activity of Op18/stathmin downstream of Rac1. *J Biol Chem.* 279:6196-203.
- Xiao, H., P. Verdier-Pinard, N. Fernandez-Fuentes, B. Burd, R. Angeletti, A. Fiser, S.B. Horwitz, and G.A. Orr. 2006. Insights into the mechanism of microtubule stabilization by Taxol. *Proc Natl Acad Sci U S A.* 103:10166-73.
- Yuan, R.H., Y.M. Jeng, H.L. Chen, P.L. Lai, H.W. Pan, F.J. Hsieh, C.Y. Lin, P.H. Lee, and H.C. Hsu. 2006. Stathmin overexpression cooperates with p53 mutation and

- osteopontin overexpression, and is associated with tumour progression, early recurrence, and poor prognosis in hepatocellular carcinoma. *J Pathol.* 209:549-58.
- Zhai, Y., P.J. Kronebusch, P.M. Simon, and G.G. Borisy. 1996. Microtubule dynamics at the G2/M transition: abrupt breakdown of cytoplasmic microtubules at nuclear envelope breakdown and implications for spindle morphogenesis. *J Cell Biol.* 135:201-14.
- Zhang, H.Z., Y. Wang, P. Gao, F. Lin, L. Liu, B. Yu, J.H. Ren, H. Zhao, and R. Wang. 2006. Silencing stathmin gene expression by survivin promoter-driven siRNA vector to reverse malignant phenotype of tumor cells. *Cancer Biol Ther.* 5:1457-61.

Bruce Carney, Ph.D

Contact Information

---

Home Address

408 West 9<sup>th</sup> St  
Bethlehem, PA 18015

Work Address

111 Research Drive  
Bethlehem, PA 18015

Cell Phone: 908-319-7431

Office Phone: 610-758-5603

Email: [bkc205@lehigh.edu](mailto:bkc205@lehigh.edu)

Education

---

Lehigh University <i>Molecular Biology, Ph.D. program</i>	Bethlehem, PA Current Student
--	----------------------------------

Virginia Tech <i>B.S. in Biology, GPA: 3.63</i>	Blacksburg, VA Graduation: May 2004
--	--

Research Experience

---

2005-Present Lehigh University  
Graduate Student, Molecular Biology Doctoral Program

Dissertation: "Stathmin Depletion from Cells Lacking p53 Leads to Delayed Cell Cycle Progression and Apoptosis Due to Increased Microtubule Stability."

Expected Graduation: September 2011

Extensive use of human cell culture, immunoblotting, immunofluorescence, wide field and confocal light microscopy, live cell imaging, FACs, vector transfection, RNA Interference, PCR, and nucleic acid techniques in pursuit of my Ph.D.

2004-2005 Metaphore Pharmaceuticals

Consultant (Assistant Scientist)

Employed in development under Dr. Robert Medve, MD assisting in data analysis, interpretation, and clinical development of a new experimental pain relieving drug.

1998-1999 Rutgers University Snyder Research and Extension Farm

Assistant in Wildlife Damage Control

Assisted in performing experiments intended to prevent crop damage by animals. Was involved with collecting, analyzing, and interpreting data.

## Teaching Experience

---

2008-present Lehigh University – Teaching Assistant

- Cell Biology Lab (2)
- Biochemistry
- Intro to Cell Biology (2)
- Genetic

2008 Biological Dynamics Summer Institute (BDSI) sponsored by HHMI

Mentored two undergraduates in a group research project that including mRNA isolation and microarray analysis of gene expression changes.

2005-2006 Lehigh University - Teaching Assistant

- Immunology Lab
- Intro to Cell Biology Lab

## Honors and Awards

---

2009-2010 President of Biological Organization of Graduate Students

2008 Biological Dynamics Summer Institute (BDSI) sponsored by HHMI  
(Graduate Fellow)

2007-2008 Vice President of Biological Organization of Graduate Students

## Professional Memberships

---

American Society for Cell Biology

American Association for the Advancement of Science

## Publications

---

1. Cassimeris, L., B. Becker and **B. Carney**. 2009. TOGp Regulates Microtubule Assembly and Density during Mitosis and Contributes to Chromosome Directional Instability. *Cell Motil. Cytoskel.* 66:535-545.

2. **Carney BK**, Cassimeris L. Stathmin/oncoprotein 18, a microtubule regulatory protein, is required for survival of both normal and cancer cell lines lacking the tumor suppressor, p53. *Cancer Biol Ther* 2010; 9:699-709.

## Presentations

---

Dissertation Public Defense: **B.K. Carney**. Stathmin Depletion from Cells Lacking p53 Leads to Delayed Cell Cycle Progression and Apoptosis Due to Increased Microtubule Stability. Lehigh University, July 15, 2011.

Biology Department Departmental Seminar Series: **B.K. Carney**. Targeted killing of cancer cells. Lehigh University, March 23, 2010.

---

Ringhoff, D., **B. Carney**, A. Lefkowitz, E. Smith, J. Marzillier, P.-S. Wu and L. Cassimeris. Gene expression profiles of HCT116<sup>p53<sup>-/-</sup></sup> cells treated with paclitaxel of stathmin siRNA. Lehigh University – BDSI Symposium, July 2008.

Abstracts/Poster Presentations

---

1. **B. Carney**, B. Becker, and L. Cassimeris. 2006. Fragmentation of the Centrosome. Mol. Biol. Cell. 17 (Suppl.) 762 (CD-ROM). Presented by BC at 46<sup>th</sup> Annual Meeting of the American Society for Cell Biology, San Diego, CA.

2. L. Cassimeris, D. Ringhoff, **B. Carney**, D. Odde and M. Gardner. (2007) “Probing the Function of Oncoprotein18/Stathmin and Mutant Variants in Microtubule Polymerization and Dynamics *in vivo*.” Presented by LC (FASEB summer conference Mitosis: Spindle Assembly and Function) Indian Wells, CA.

3. Ringhoff, D., **B. Carney**, A. Lefkowitz, E. Smith, J. Marzillier, P.-S. Wu and L. Cassimeris. 2008. Gene expression profiles of HCT116p53<sup>-/-</sup> cells treated with paclitaxel or stathmin siRNA. Mol. Biol. Cell. 19 (Suppl.). 1077 (CD-ROM). Presented by Ringhoff at 48<sup>th</sup> Annual Meeting of the American Society for Cell Biology, San Francisco, CA.

4. **Carney, B.** and L. Cassimeris. 2008. Stathmin/oncoprotein 18 depletion leads to apoptosis in cells lacking p53. Mol. Biol. Cell. 19 (Suppl.). 1078 (CD-ROM). Presented by BC at 48<sup>th</sup> Annual Meeting of the American Society for Cell Biology, San Francisco, CA.

5. **Carney, B.** and Cassimeris, L. 2010. Stathmin/oncoprotein 18, a microtubule regulatory protein, is required for survival of both normal and cancer cell lines lacking the tumor suppressor, p53. Presented by BC at the Pennsylvania Muscle Institute Retreat and Symposium, Philadelphia, PA.

6. **Carney, B.** and L. Cassimeris. 2010. Increasing Stable Microtubules Leads to Apoptosis in Human Cell Lines Lacking p53. Mol. Biol. Cell. 21 (Suppl.). 139 (CD-ROM). Presented by BC at 50<sup>th</sup> Annual Meeting of the American Society for Cell Biology, Philadelphia, PA.

---